Quantum World at Atomic Scale: Spin-Polarized Scanning Tunneling Microscopy

Pin-Jui Hsu[1,2] (徐斌睿)

1. Institute of Applied Physics, University of Hamburg, Jungiusstrasse 11, D-20355 Hamburg, Germany
2. Department of Physics, National Tsing Hua University, No. 101, Section 2, Kuang-Fu Road, Hsinchu 30013, Taiwan

Fe-DL/ Rh(001)

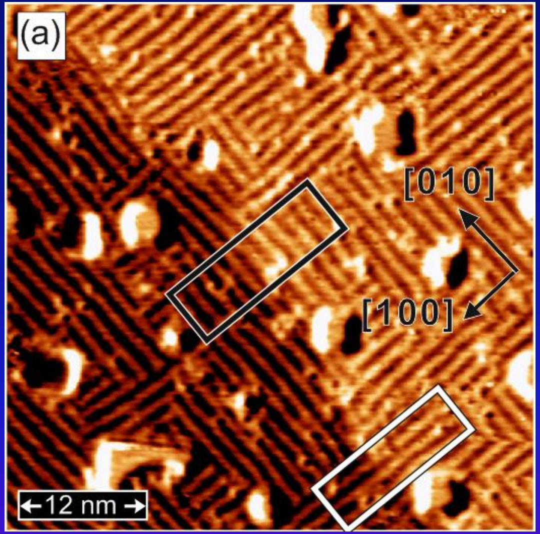

Fe-TL/ Ir(111)

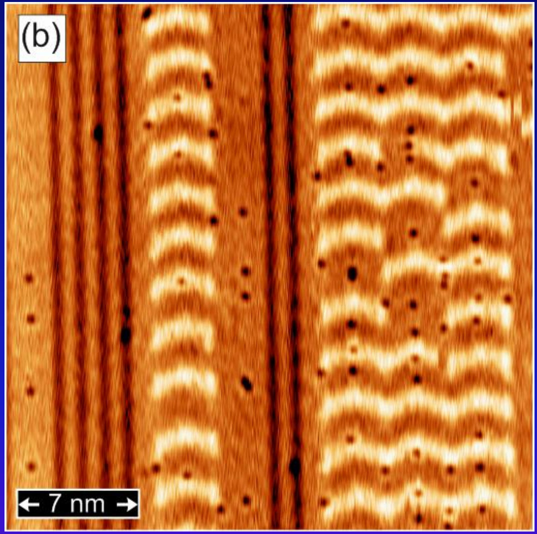

H/ Fe-DL/ Ir(111)

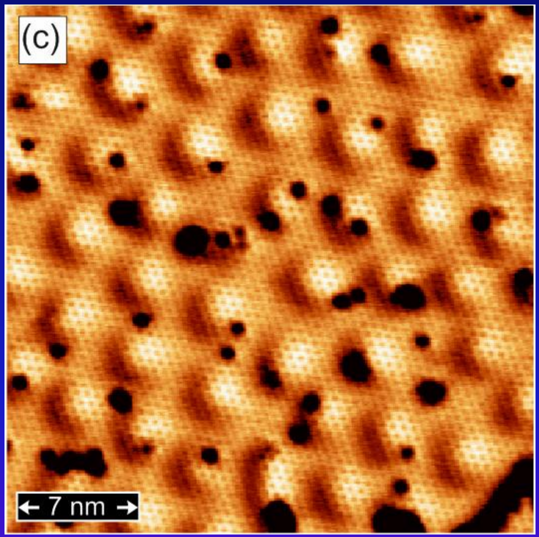

Outline

- ***Research Motivation***
  - *To image, detect, and manipulate low-dimensional systems by SP-STM with spin resolution.*
- ***Introductions & Literatures***
  - *What SP-STM can do ?*
    - *Atomic Spin Lattice : Non-collinear Magnetism*
      - *Chiral Domain Wall, Spin Spiral, Magnetic Skyrmions*
    - *SP-STS : LDOS, QPI, IETS, Image State, Landau Splitting, QPC*
      - *Kondo Resonance, Band Dispersion, Phonon Excitation*
    - *Atom Manipulation : Zeeman Splitting, Magnetic Hysteresis*
      - *Magnetic Moment, Magnetocrystalliine Anisotropy, RKKY Coupling Strength*
    - *Time Resolution : Pump-Probe Dynamics, Atomic Dipolar Fields*
      - *Electron Spin Resonance, Dipole-dipole Interaction*
- ***Summary & Future Highlights***

The Nobel Prize in Physics 1986 ~

"See" the atomic scale world !!

"for his fundamental work in electron optics, and for the design of the first electron microscope"

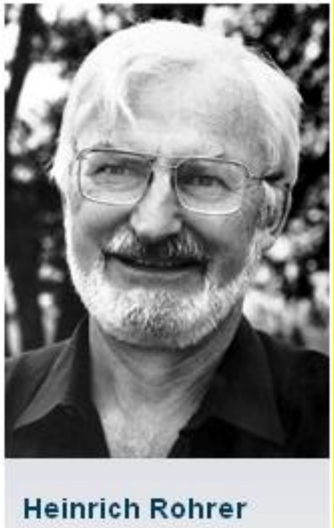

"for their design of the scanning tunneling microscope"

Working Principle

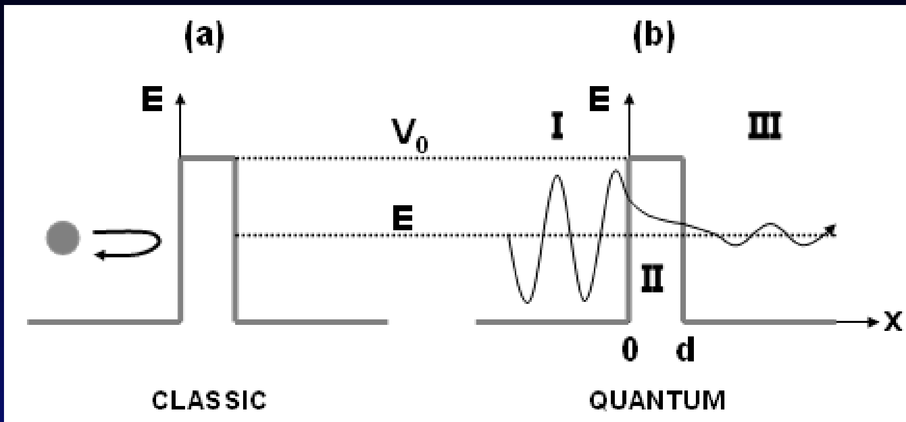

$$T = \frac{j_t}{j_i} = \left|\frac{F}{A}\right|^2 = \frac{1}{1 + \frac{(k^2+\kappa^2)^2}{(4k^2\kappa^2)}\sinh^2(\kappa d)}$$

$$T \approx \frac{16k^2\kappa^2}{(k^2+\kappa^2)^2} \cdot e^{-2\kappa d}, \kappa d \gg 1$$

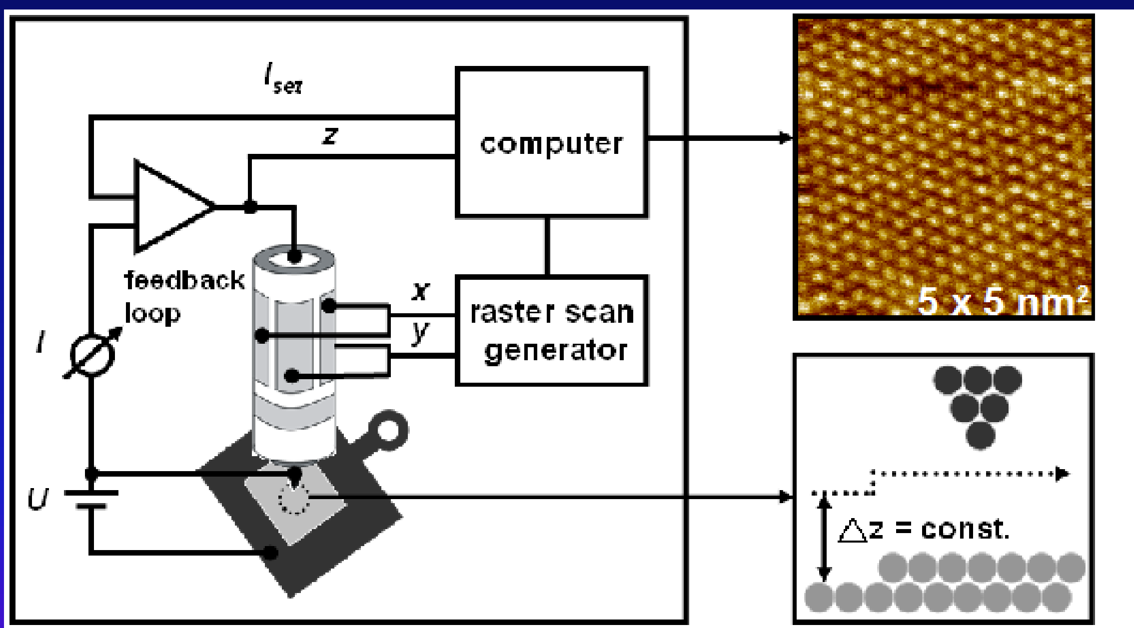

$$I \propto e^{-\lambda z}$$

- Atomic Resolution
- Surface Sensitivity
- Local Density of States

↓

(Tunneling Spectroscopy)

....

Operation Modes

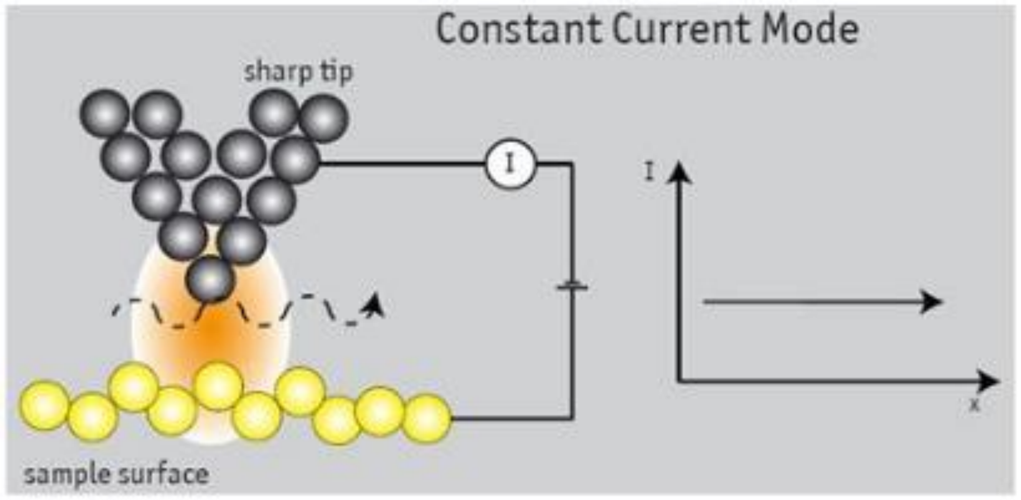

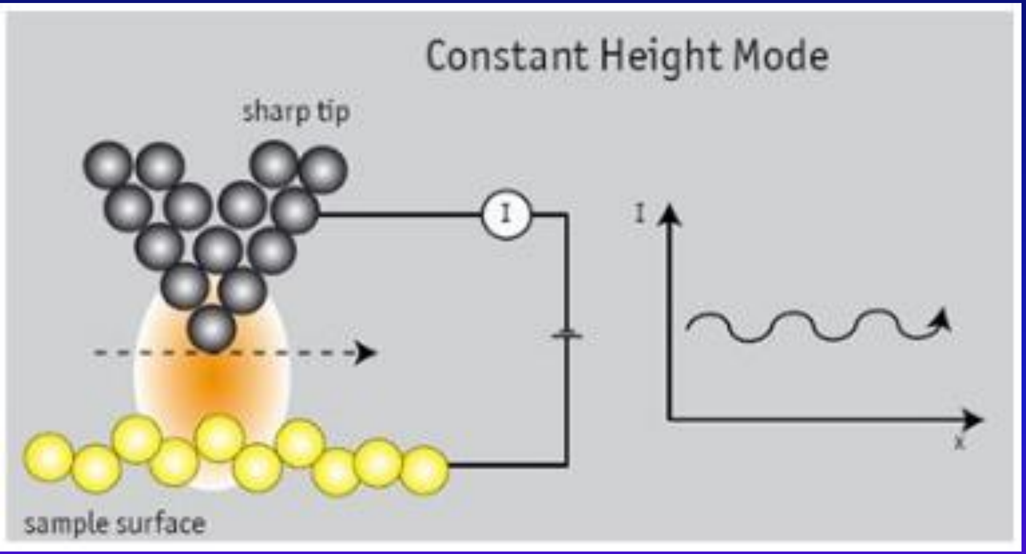

Scanning Tunneling Microscopy

Working Principle

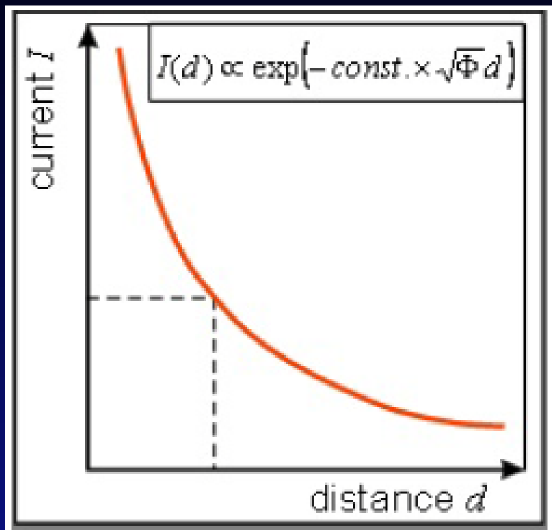

$$I(d) = constant \times eV \exp\left(-2\frac{\sqrt{2m\Phi}}{\hbar}d\right)$$

Φ: the work function (energy barrier),
e: the electron charge,
m: the electron mass,
h: the Planck's constant,
V: applied voltage,
d: tip-sample distance.

- A thin metal tip is brought in close proximity of the sample surface. At a distance of only a few Å, the overlap of tip and sample electron wavefunctions is large enough for an electron tunneling to occur.
- When an electrical voltage *V* is applied between sample and tip, this tunneling phenomenon results in a net electrical current, the 'tunneling current'. This current depends on the tip-surface distance *d*, on the voltage *V*, and on the height of the barrier Φ:
- This (approximate) equation shows that the tunneling current obeys Ohm's law, i.e. the current *I* is proportional to the voltage *V*.
- The current depends exponentially on the distance *d*.
- For a typical value of the work function Φ of 4 eV for a metal, the tunneling current reduces by a factor **10** for every **0.1** nm increase in *d*. This means that over a typical atomic diameter of e.g. **0.3 nm**, the tunneling current changes by a factor **1000**! *This is what makes the STM so sensitive.*
- The tunneling current depends so strongly on the distance that it is dominated by the contribution flowing between the last atom of the tip and the nearest atom in the specimen --- single-atom imaging!

Scanning Tunneling Microscopy

Various Systems

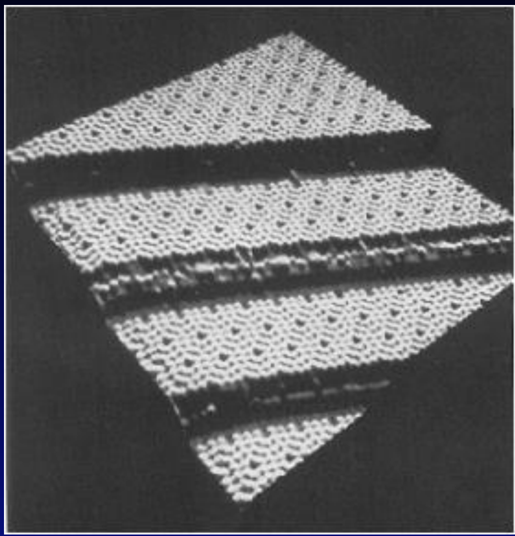

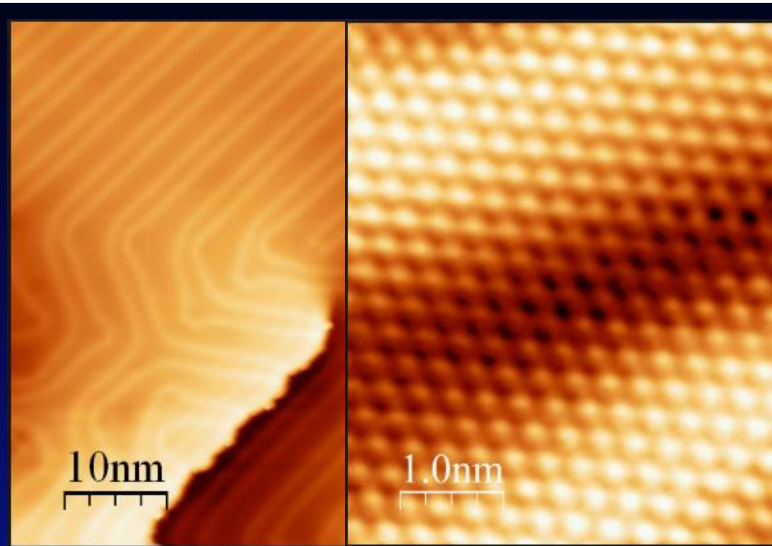

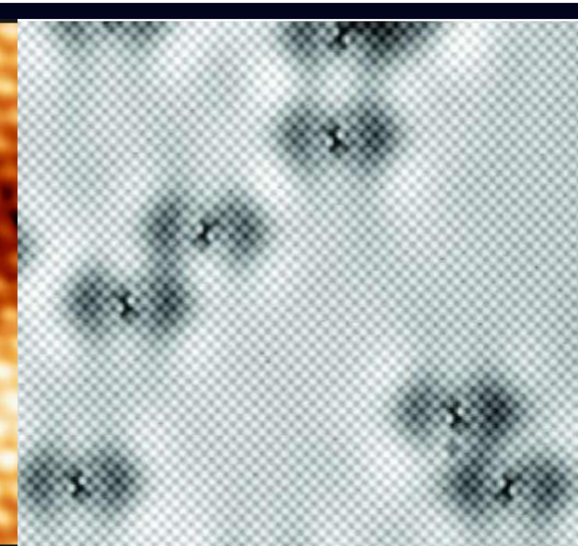

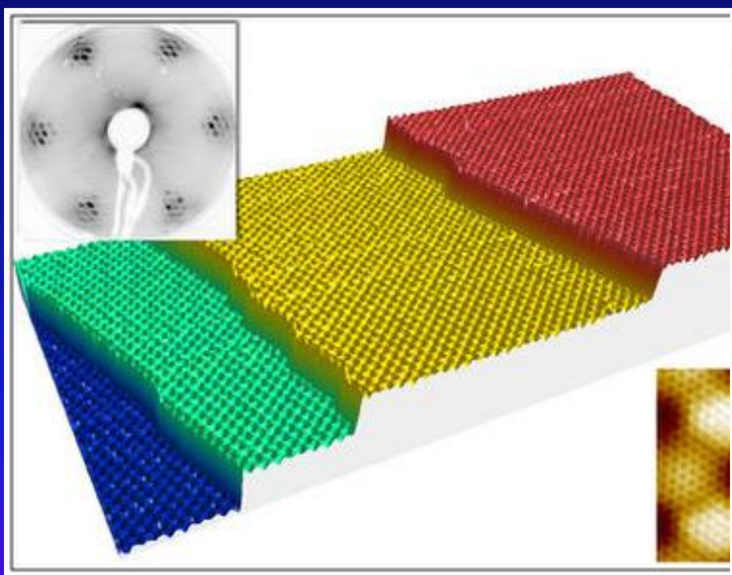

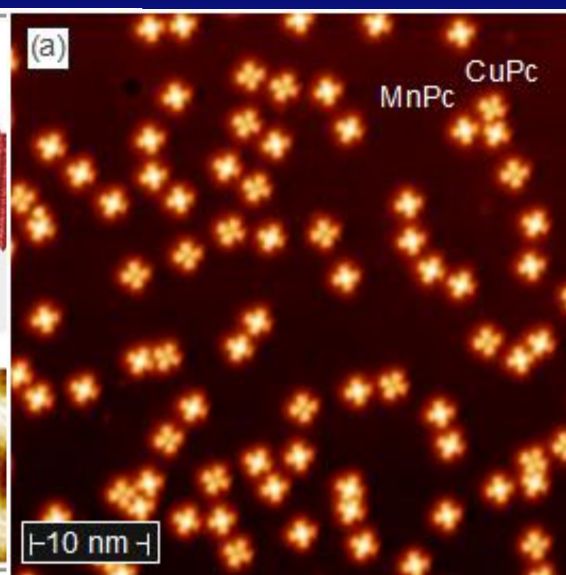

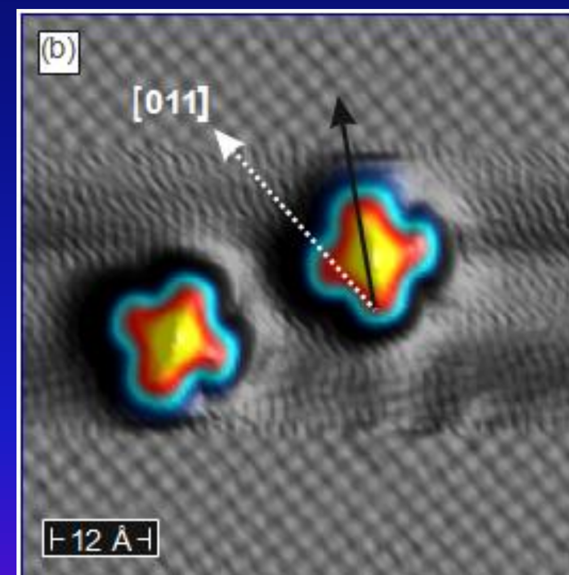

Experimental Instruments

Various types of STM in Hamburg

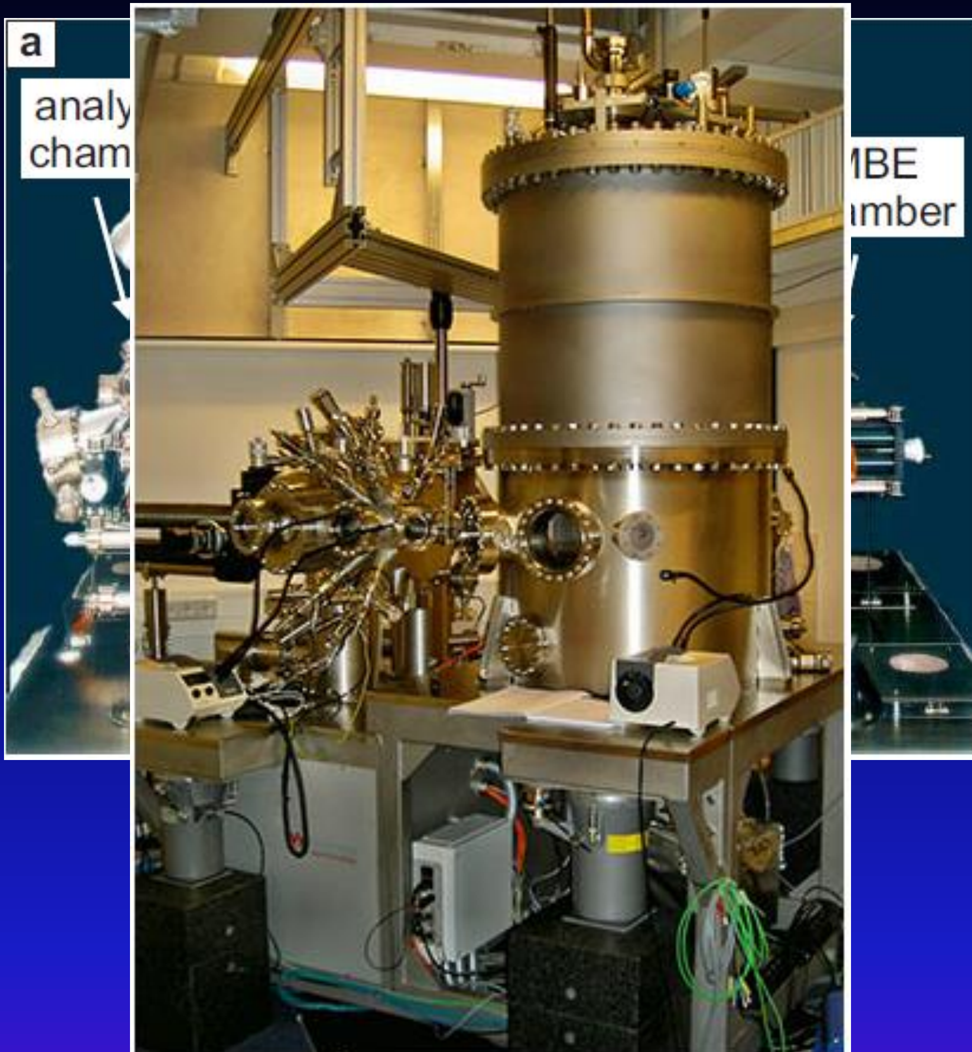

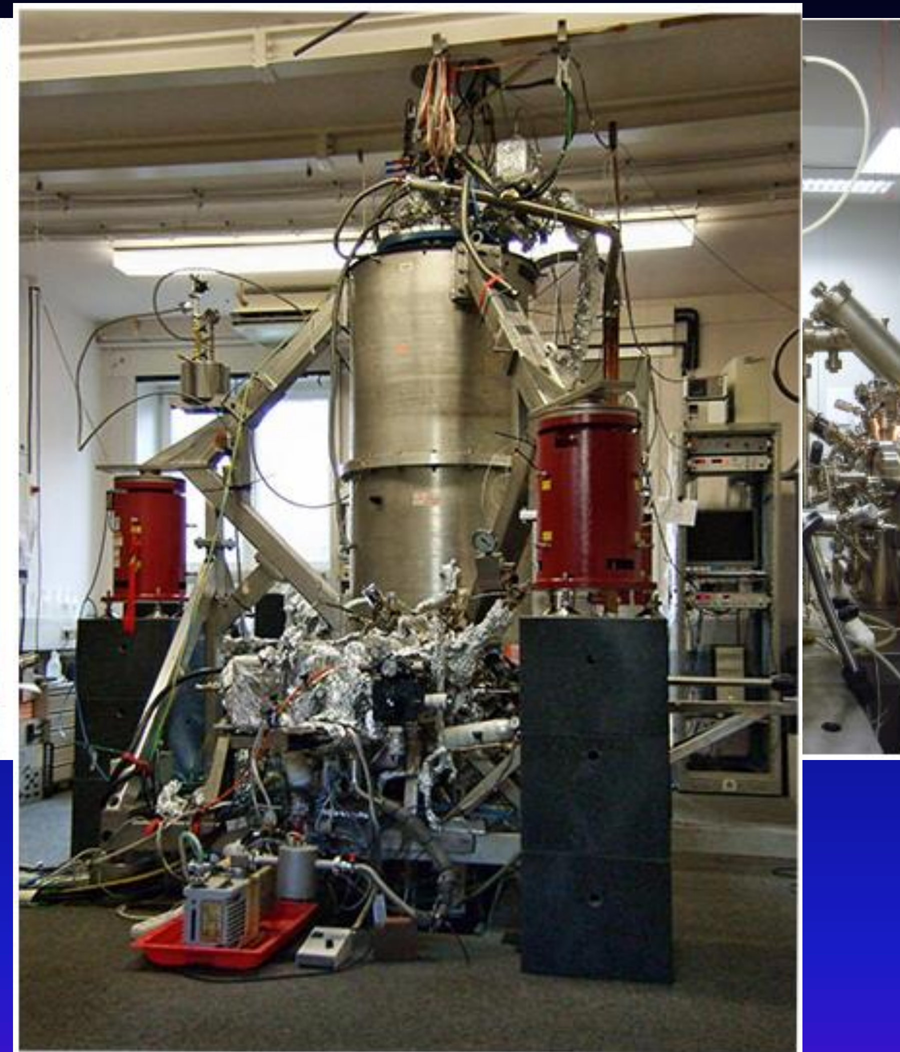

- Home built 4K-STM with 3D Magnets
- Home built 300 mK-STM with 12T Magnet

Experimental Instruments

Various types of STM in Hamburg

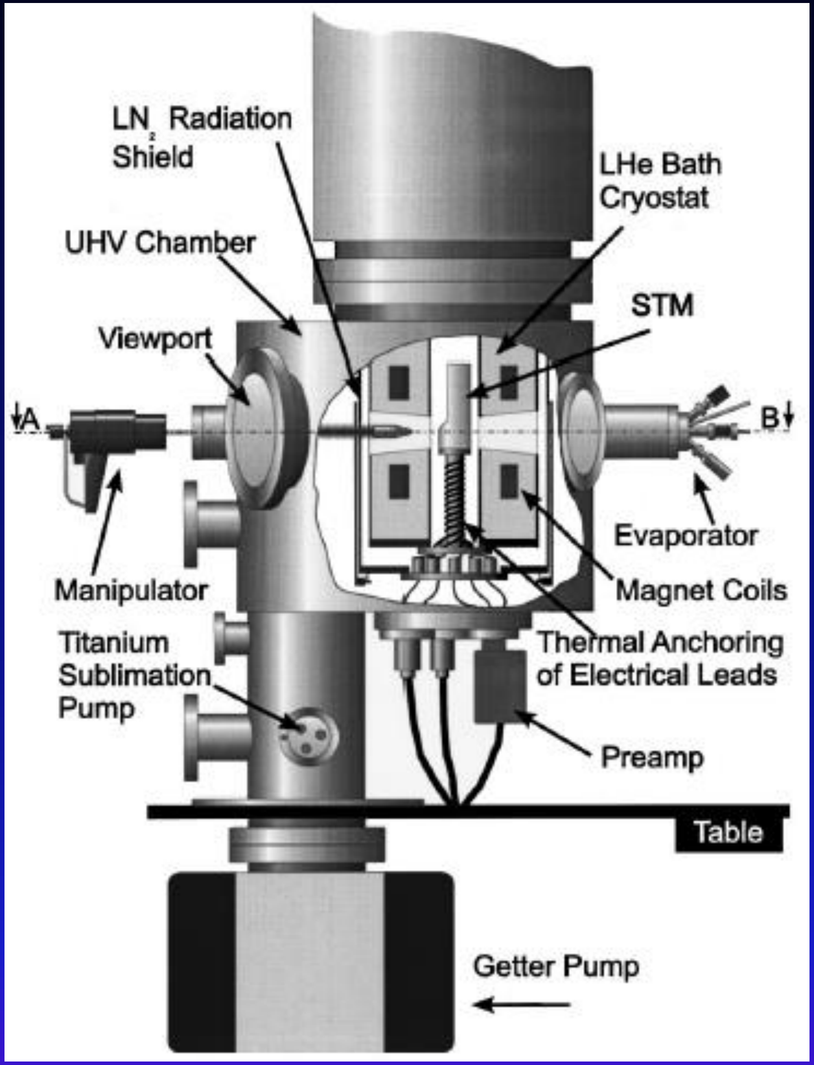

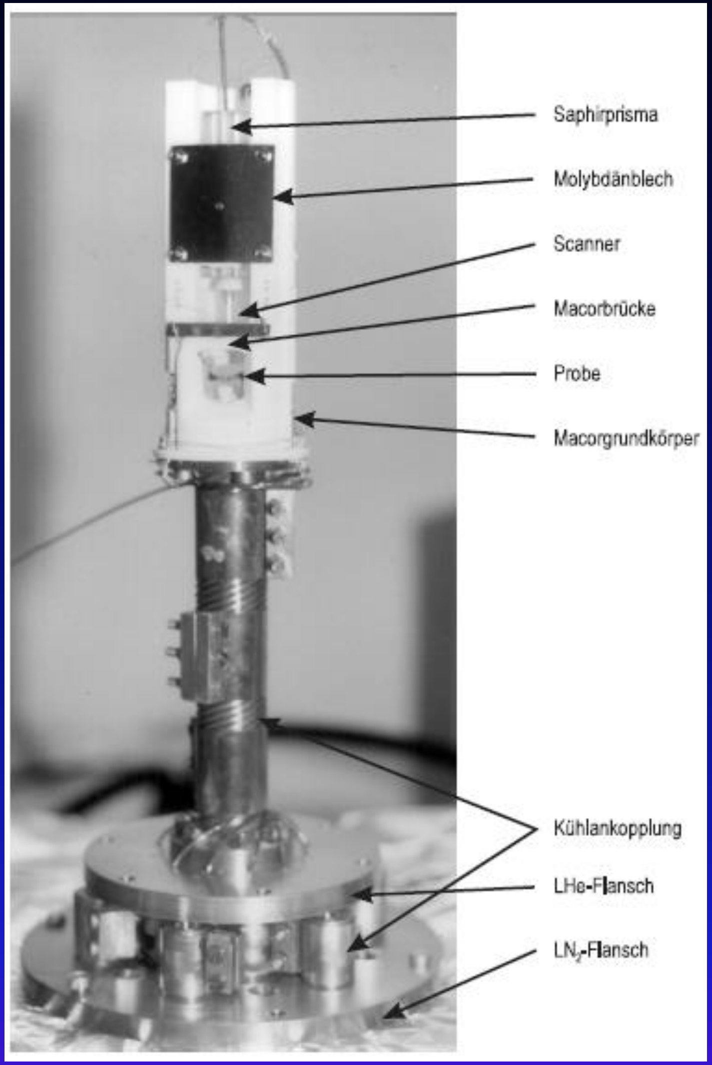

Experimental Instruments

Various types of STM in Hamburg

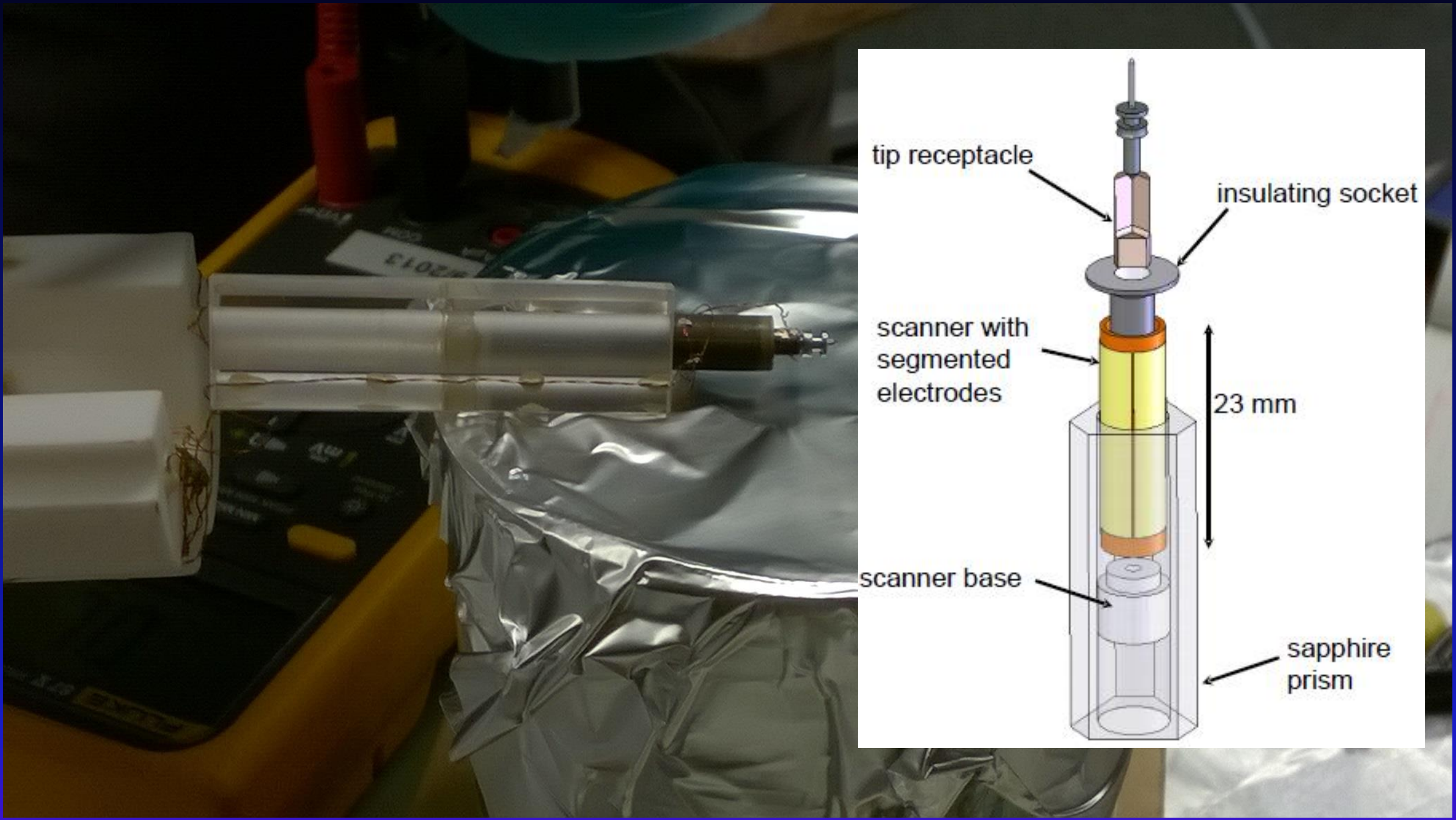

Scanner Piezo Tube

Tube Scanners

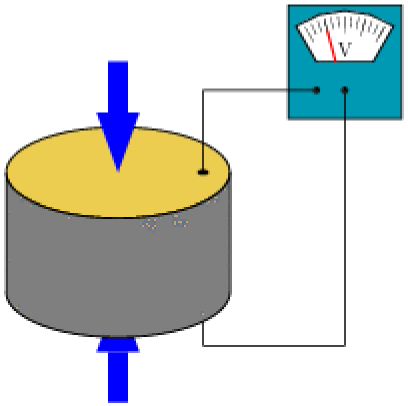

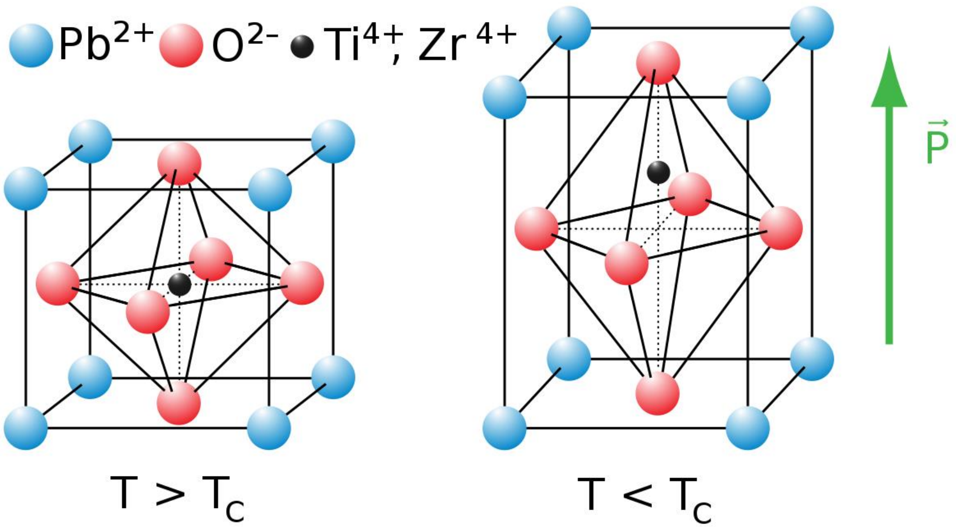

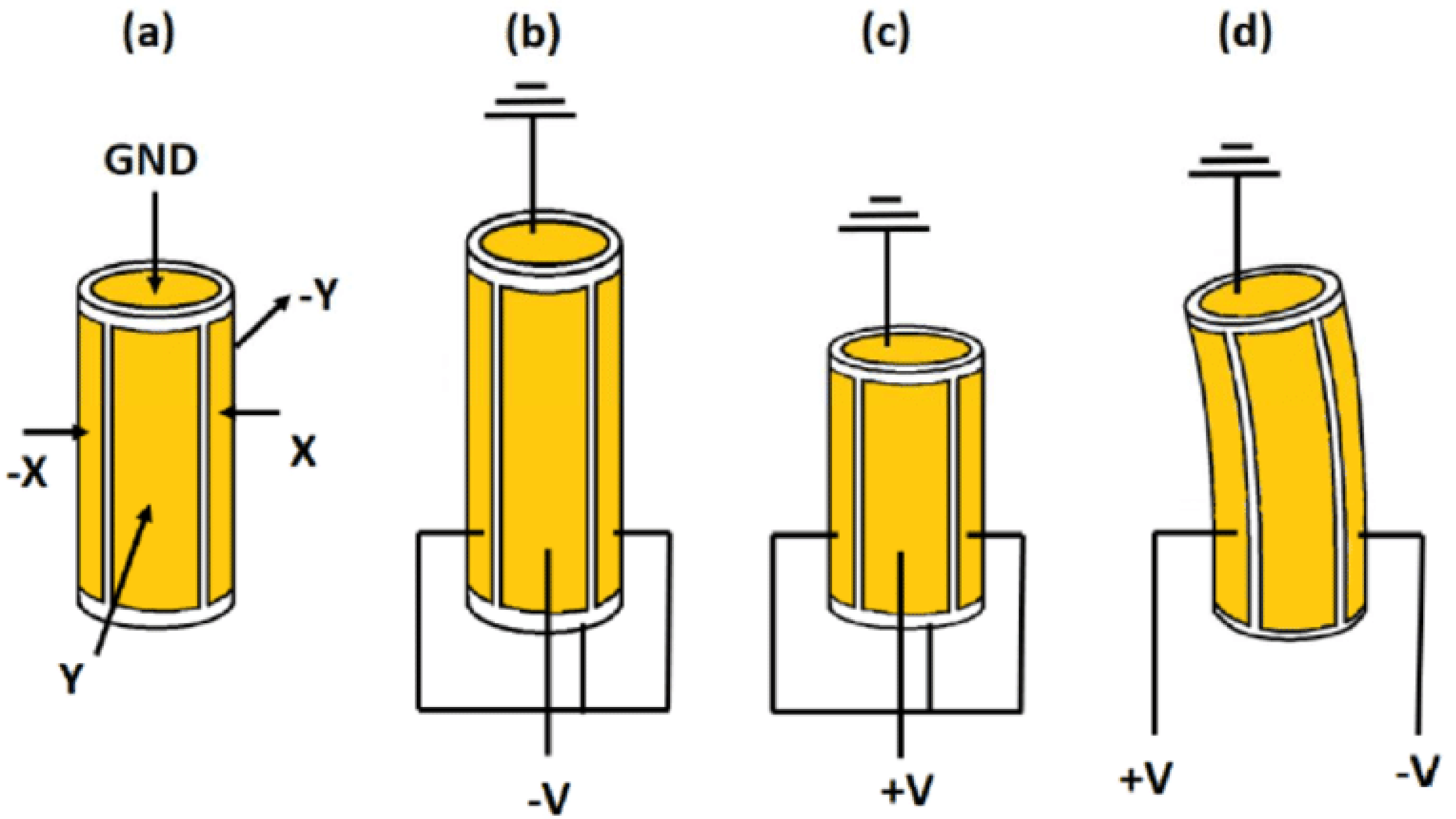

(a)
(b)
(c)
(d)
GND
-Y
-X
X
Y
-V
+V
+V
-V

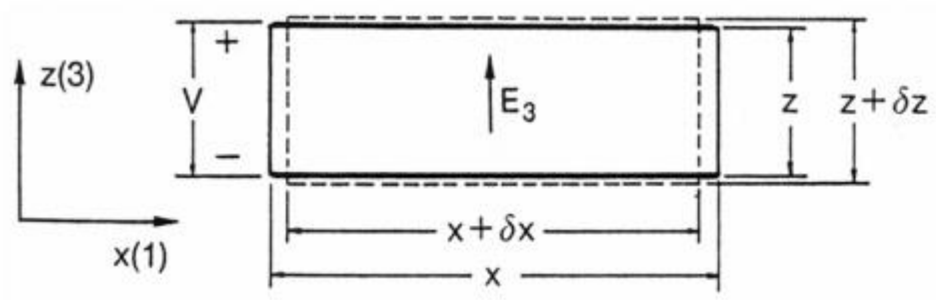

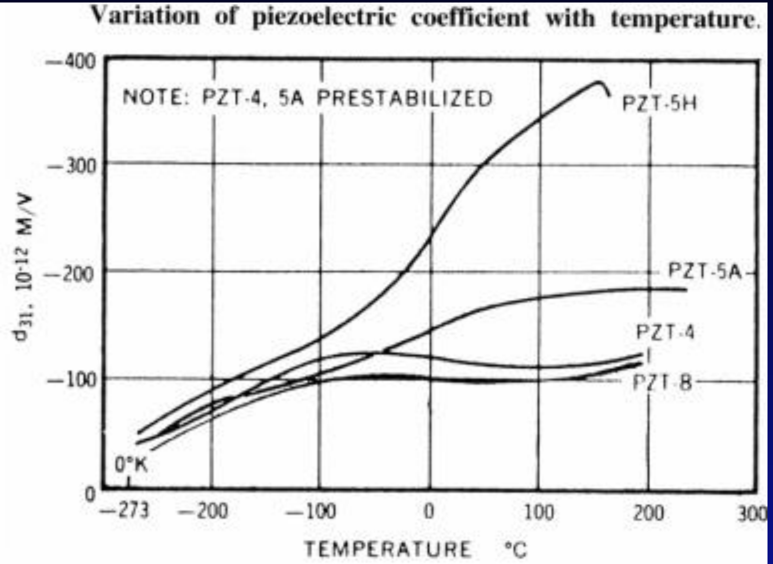

Strain: $S_1 = \delta x/x$, $S_3 = \delta z/z$

Electric field: $E_3 = V/z$

Piezoelectric Coeff.: $d_{33} = S_3/E_3$, $d_{31} = S_1/E_3$

Typical values for $d_{31} \sim -1$ Å/V, $d_{33} \sim 3$ Å/V.

Scanner Piezo Tube

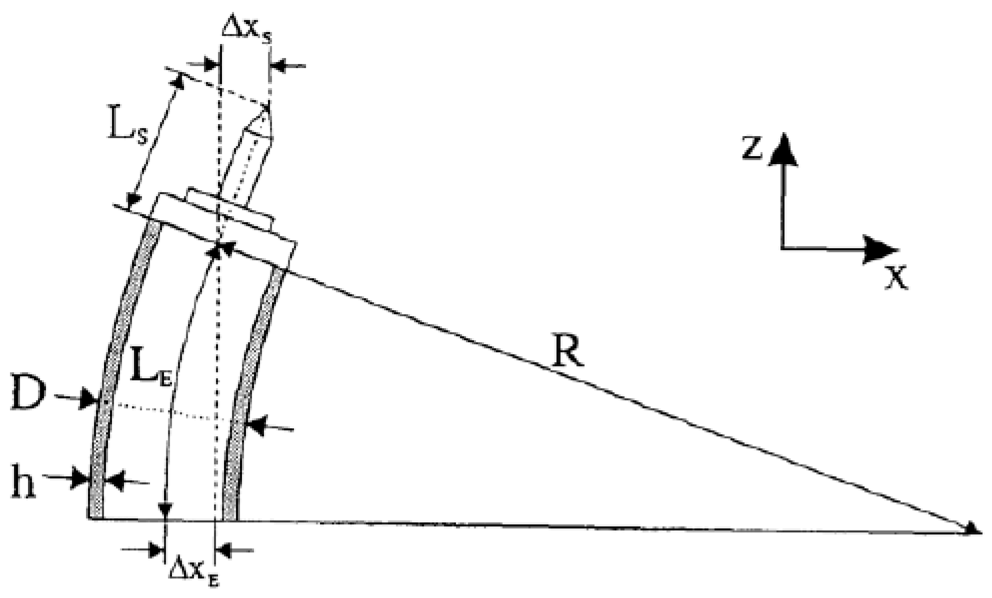

$$\Delta x = 2(\Delta x_{\mathrm{E}} + \Delta x_{\mathrm{S}})$$

$$\Delta x = \Delta y = \frac{2\sqrt{2} d_{31} U}{\pi D w}(L_{\mathrm{E}}^2 + 2 L_{\mathrm{E}} L_{\mathrm{S}})$$

$$\Delta z = d_{31} U \frac{L_{\mathrm{E}}}{w}$$

The scanner used has a wall thickness $w = 0.5$ mm and an outer diameter $D = 6.4$ mm. The length of the electrodes and the extension is $L_{\mathrm{E}} = 19.5$ mm and $L_{\mathrm{S}} = 8.6$ mm, respectively. The piezoelectric constant is $d_{31} = 9.5 \cdot 10^{-12}$ m/V and the maximal voltage which can be applied is $U = \pm 130$ V. The resulting scan range is:

$$\begin{aligned} \Delta x = \Delta y &= 4.934 \mu\mathrm{m} \\ \Delta z &= 0.948 \mu\mathrm{m} \end{aligned}$$

The transverse and longitudinal eigenfrequencies – f_t and f_l – of the scanner have to be larger than the typical cut-off frequencies used in STM-experiments (about 1.5 kHz).

$$f_l = \frac{1}{4L}\sqrt{\frac{E}{\rho}} = 36.592 \text{ kHz}$$

$$f_t = \frac{1.88^2 D}{4\sqrt{2}\pi L^2}\sqrt{\frac{E}{\rho}} = 8.037 \text{ kHz}$$

$L = 23$ mm is the entire scanner length, $D = 6.4$ mm is the diameter of the tube. $E = 8.5 \cdot 10^{10}$ N/m^2 is Young's modulus and $\rho = 7500$ kg/m^3 is the density of the tube's material.

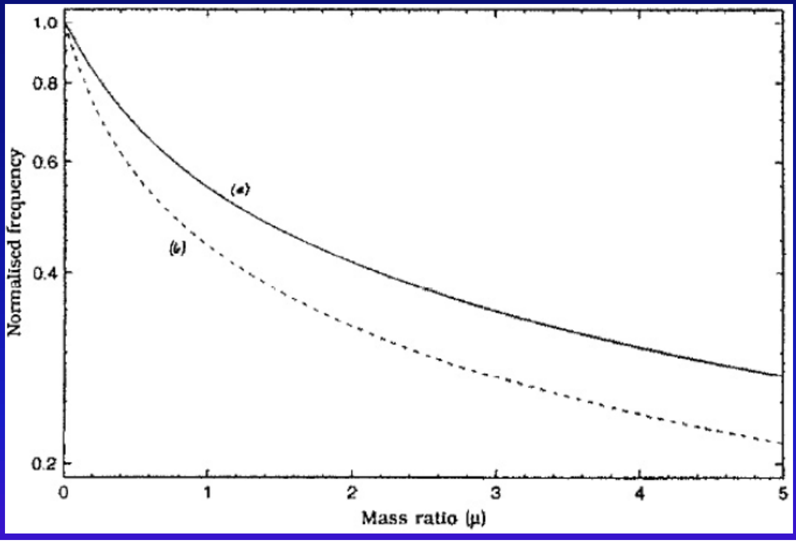

Dependence of the eigenfrequencies (extension (a), deflection (b))

The frequencies are lowered due to the load of the scanner. i.e. the entire mass of insulating socket, tip receptacle, tip holder and tip. Figure 3.8 shows that the mass ratio $\mu = 0,5$, i.e. external load divided by the tube's mass, can be used to determine the normalized eigenfrequencies:

$$f_l = 18.296\text{kHz}$$

$$f_t = 4.661\text{kHz}$$

Scanning Tunneling Microscopy

Coarse Piezo Motor

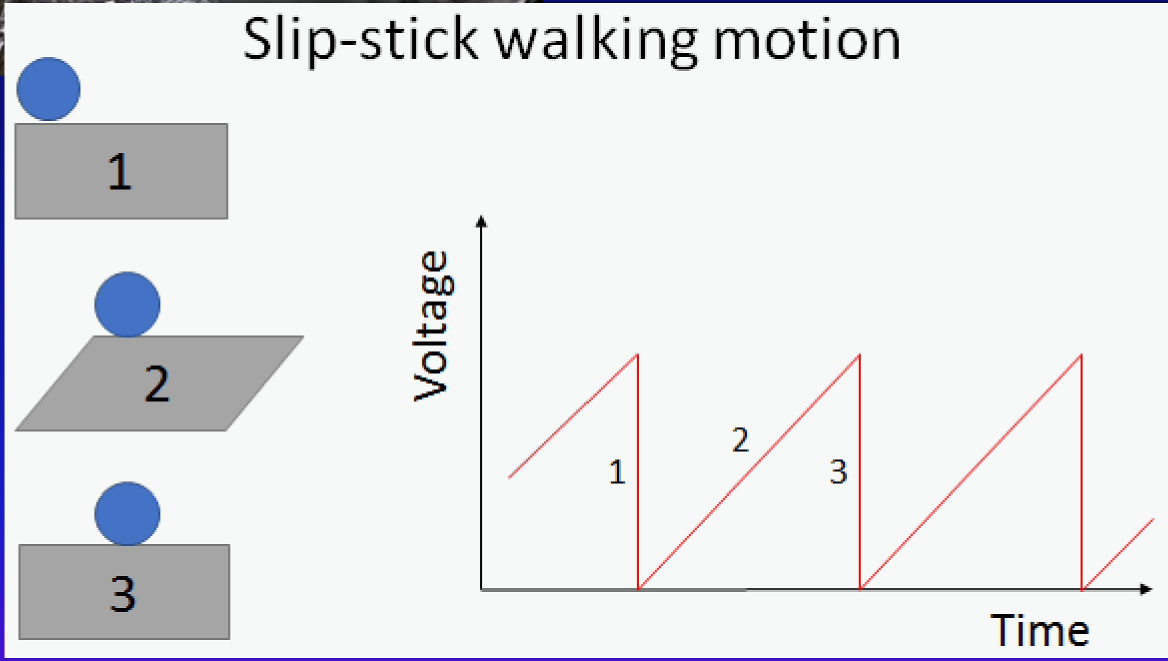

Scanning Tunneling Microscopy

Coarse Piezo Motor

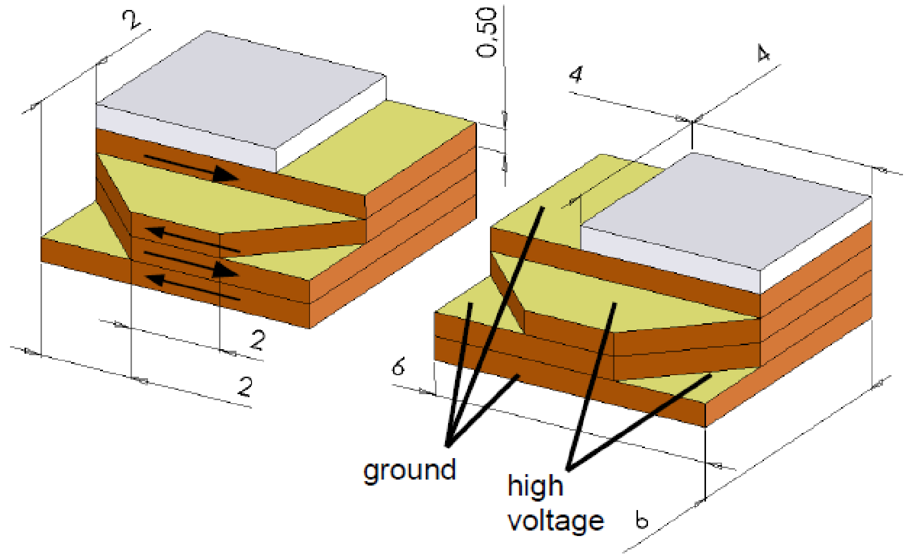

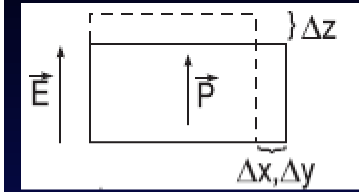

Längs-Effekt: $\Delta z = d_{33} E_z L_z$

Quer-Effekt: $\Delta x = d_{31} E_z L_x$

$\Delta y = d_{31} E_z L_y$

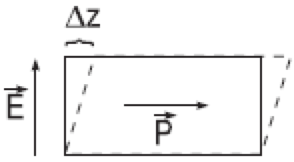

Scher-Effekt: $\Delta z = d_{15} E_x L_x$

The shear width Δz depends on the shear-piezoelectric constant k_{15}, the electric field in x-direction E_x, and the thickness in x-direction d, and is given by:

$$\Delta z = k_{15} E_\mathrm{x} d_\mathrm{total} = k_{15} E_\mathrm{x} 4d = 4k_{15} \frac{\Delta U}{d} d = 4k_{15} \Delta U$$

For a voltage of $U = \pm 400$ V the step width is $\Delta z_\mathrm{coarse} = 1.056\ \mu\mathrm{m}$.

⇨ $\Delta Z_{fine} \geq \Delta Z_{coarse}$

Scanning Tunneling Spectroscopy

Working Principle

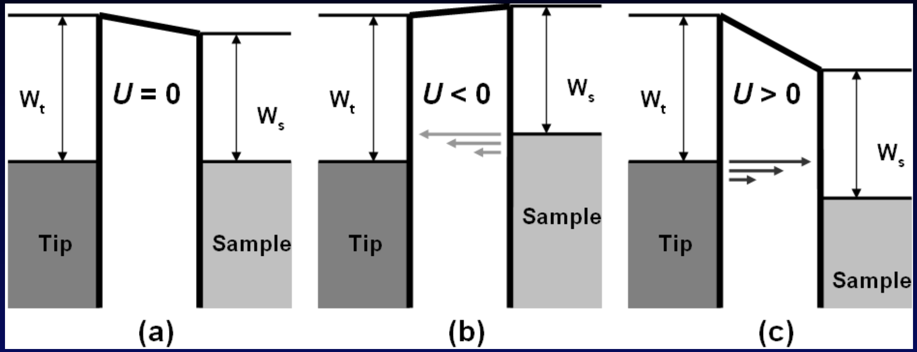

$$I \propto \int_0^{eU} \rho_s(\vec{r}_0, E_F+\varepsilon)\cdot\rho_t(E_F-eU+\varepsilon)\,d\varepsilon$$

$$\frac{dI}{dU} \propto \rho_s(\vec{r}_0, E_F+eU)$$

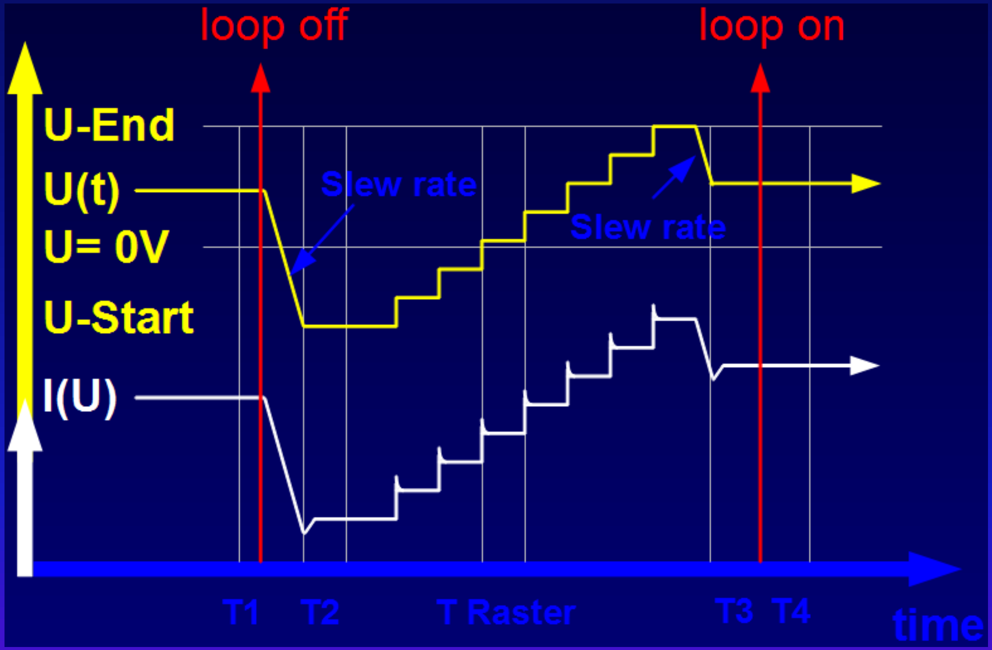

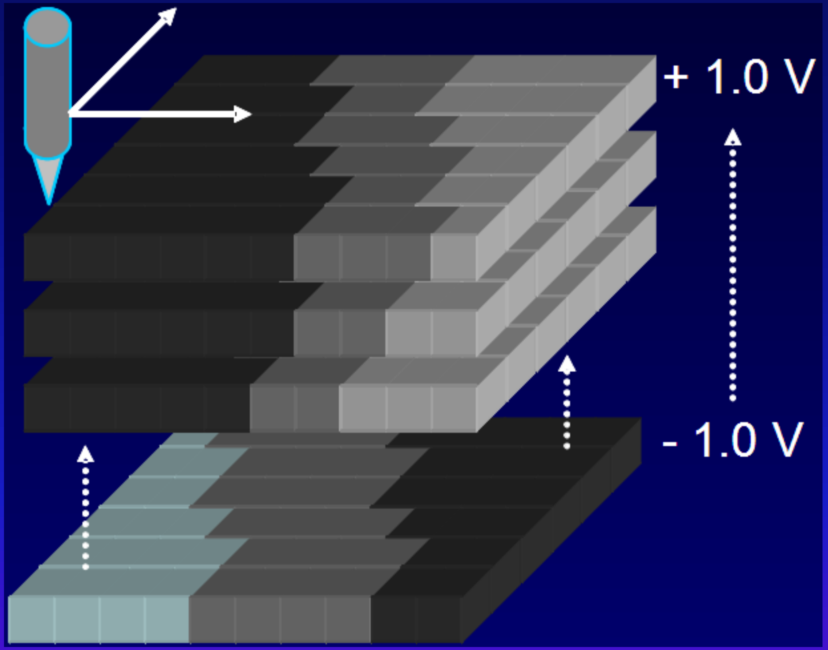

Scanning Tunneling Spectroscopy

Working Principle

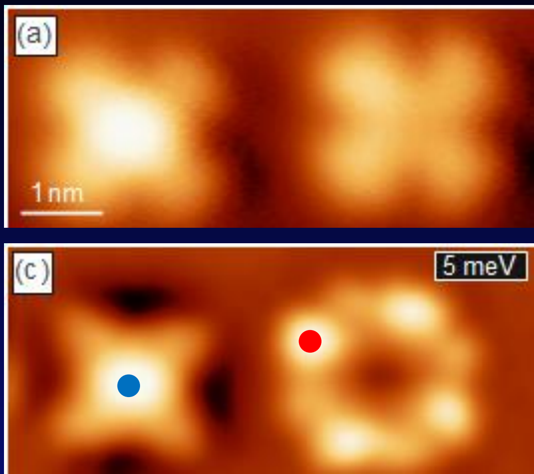

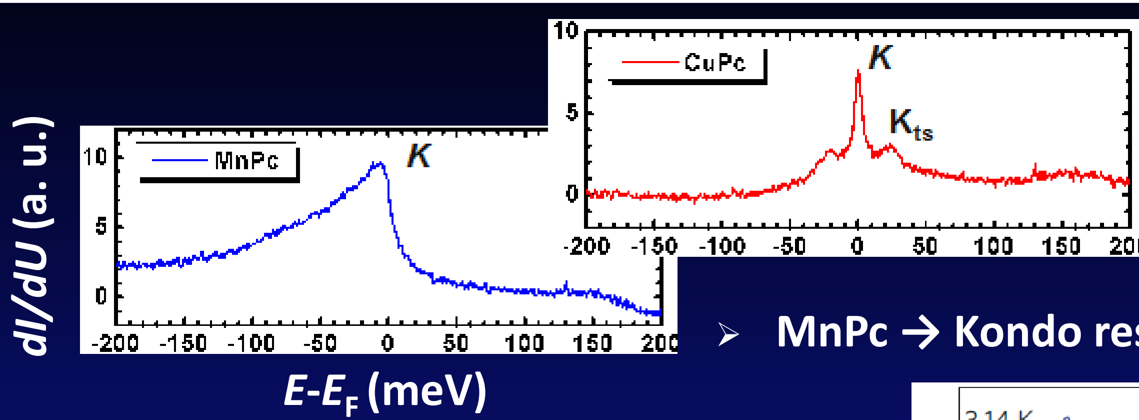

- MnPc → Kondo resonance.

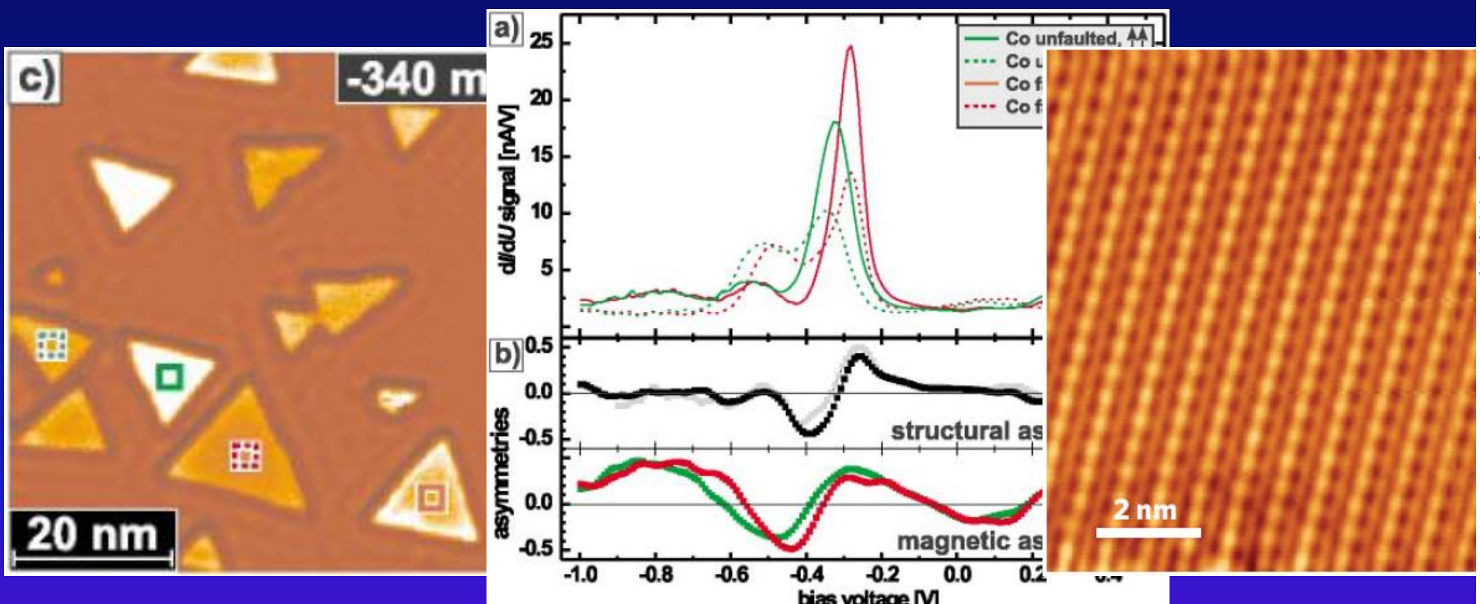

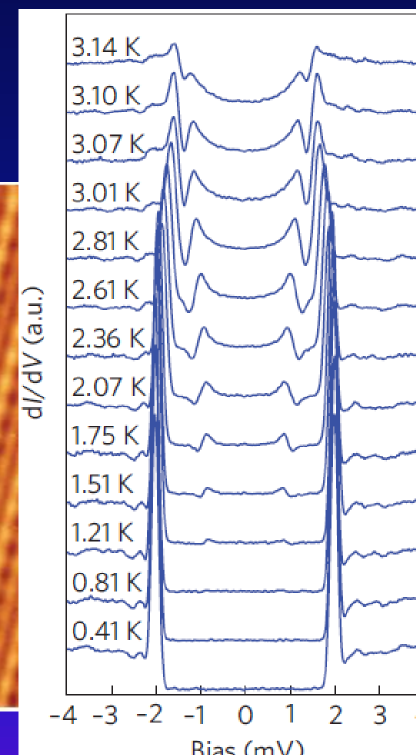

Scanning Tunneling Spectroscopy

Working Principle

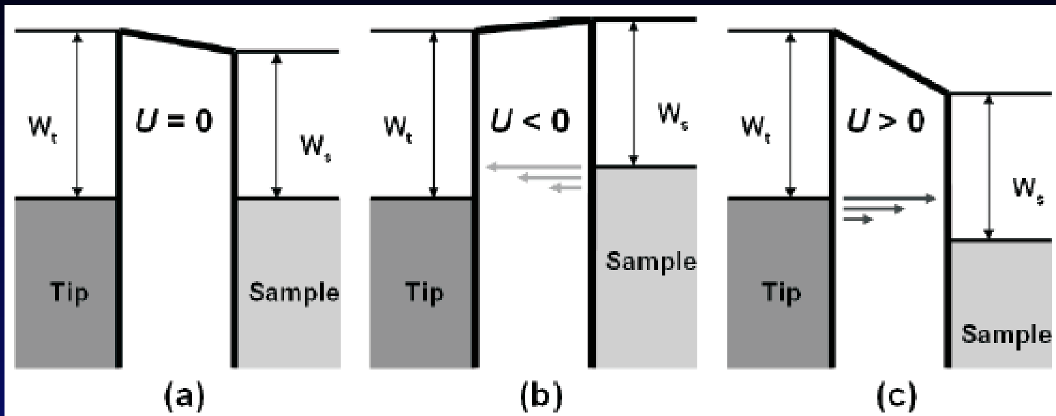

$$I \propto \int_0^{eU} \rho_s(E_F+\epsilon)\cdot\rho_t(E_F-eU+\epsilon)\cdot T(\epsilon,U,s)d\epsilon.$$

In the framework of a semi-classical WKB-approximation

$$T(E,U,s) \cong exp\left[-2\kappa(E,U,s)\right],$$

$$\kappa(E,U,s)=\sqrt{\frac{2m}{\hbar^2}(\bar{W}+\frac{eU}{2}-(E-E_{\|}))}.$$

$$\frac{dI}{dU}(U,s) \propto \rho_s(E_F+eU)\cdot\rho_t(E_F)\cdot T(eU,U,s)$$
$$+\int_0^{eU}\rho_s(E_F+\epsilon)\cdot\rho_t(E_F+\epsilon-eU)\cdot\frac{d}{dU}T(\epsilon,U,s)d\epsilon$$
$$+\int_0^{eU}\rho_s(E_F+\epsilon)\cdot T(\epsilon,U,s)\cdot\frac{d}{dU}\rho_t(E_F+\epsilon-eU)d\epsilon.$$

$+ R$ is the effective tunnel distance and $\bar{W}=(W_s+W_t)/2$ the average
ion. The decay constant $\kappa(\epsilon,U,k_{\|})$ becomes minimal at a certain energy
for states that have a vanishing wave vector parallel to the surface ($k_{\|}=0$).
urface Brillouin zone are more pronounced

In the first term, we have the LDOS $\rho_s(E_F+eU)$ of the sample. Assuming a constant or weakly varying LDOS ρ_t of the tip, the third term can be neglected. The second term mainly contributes at high bias voltage due to the increase of the transmission coefficient T at high bias voltages.

Scanning Tunneling Spectroscopy
Working Principle

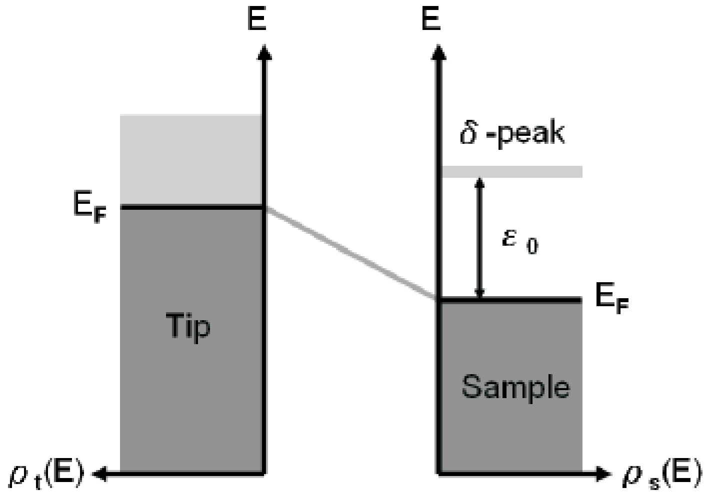

$$\frac{dI}{dU}(U) \propto \frac{1}{k_BT} \cdot \frac{1}{cosh^2(\frac{\epsilon_0+eU}{2k_BT})}.$$

$$\rho_s(\epsilon) = A\delta(\epsilon - \epsilon_0)$$

The differential tunnel conductance has a pronounced maximum at $-eU = \epsilon_0$ and the dI/dU signal can be approximated by a Gaussian line shape with full width at half maximum (FWHM) of $2\sigma = 3k_BT/e$.

$$\Delta E = 3k_BT.$$

A high energy resolution can only be achieved at low temperatures and an estimation leads to $\Delta E \approx 1$ meV for $T = 4$ K.

$$I = \frac{2\pi e}{\hbar} \int_{-\infty}^{\infty} [f(\epsilon + eU) - f(\epsilon)] \cdot |M_{\mu\nu}|^2 \cdot \rho_t(\epsilon + eU) \cdot \rho_s(\epsilon) d\epsilon.$$

$$\Delta E = \sqrt{\delta E_{therm}^2 + \delta E_{mod}^2} = \sqrt{(3k_BT)^2 + (2.5 \cdot eU_{mod})^2}.$$

Here U is the difference of the potentials of tip and sample, $\epsilon = E - E_F$ the relative energy of the electrode with respect to the Fermi level and $f(\epsilon) = [exp\,(\epsilon(k_BT)+1]^{-1}$ the Fermi-Dirac distribution. While looking at a small energy window, the tunnel matrix elements $M_{\mu\nu}$ are constant.

$$\frac{dI}{dU}(U) \propto |M_{\mu\nu}|^2 \cdot \rho_t \int_{-\infty}^{\infty} [\frac{(1/k_BT)exp\,[(\epsilon + eU)/k_BT]}{(exp\,[(\epsilon + eU)/k_BT] + 1)^2} \cdot \rho_s(\epsilon) d\epsilon.$$

Quantum World at Atomic Scale:
Spin-Polarized Scanning Tunneling Microscopy

Pin-Jui Hsu[1,2] (徐斌睿)

1. Institute of Applied Physics, University of Hamburg, Jungiusstrasse 11, D-20355 Hamburg, Germany
2. Department of Physics, National Tsing Hua University, No. 101, Section 2, Kuang-Fu Road, Hsinchu 30013, Taiwan

Fe-DL/ Rh(001)

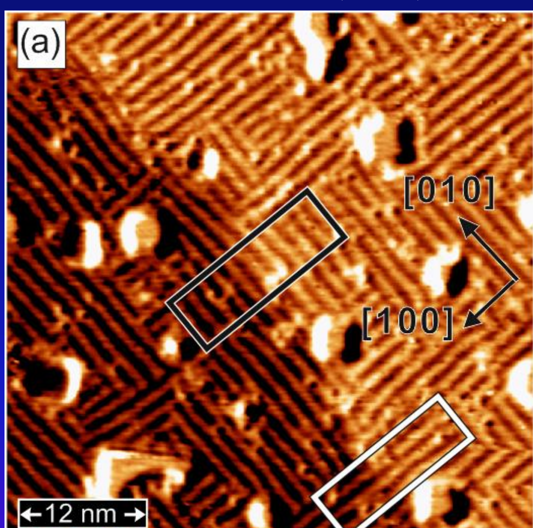

Fe-TL/ Ir(111)

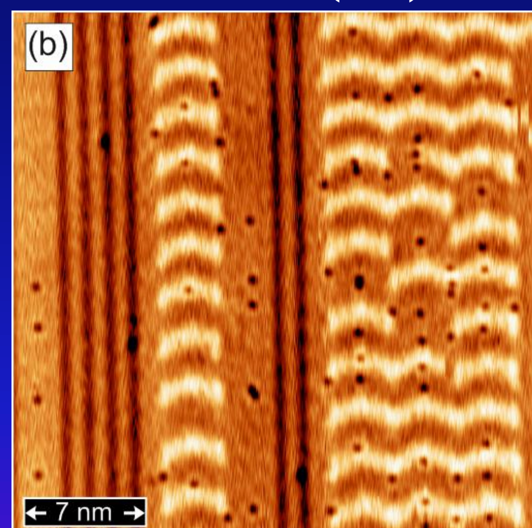

H/ Fe-DL/ Ir(111)

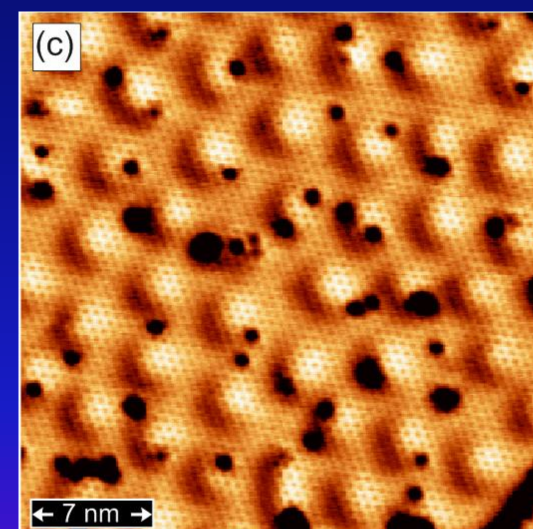

Working Principle

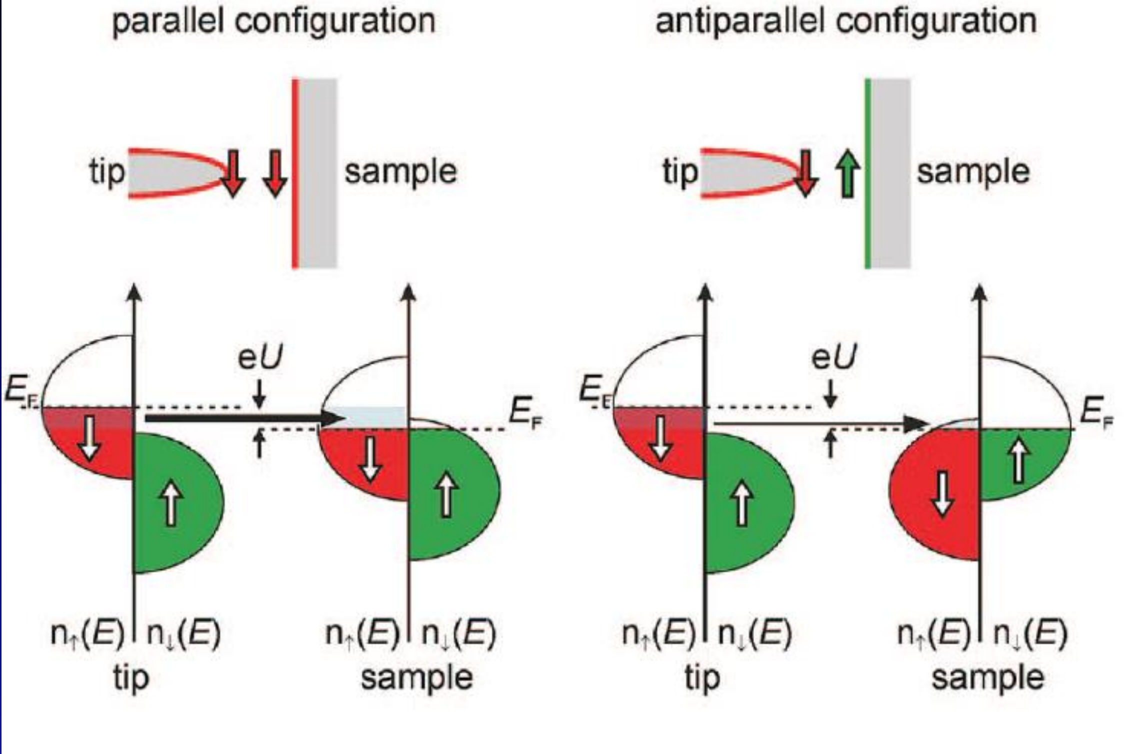

$$I_{SP}(U_0) \propto I_0 \cdot [1 + P_{tip} \cdot P_{sample} \cdot \cos(\vec{m}_{tip}, \vec{m}_{sample})]$$

$$n_t = n_t^\uparrow + n_t^\downarrow, \quad n_s = n_s^\uparrow + n_s^\downarrow$$

$$m_t = n_t^\uparrow - n_t^\downarrow, \quad m_s = n_s^\uparrow - n_s^\downarrow,$$

$$P_t = m_t / n_t, \quad P_s = m_s / n_s,$$

$$I(\vec{r}_0, U, \theta) = I_0(\vec{r}_0, U) + I_{sp}(\vec{r}_0, U, \theta) = \frac{4\pi^3 C^2 \hbar^3 e}{\kappa^2 m^2} [n_t \tilde{n}_s(\vec{r}_0, U) + \vec{m}_t \tilde{\vec{m}}_s(\vec{r}_0, U)]$$

where n_t is the non-spin-polarized LDOS at the tip apex, $\tilde{n}_S$ is the energy-integrated LDOS of the sample, and $\vec{m}_t$ and $\tilde{\vec{m}}_s$ are the corresponding vectors of the (energy-integrated) spin-polarized (or magnetic) LDOS

$$\tilde{\vec{m}}_s(\vec{r}_0, U) = \int^{eU} \vec{m}_s(\vec{r}_0, E) dE,$$

with

$$\vec{m}_s = \sum \delta(E_\mu - E) \Psi_\mu^S(\vec{r}_0) \sigma \Psi_\mu^S(\vec{r}_0).$$

Ψ_μ^S denotes the spinor of the sample wave function

$$\Psi_\mu^S = \begin{pmatrix} \Psi_{\mu\uparrow}^S \\ \Psi_{\mu\downarrow}^S \end{pmatrix}$$

and σ is Pauli's spin matrix. As an important result, the spin-dependent contribution I_{sp} to the total tunneling current is found to scale with the projection of $\tilde{\vec{m}}_s$ onto $\vec{m}_t$, and therefore with the cosine of the angle θ between the magnetization directions of the two electrodes, in agreement with the limiting case of vanishing applied bias voltage

Spin-Polarized STM
Working Principle

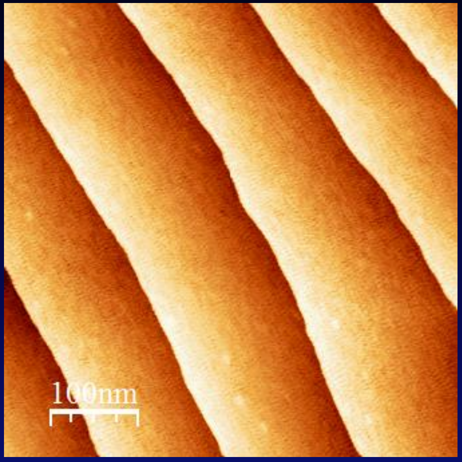

Topo.

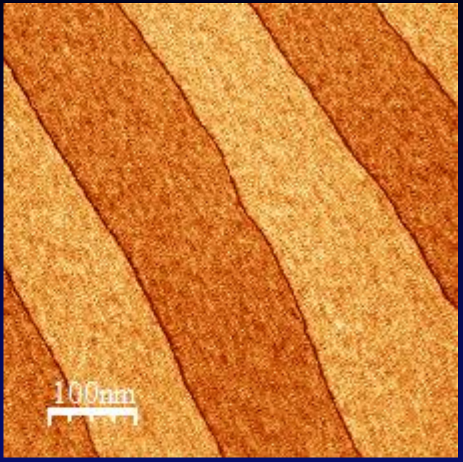

dI/dU Cr(001)

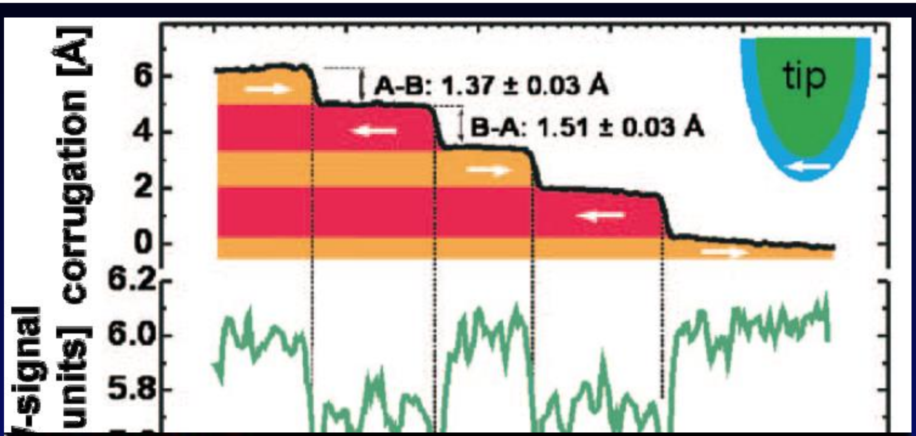

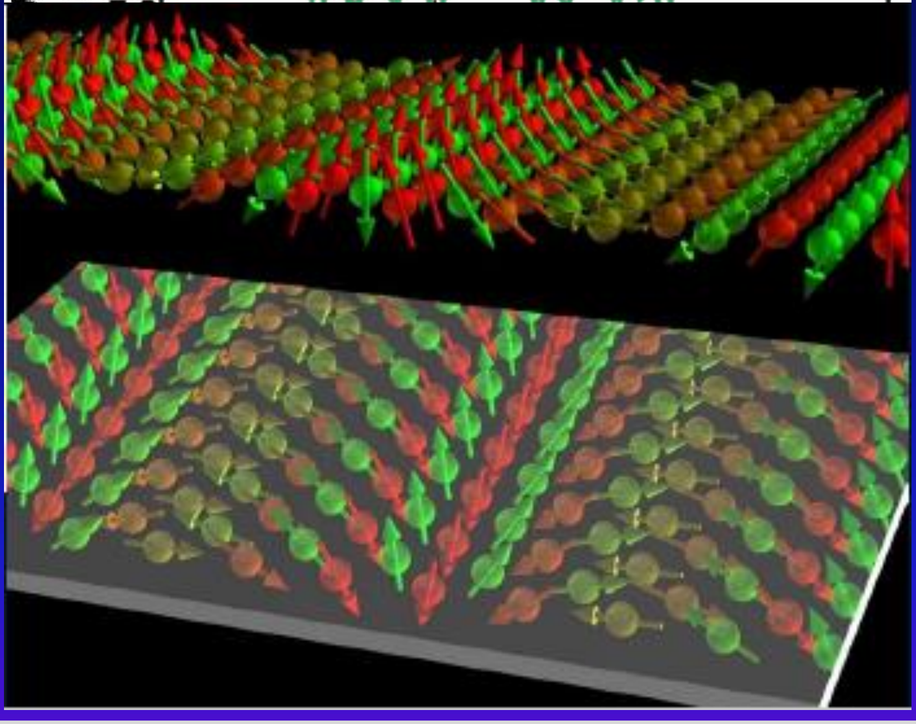

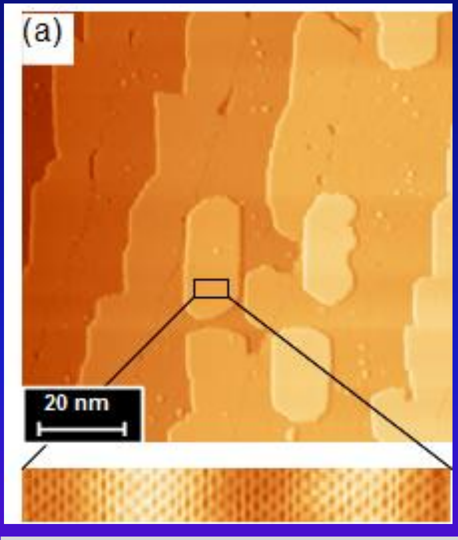

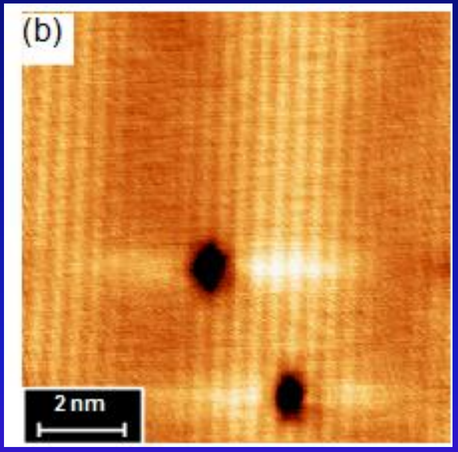

Mn/ W(110)

Magnetic Domain Wall

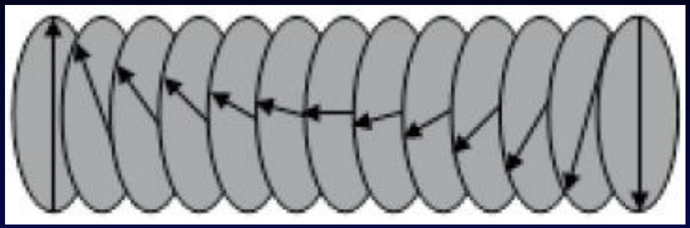

Bloch Wall

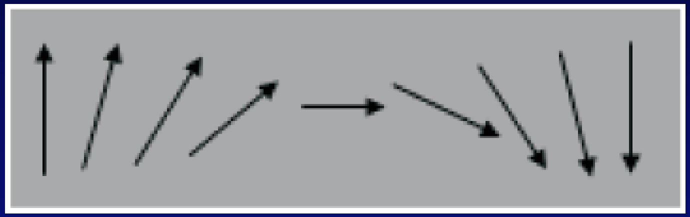

Neél Wall

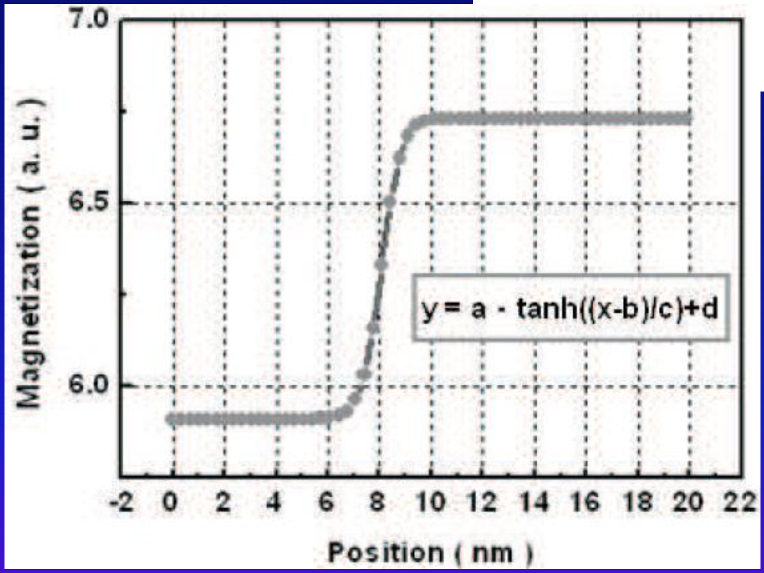

the exchange energy intends to make the wall wider in order to make the angle ϕ between adjacent spins become smaller and the anisotropy energy tries to make the wall thinner in order to reduce the number of spins aligning to non-easy axis directions. As a consequence of these two energy competition, there is a certain finite width and a certain spin structure of the magnetic domain wall.

Besides, the domain wall width can be expressed in the form of $\phi(x)$ dependence,

$$E_{ex} = E_{an} \Rightarrow J\frac{d\phi}{dx} = Kcos^2\phi$$

$$\Rightarrow \sqrt{\frac{K}{J}}dx = \frac{d\phi}{cos\phi}$$

$$\sqrt{\frac{K}{J}}x = tanh^{-1}(tan\phi)$$

Spin-Polarized STM

Magnetic Domain Wall, AFM Cr(001)

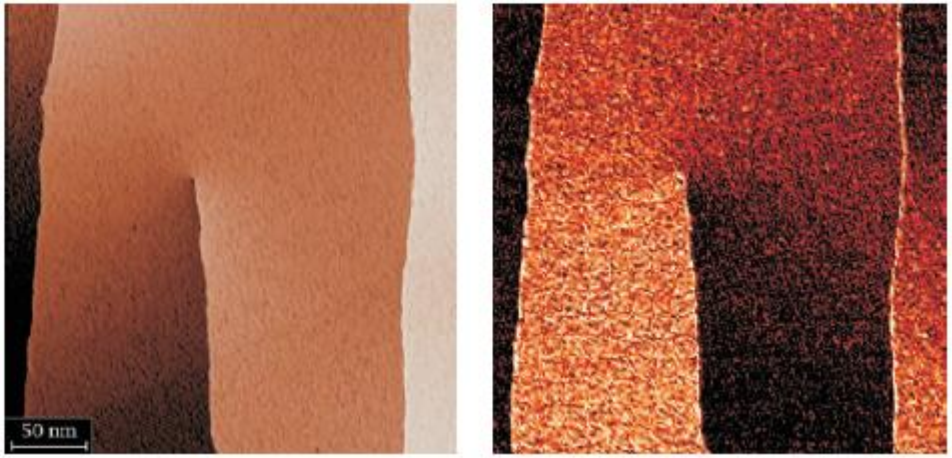

Cr(001)

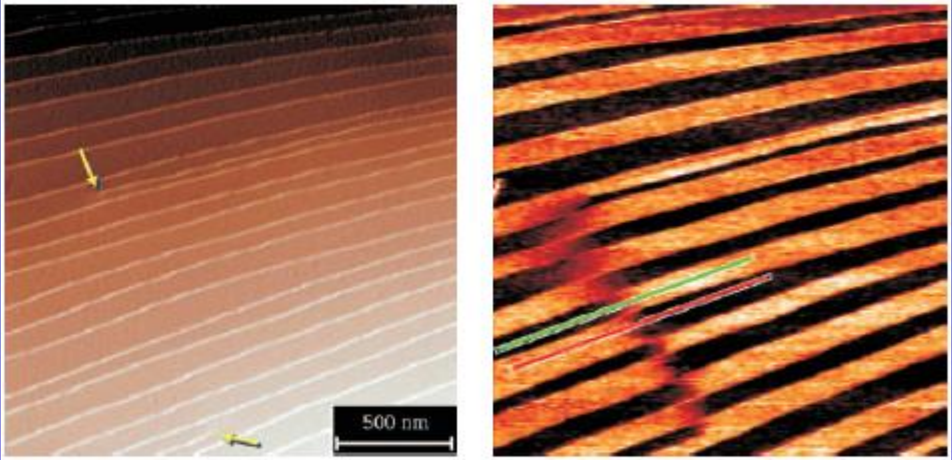

$$y(x) = y_0 + y_{sp} \tanh\left(\frac{x - x_0}{w/2}\right)$$

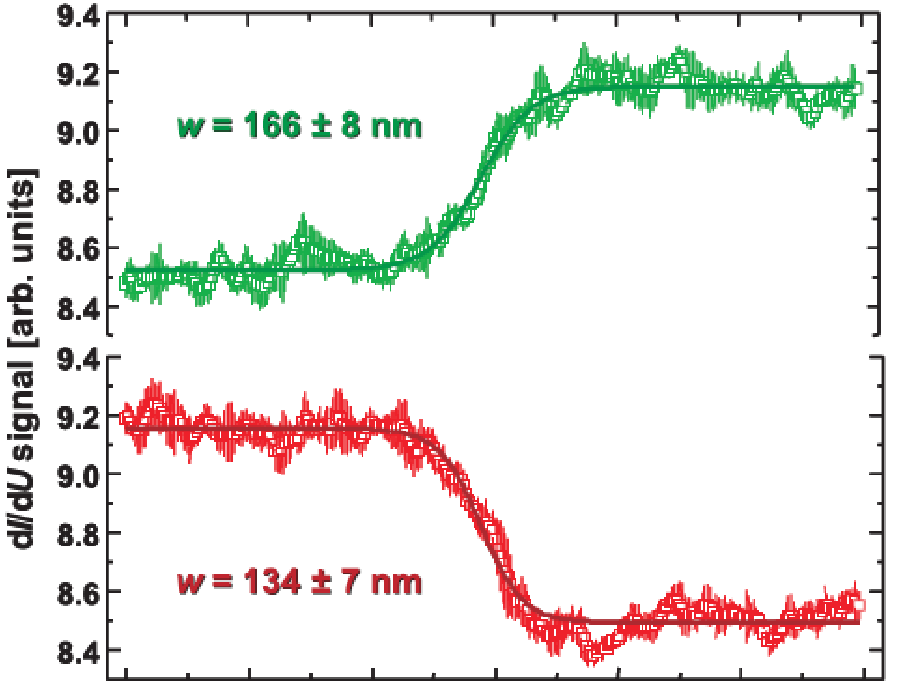

$w = 2\sqrt{A/k}$ the domain-wall width w is one-to-one determined by the ratio A/k, where A is the so-called exchange stiffness and k is the effective anisotropy energy density.

For instance, we may assume that $A_{\mathrm{Cr}} = 1 \times 10^{-11}$ J/m and $k_{\mathrm{Cr}} = 1.77 \times 10^3$ J/m^3. We believe that in consideration of the fact that the "Stoner parameter" I of Cr, $I_{\mathrm{Cr}} = 0.58$–0.68 eV,[23–25] is considerably smaller than $I_{\mathrm{Fe}} = 0.88$ eV,[26] this assumption for A_{Cr} is justified.

R. Wiesendanger, Rev. Mod. Phys., 81, 1495 (2009)

Spin-Polarized STM

Magnetic Domain Wall, FM Fe-DL/W(110)

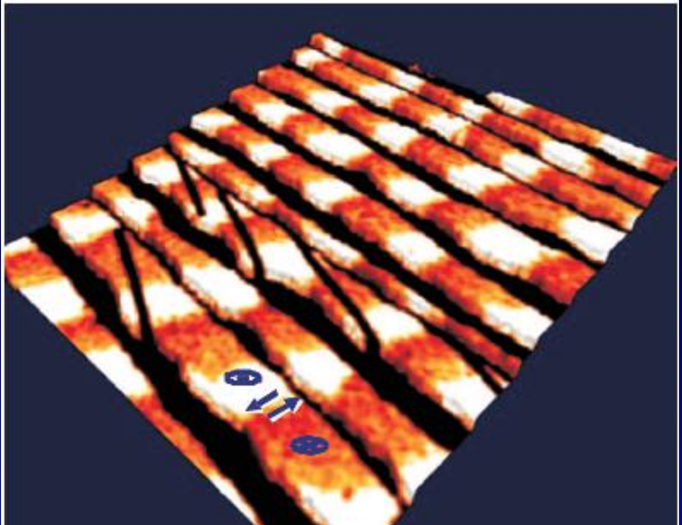

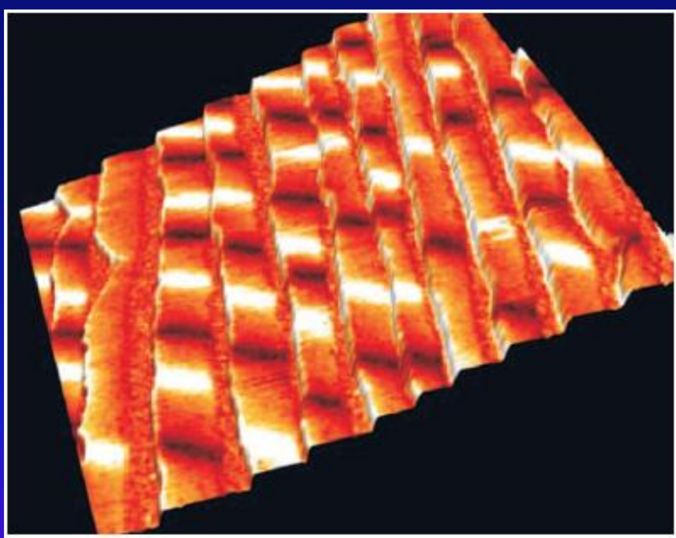

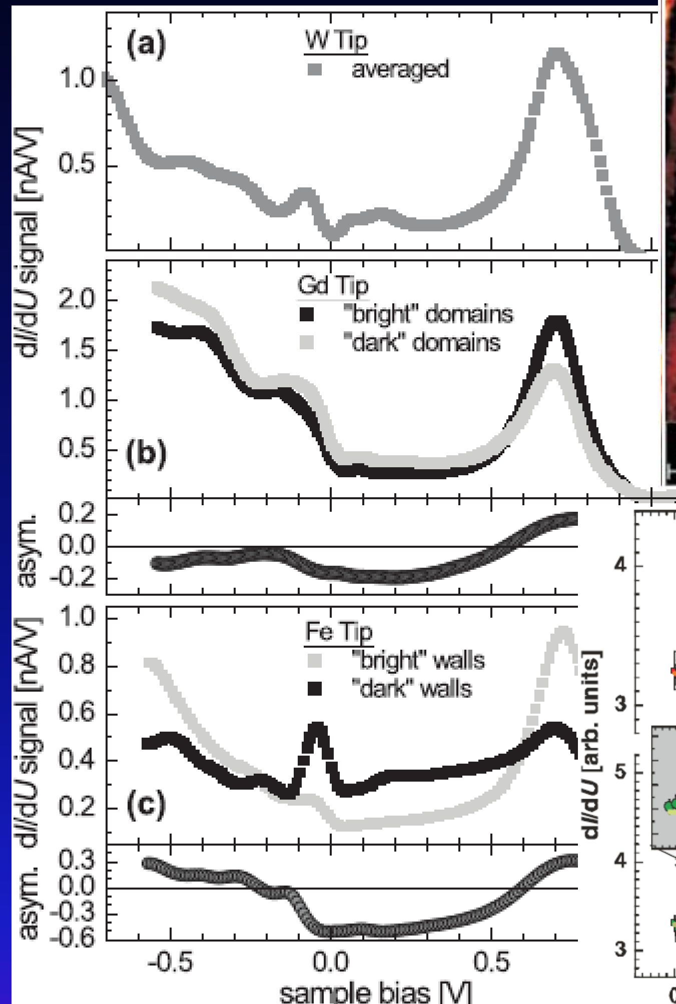

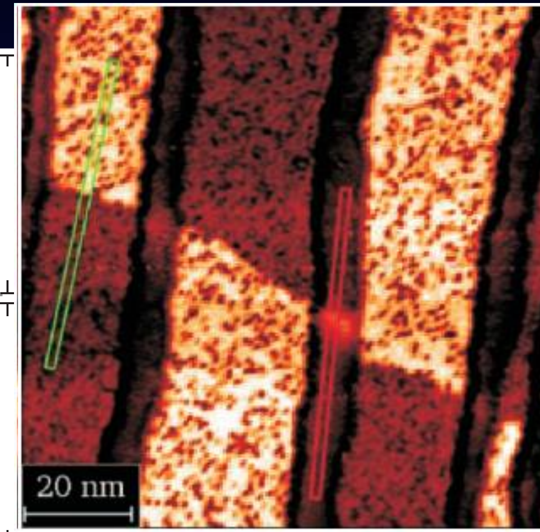

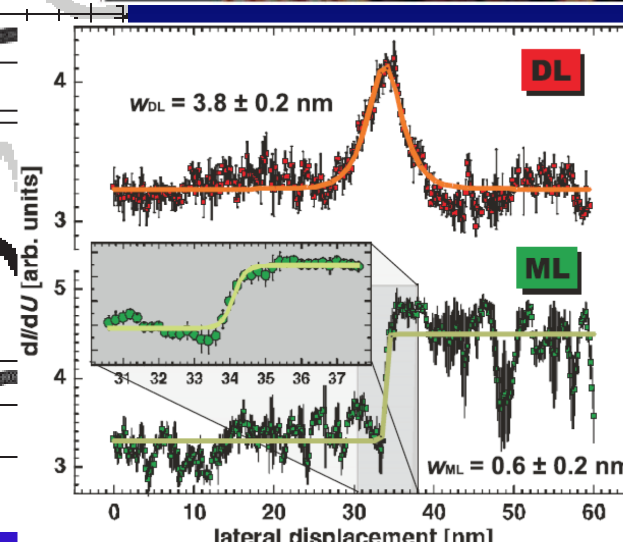

R. Wiesendanger, Rev. Mod. Phys., 81, 1495 (2009)

Spin-Polarized STM

Magnetic Domain Wall, FM Fe-DL/W(110)

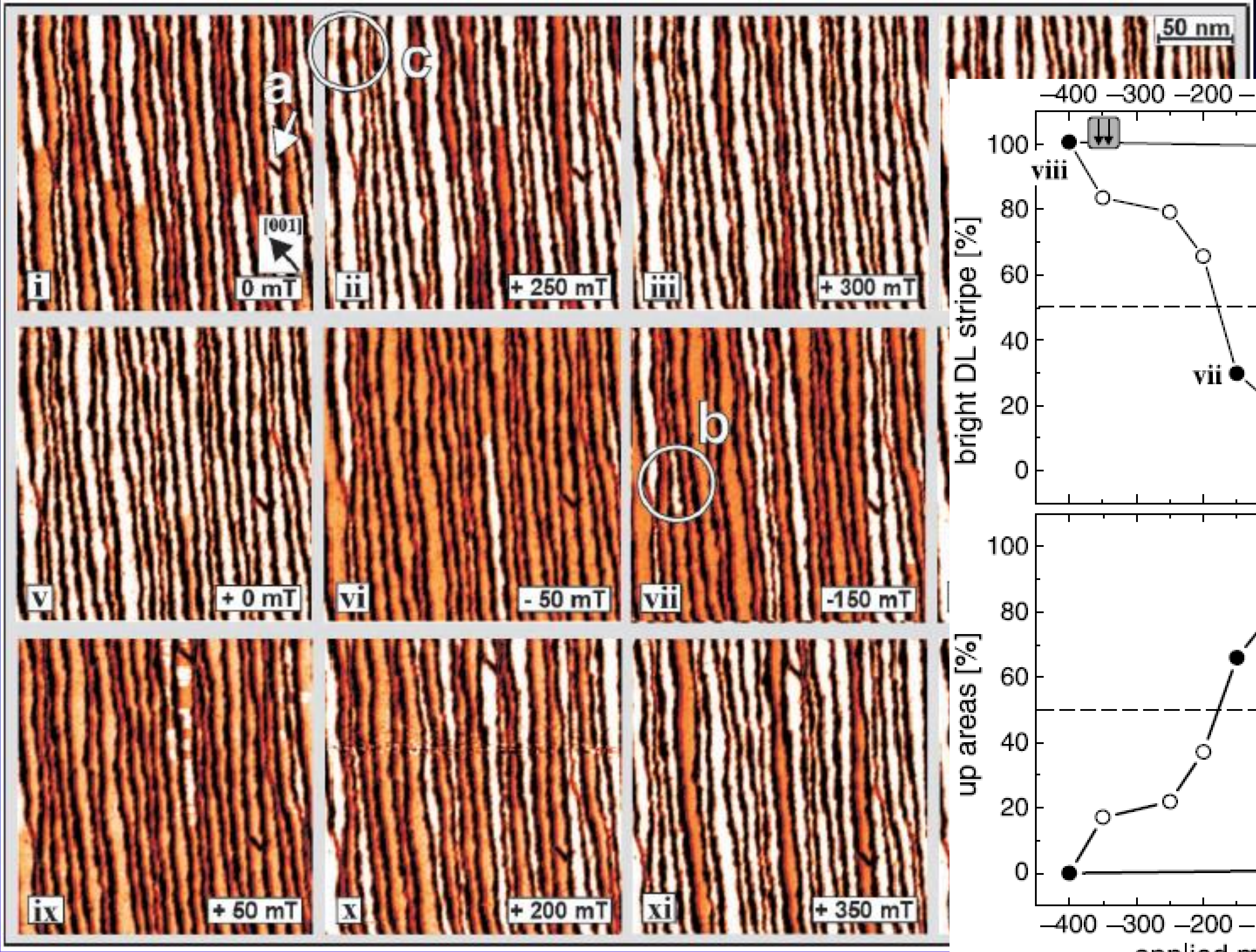

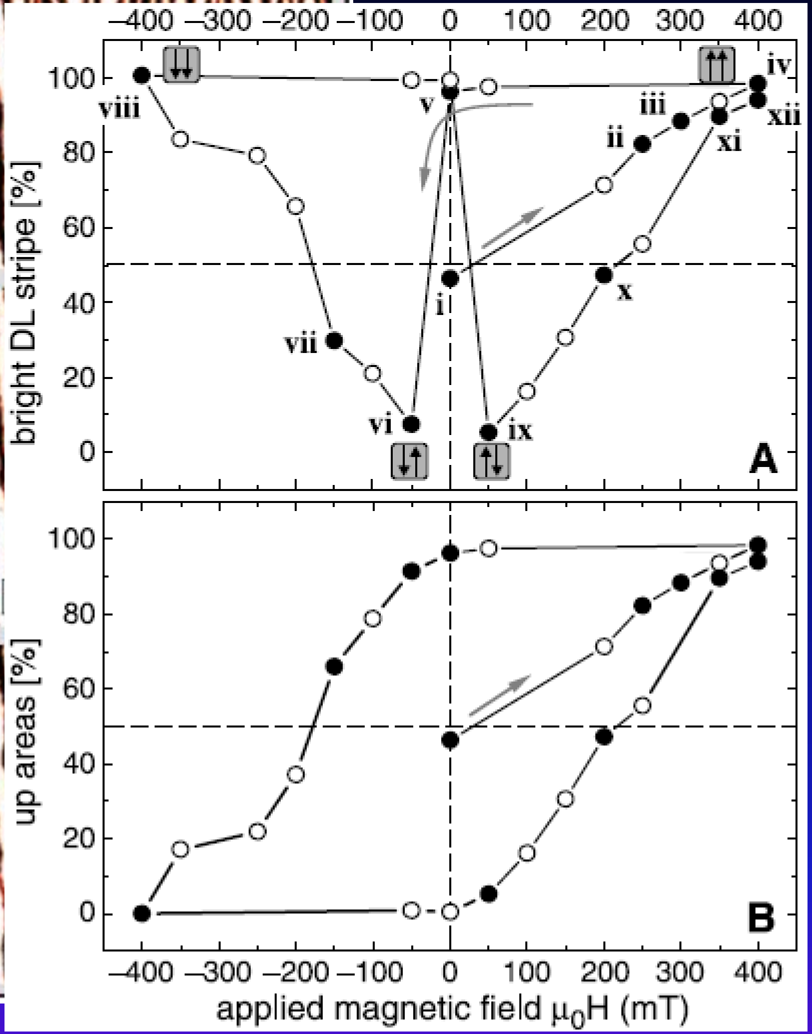

O. Pietzsch *et al*., Science, 292, 2053 (2001)

Spin-polarized States

Spin-polarized Surface State, FM Co-DL/Cu(111)

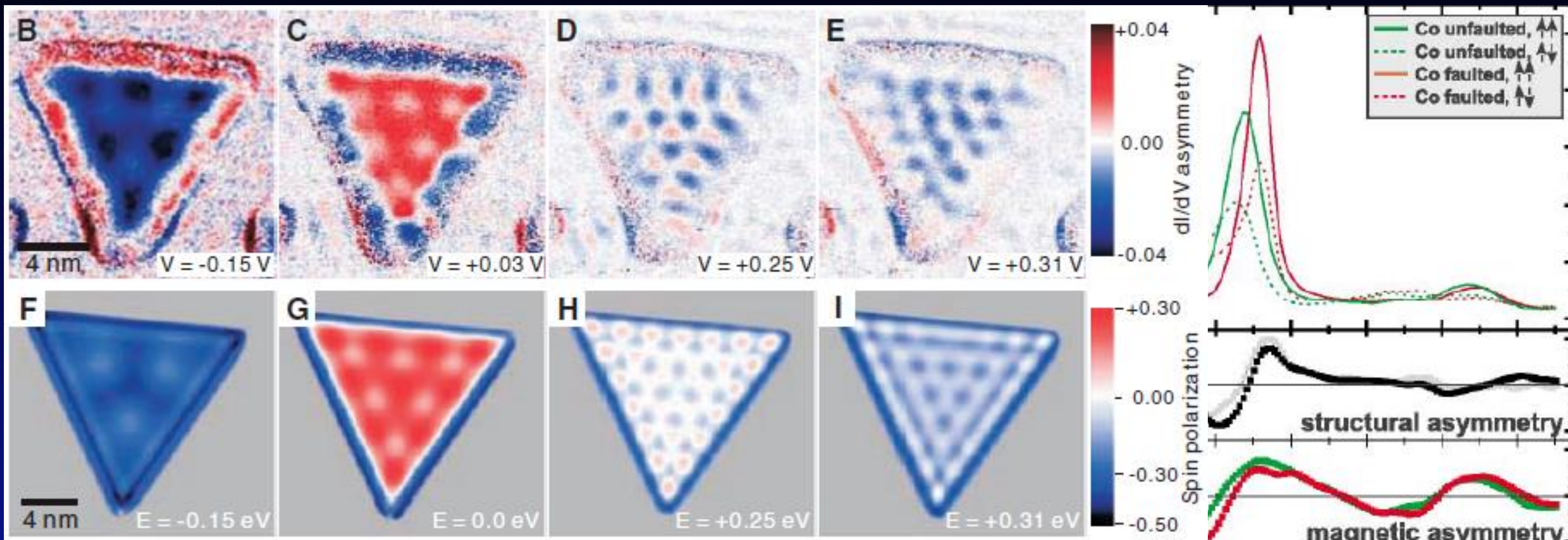

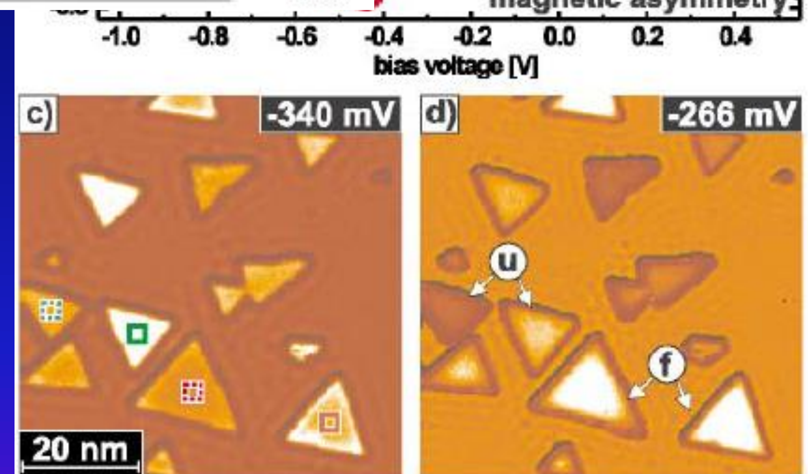

L. Diekhöner *et al*., Phys. Rev. Lett., 90, 236801 (2003)

O. Pietzsch *et al*., Phys. Rev. Lett., 92, 057202 (2004)

H. Oka *et al*., Science, 327, 843 (2010)

Spin-Polarized STM

Atomic Spin Resolution, AFM Fe-ML/W(001)

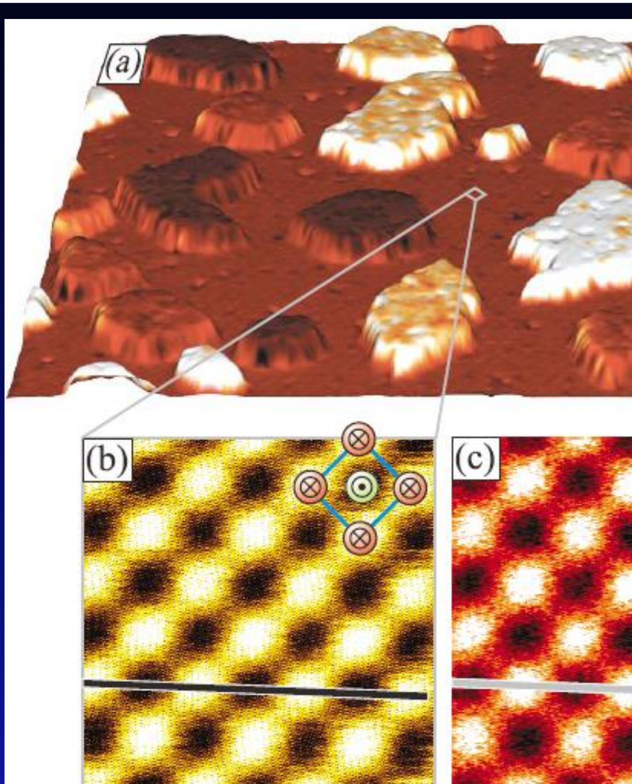

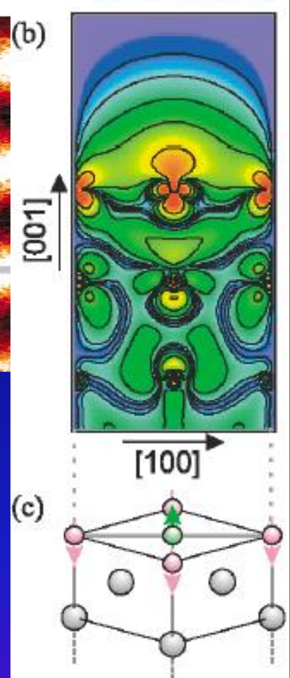

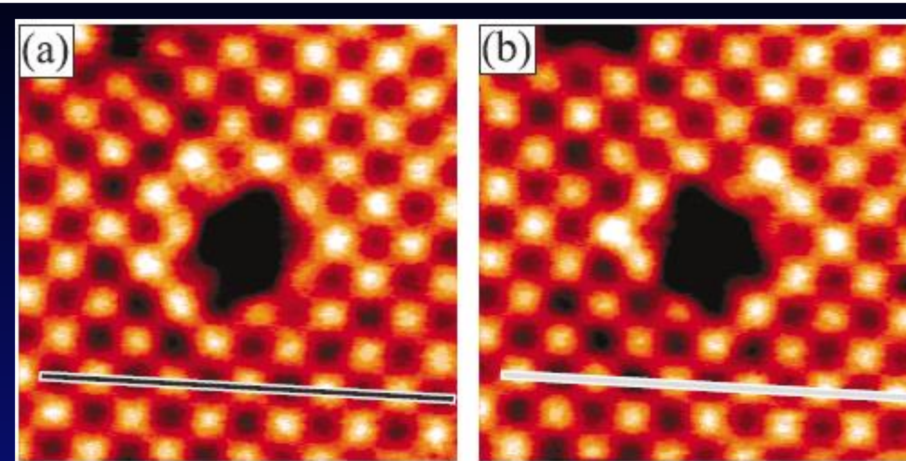

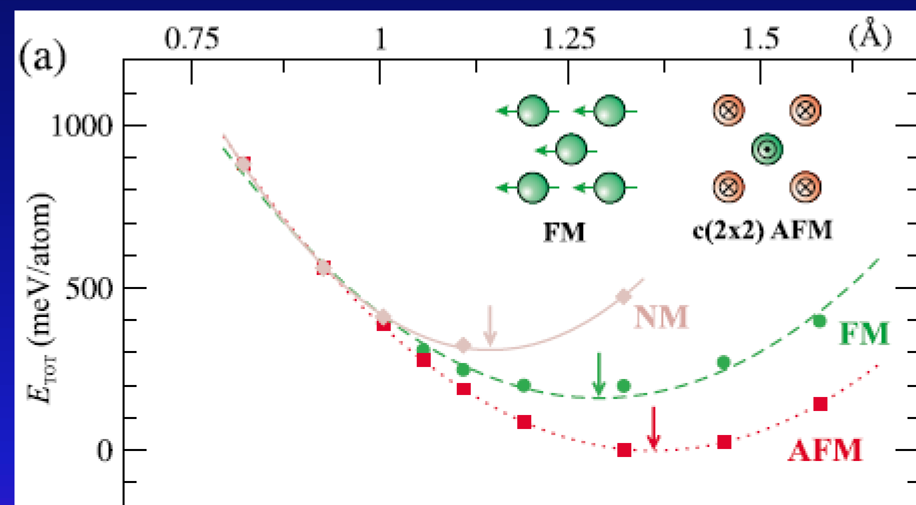

A. Kubetzka *et al*., Phys. Rev. Lett., 90, 236801 (2003)

Spin-Polarized STM

Atomic Spin Resolution, AFM Mn-ML/W(110)

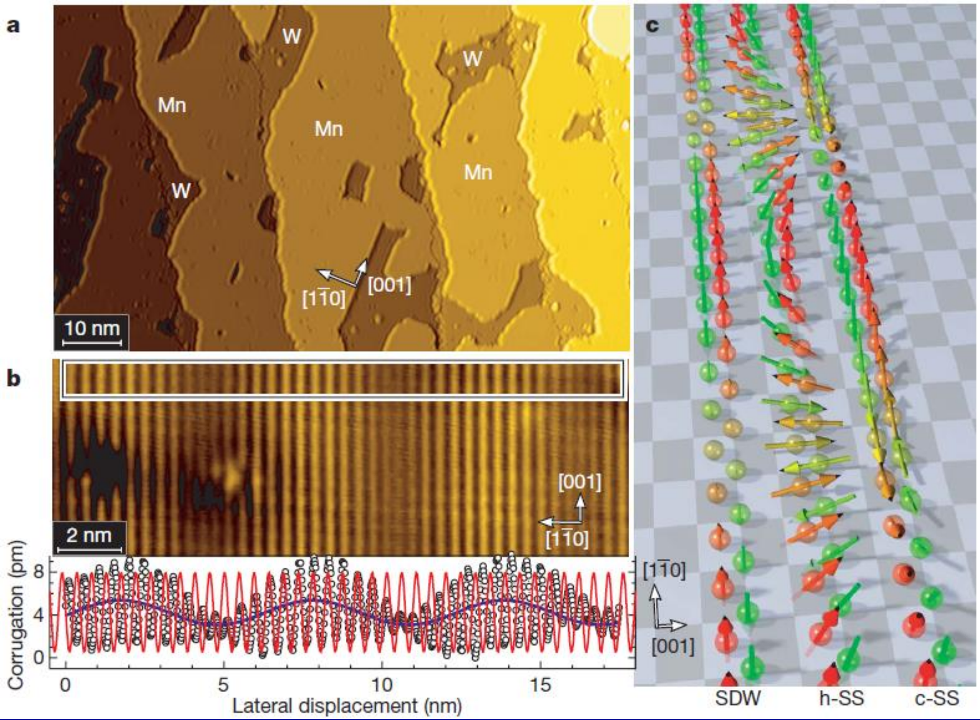

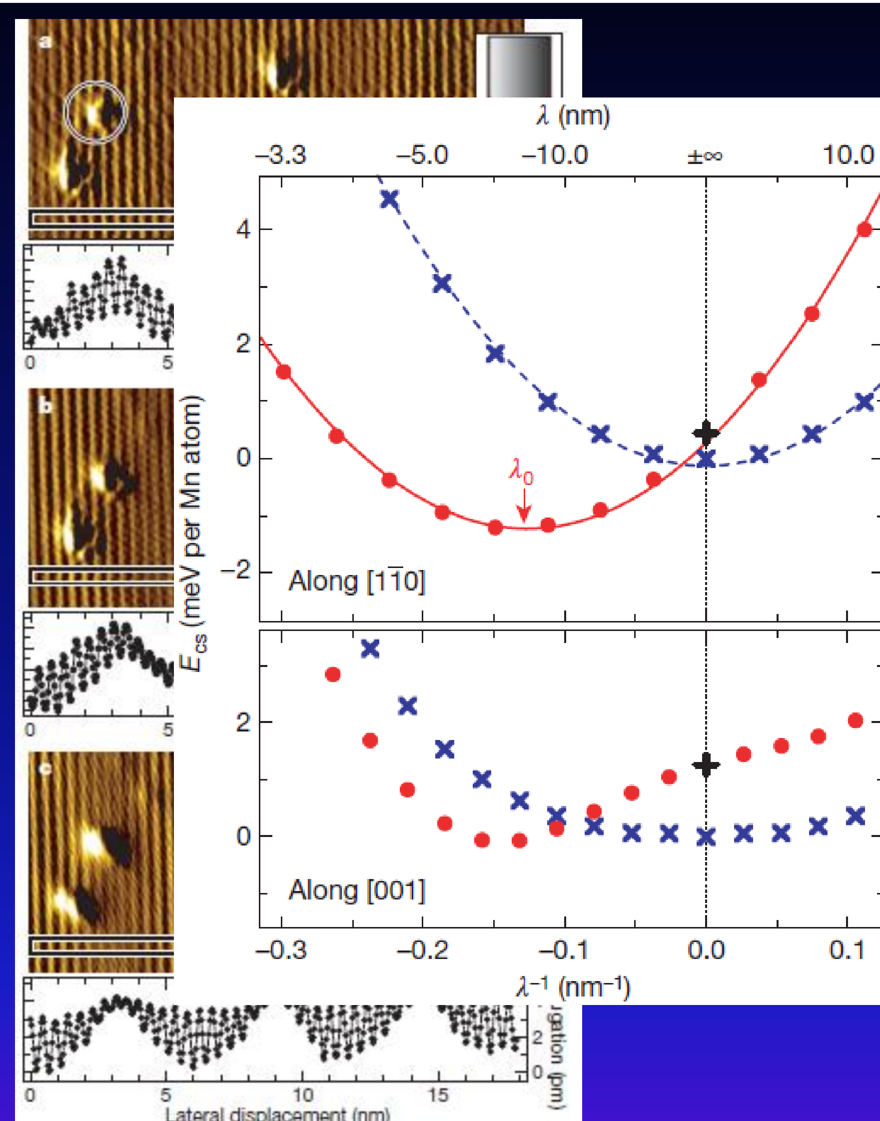

This is the Dzyaloshinskii–Moriya interaction[3,4], DMI,

$$E_{DM} = \sum_{i,j} \mathbf{D}_{ij} \cdot (\mathbf{S}_i \times \mathbf{S}_j)$$

M. Bode *et al*., Nature, 447, 190 (2007)

Magnetic Skyrmion

Dzyaloshinsky-Moriya Interaction

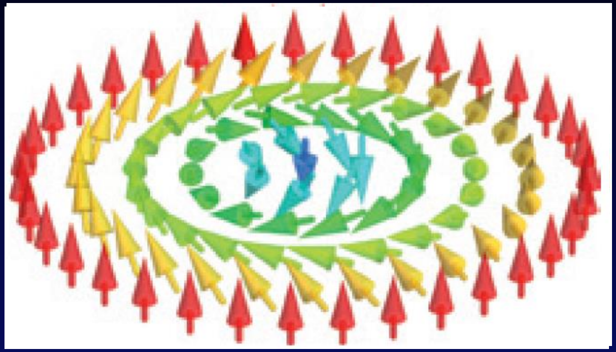

$$E_{DM} = -\sum_{ij} \mathbf{D}_{ij}\left(\mathbf{S}_i \times \mathbf{S}_j\right)$$

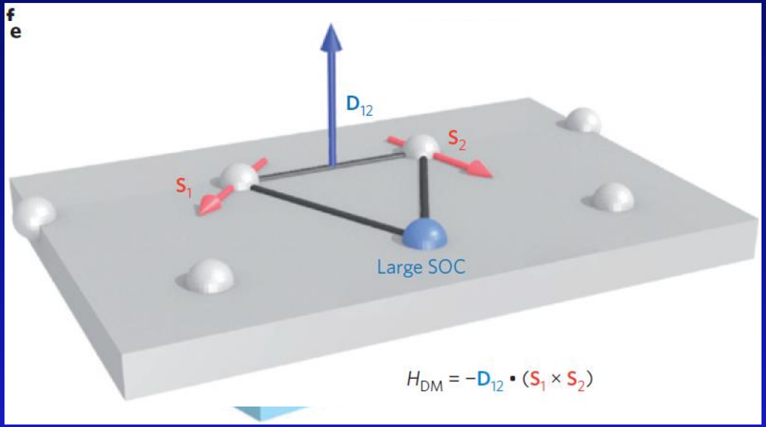

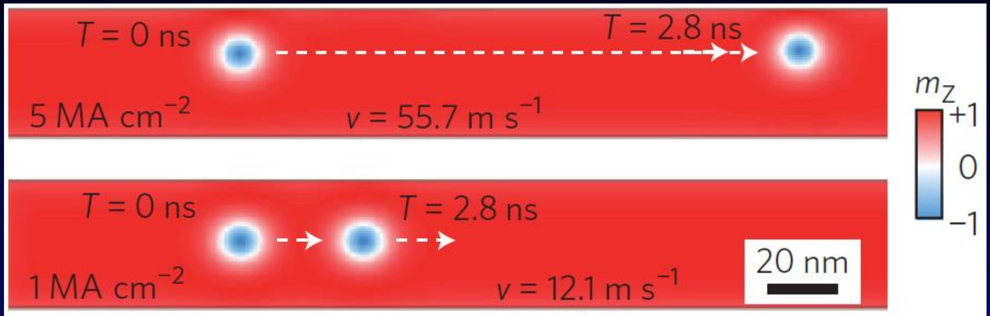

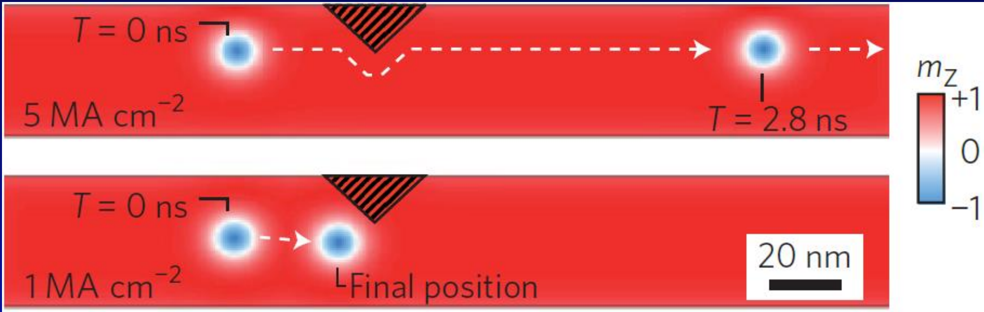

- DMI has the dominant contributions to formation of magnetic skyrmion spin texture.

- The current density required to move skyrmions has 5~6 order of magnitudes smaller than DW movement.
- Non-trivial topology and lower depinning currents lead to low energy consumption.

A, Fert, V. Cros, and J. Sampaio, Nature Nano., 8, 152 (2013)

Spin-Polarized STM

Magnetic Phase transition, Magnetic Skyrmions

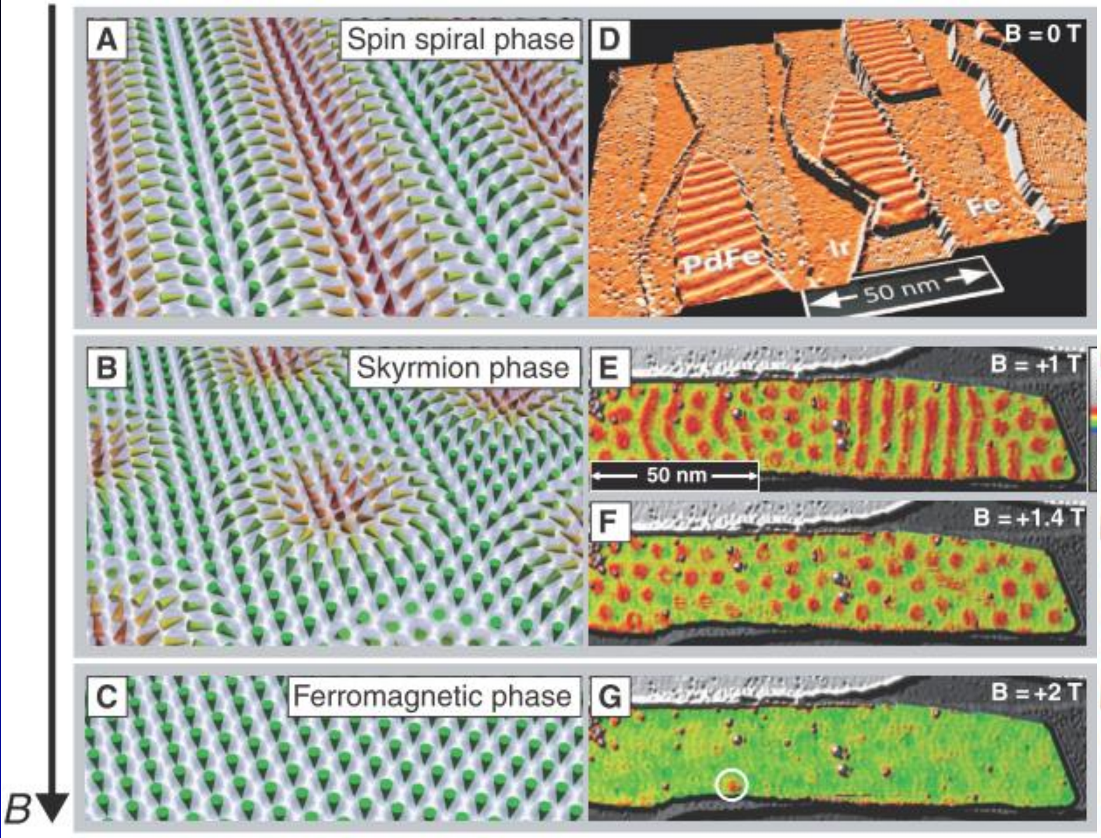

N. Romming *et al*., Science, 341, 636 (2013)

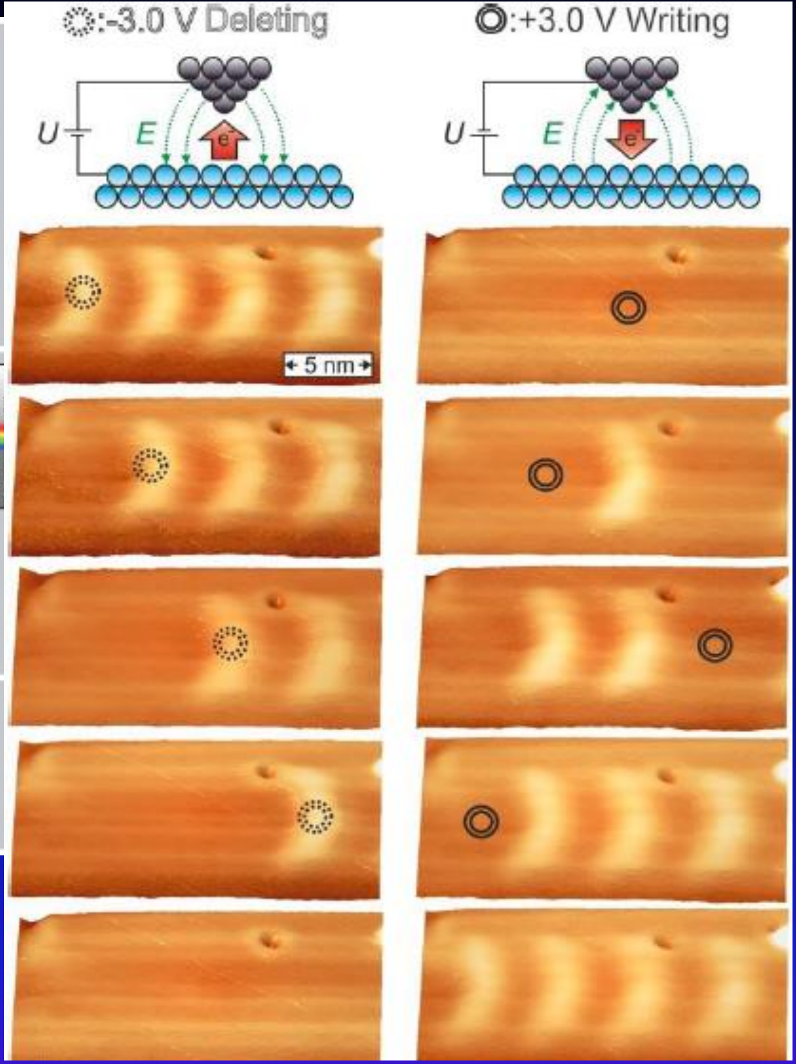

P. J. Hsu *et al*., Nat. Nano., 12, 123 (2017)

AFM skyrmion; Antiskyrmion; $|Q| > 1$

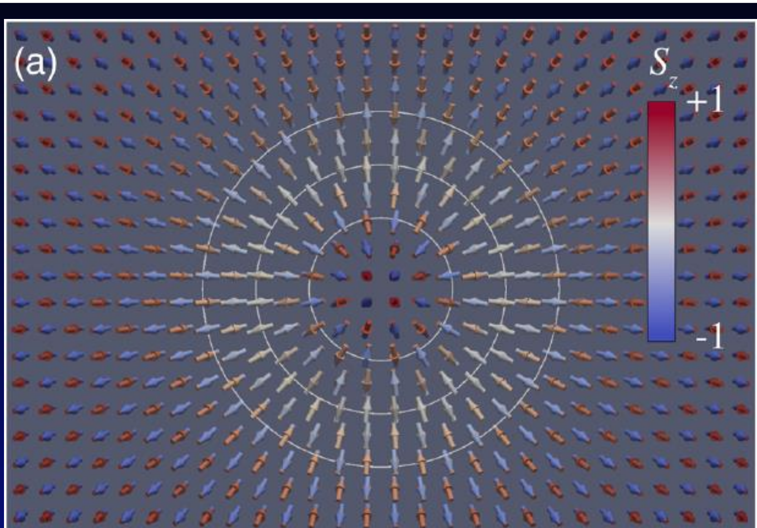

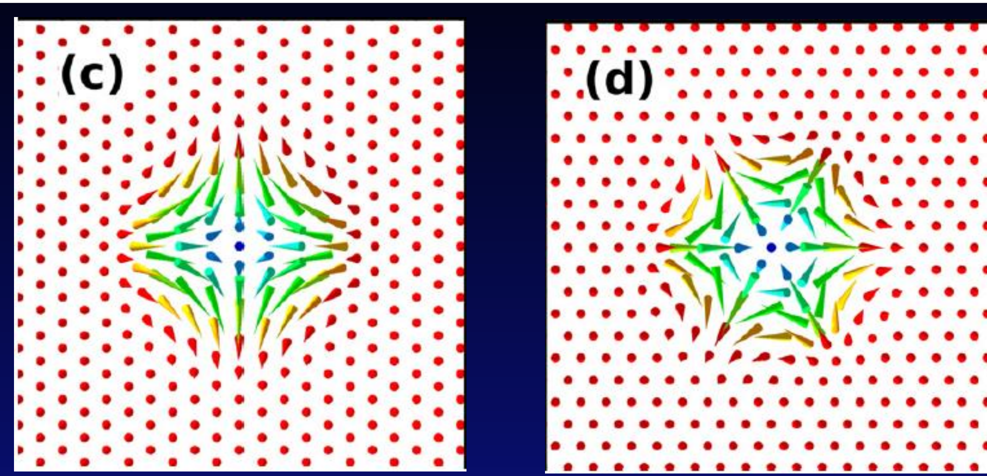

B. Dupé, C. N. Kruse, T. Dornheim, and S. Heinze, New. J. Phys., 18, 055015 (2016)

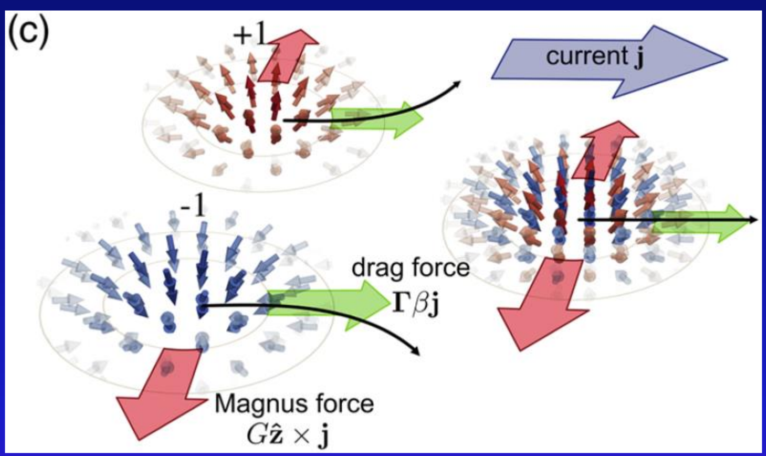

J, Barker, and O. A. Tretiakov, Phys. Rev. Lett., 116, 147203 (2016)

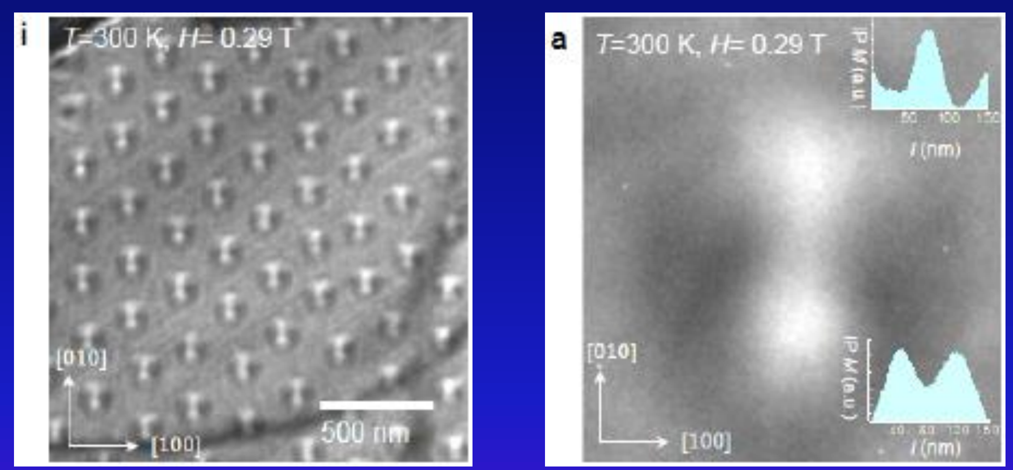

A. K. Nayak, V. Kumar, P. Werner, E. Pippel, R. Sahoo, F. Damay, U. K. Roßler, C. Felser, and S. P. Parkin, Nature, 548, 561 (2017)

Single-Atom Magnetometry
SP-STM/STS with B field, Co atoms/Pt(111)

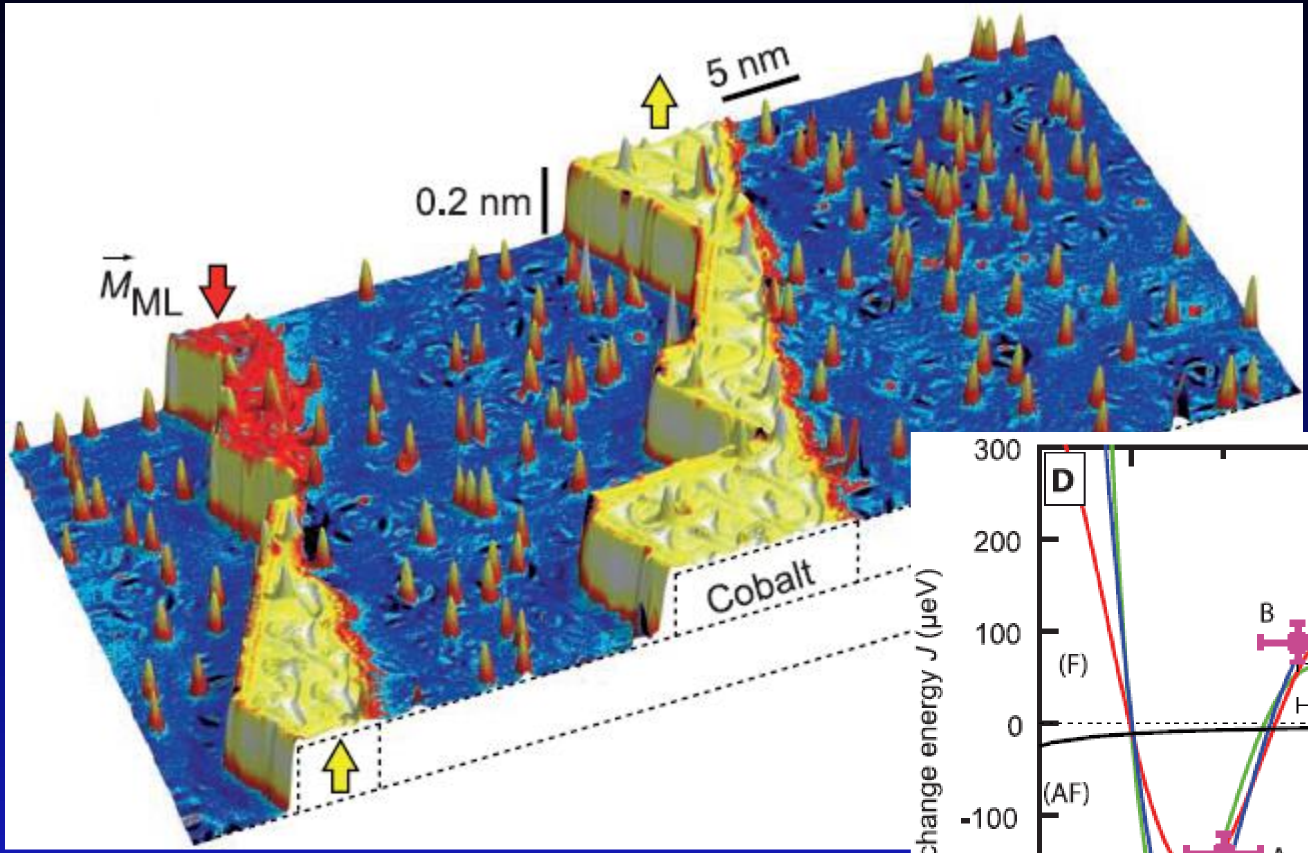

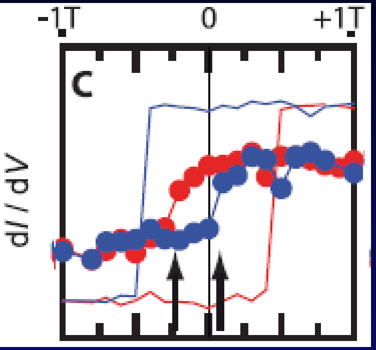

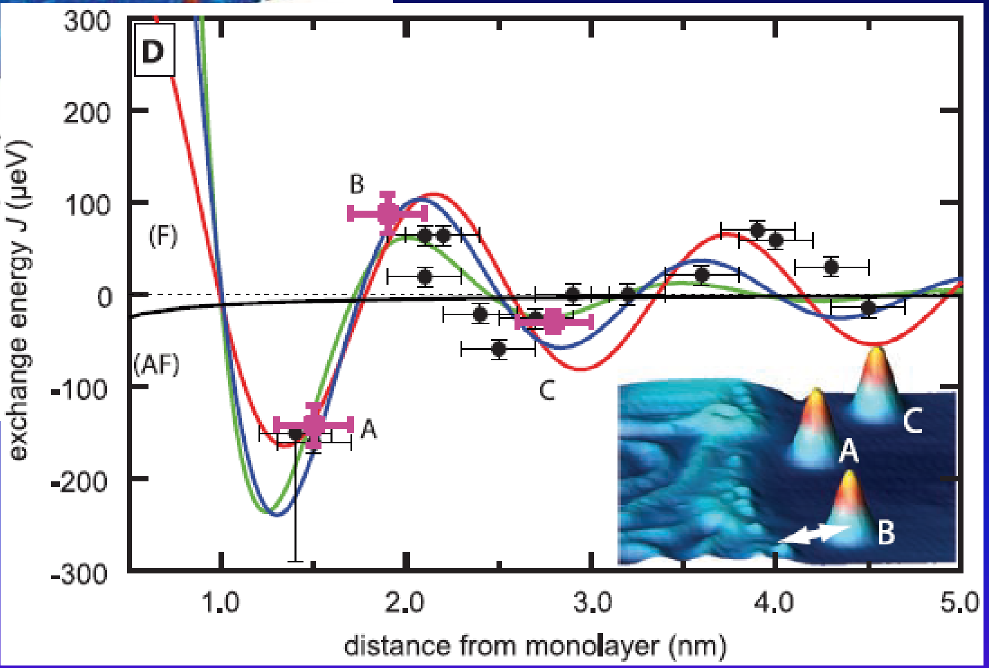

$$J(d) = J_0 \cdot \cos(2 \cdot k_F \cdot d)/(2 \cdot k_F \cdot d)^D$$

F. Meier *et al.*, Science, 320, 82 (2008)

Single-Atom Magnetometry

Moving Single Atoms

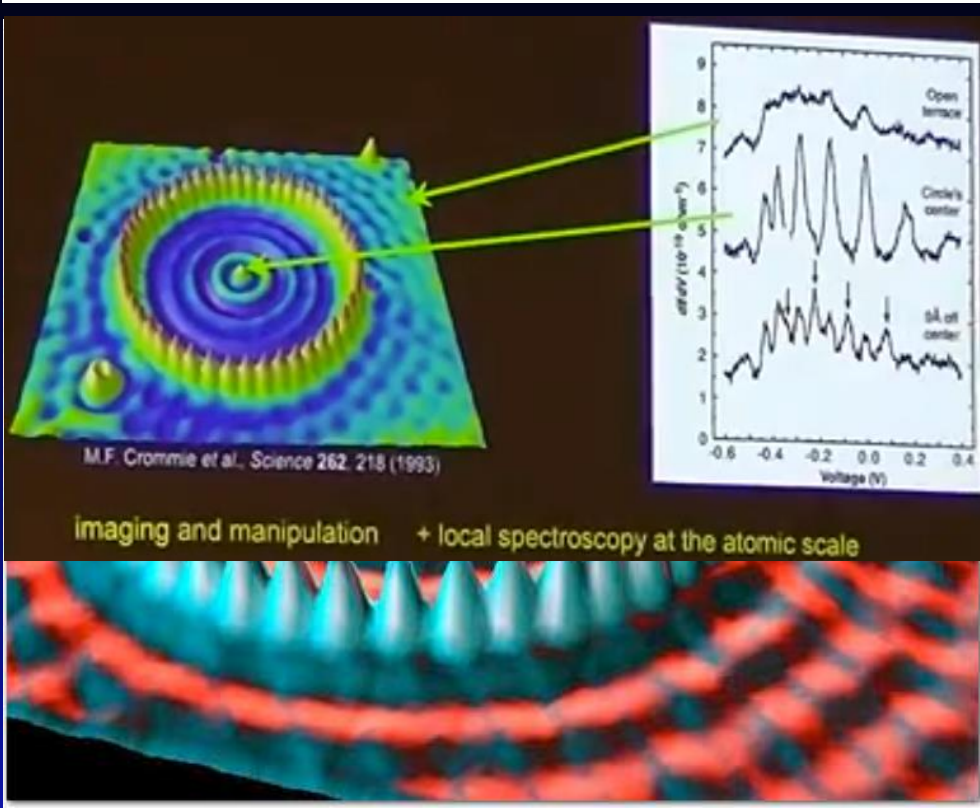

75 Fe/ Cu(111)

M. F. Crommie *et al*., Science, 262, 218 (1993)

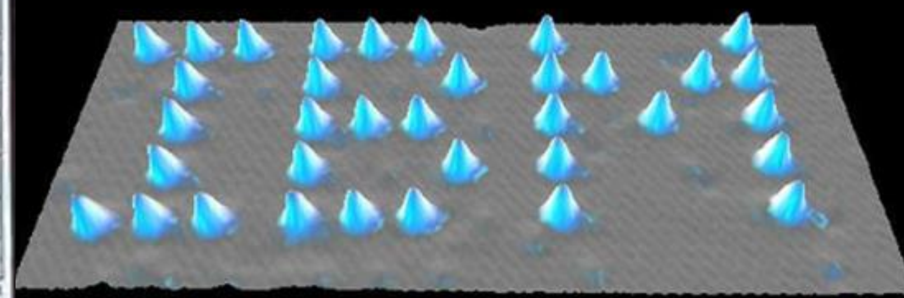

34 Xe / Ni(110)

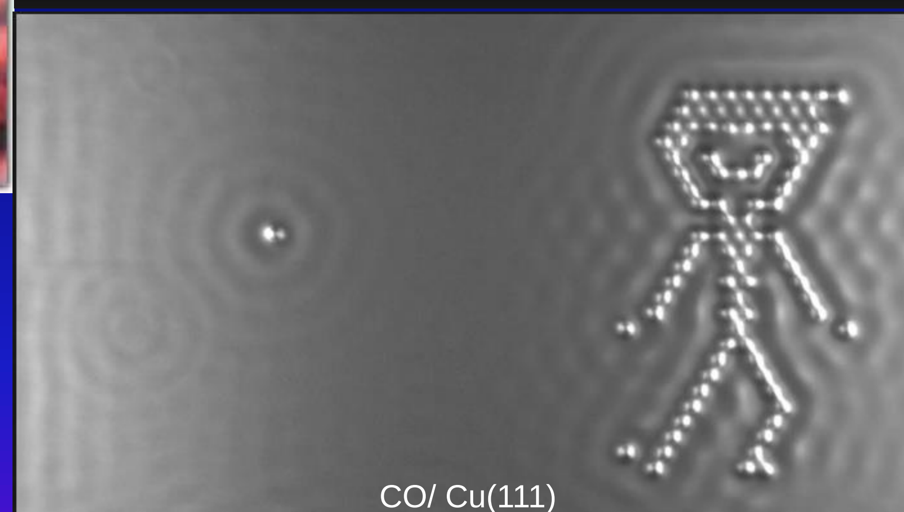

CO/ Cu(111)

Single-Atom Magnetometry

Moving Single Atoms, Lateral Movement

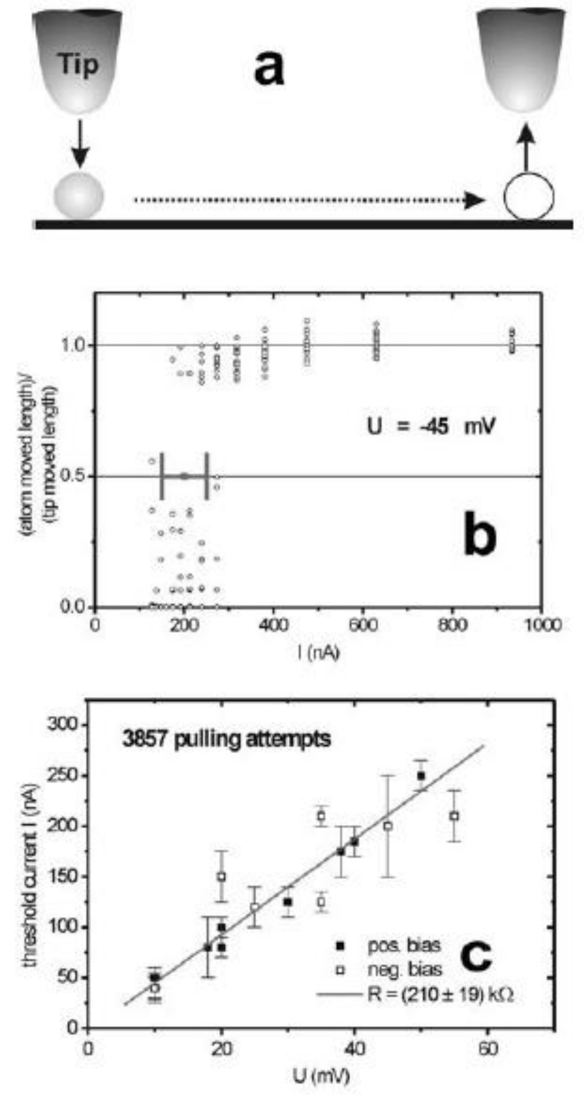

In case of a silver atom manipulation on Ag(111), R_t = 184 ± 8 kΩ is necessary[37]. This R_t corresponds to a distance of 1.9 Å between the edges of van-der-Waals radii of tip-apex and manipulated atom. Since the atomic orbitals of tip-apex and manipulated atoms are overlapping at this distance, a weak chemical bond is formed. The attractive force used in the "pulling" manipulation is originated from this chemical nature of interaction.

Three basic LM modes, "pushing", "pulling" and "sliding", has been distinguished[5]. In the "pulling" mode, the atom follows the tip due to an attractive tip-atom interaction. In the "pushing" mode, a repulsive tip-atom interaction drives the atom to move in front of the tip. In the "sliding" mode, the atom is virtually bound to or trapped under the tip and it moves smoothly across the surface together with the tip.

S. W. Hla, J. Vac. Sci. & Tech. B, 23, 1351 (2005)

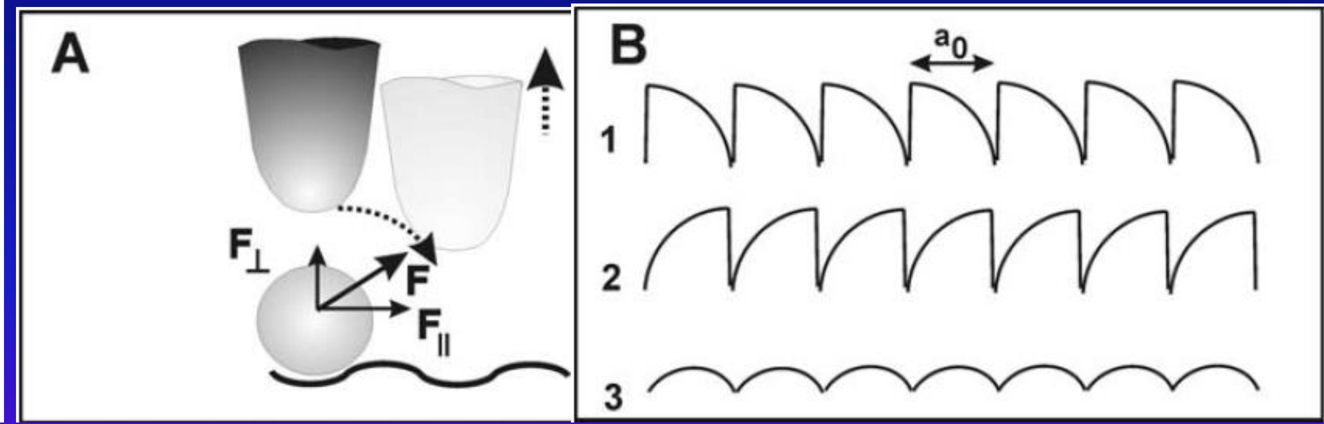

Single-Atom Magnetometry

Moving Single Atoms, Vertical Manipulation

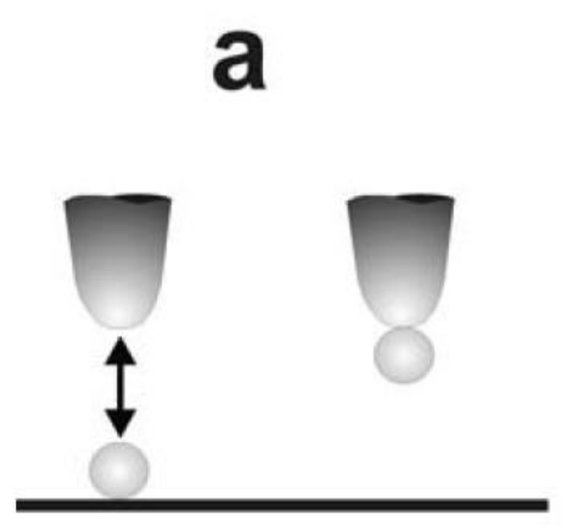

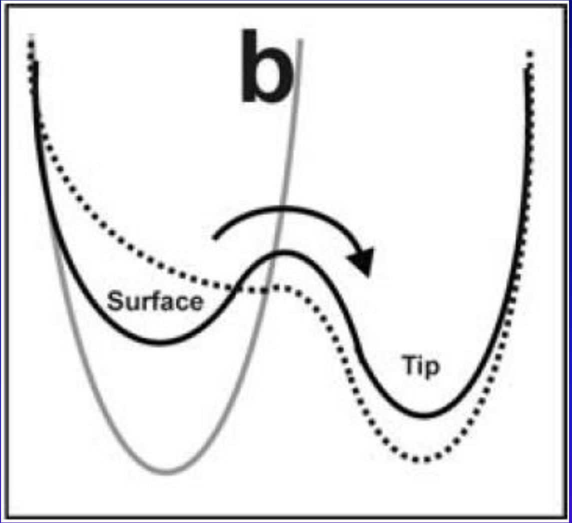

Fig. 8. Vertical manipulation (VM). (a) A schematic drawing shows the process. (b) The double-potential well model. The black (solid), dash and gray curves represent the shape of potentials (the well shapes are working assumptions) at an image-height, under an electric field, and at the tip-atom/molecule contact, respectively.

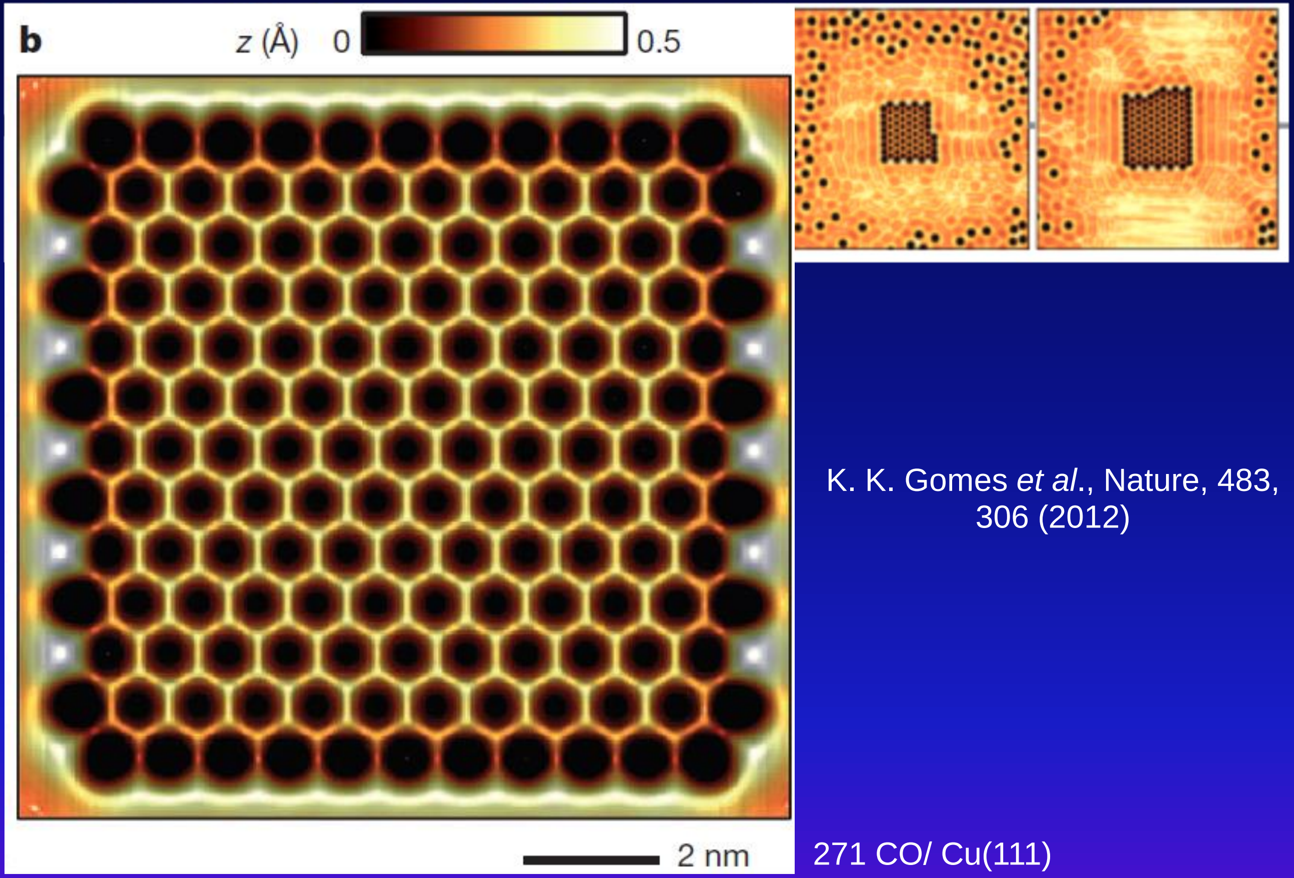

K. K. Gomes *et al.*, Nature, 483, 306 (2012)

271 CO/ Cu(111)

Spin Logic Operations

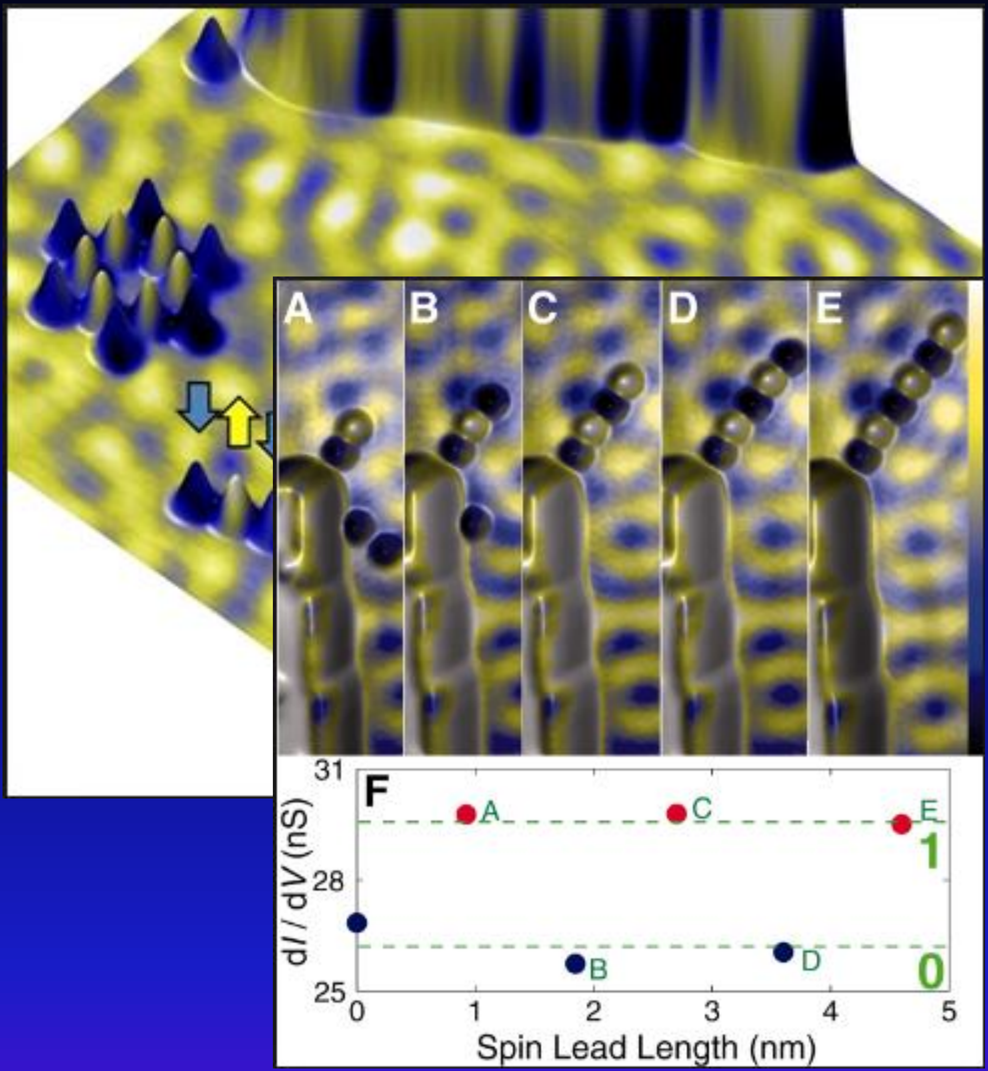

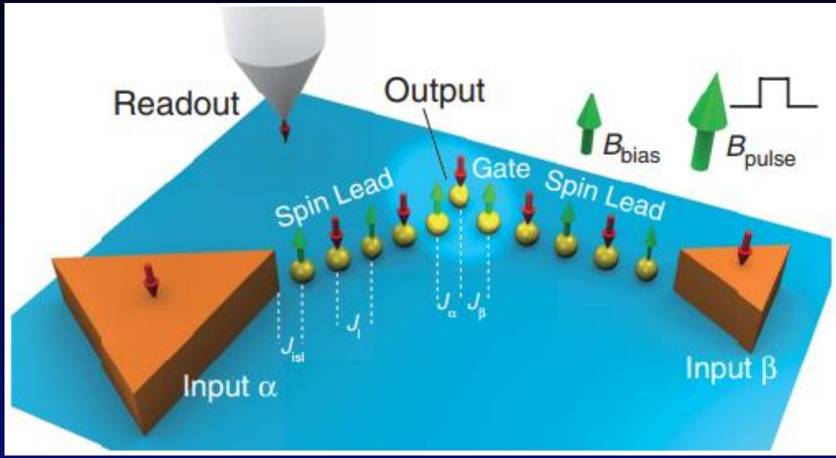

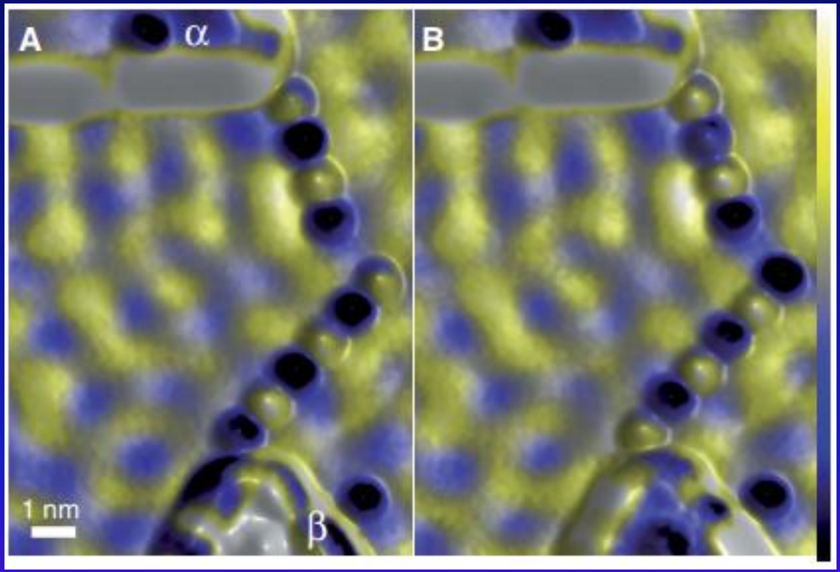

A. Khajetoorians *et al*., Science, 332, 1062 (2011)

SP-STM with Time Resolution

Single-Atom Dynamics

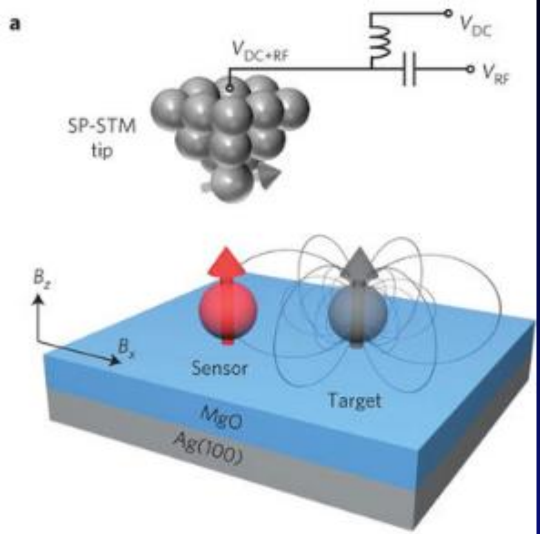

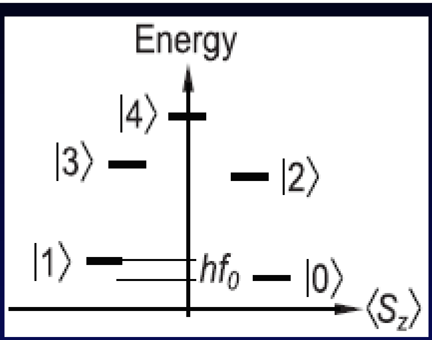

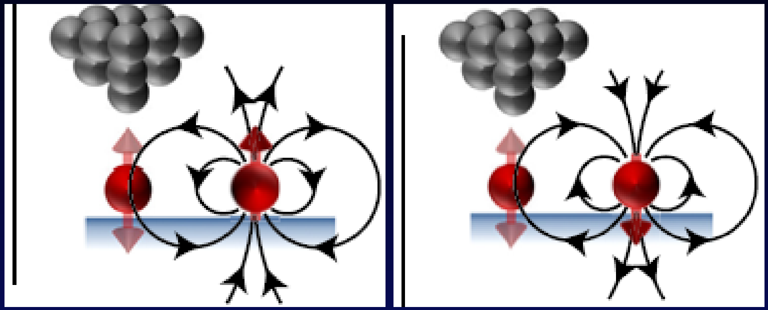

S. Baumann *et al*., Science, 417, 350 (2015)

F. D. Natterer *et al*., Nature, 543, 226 (2017)

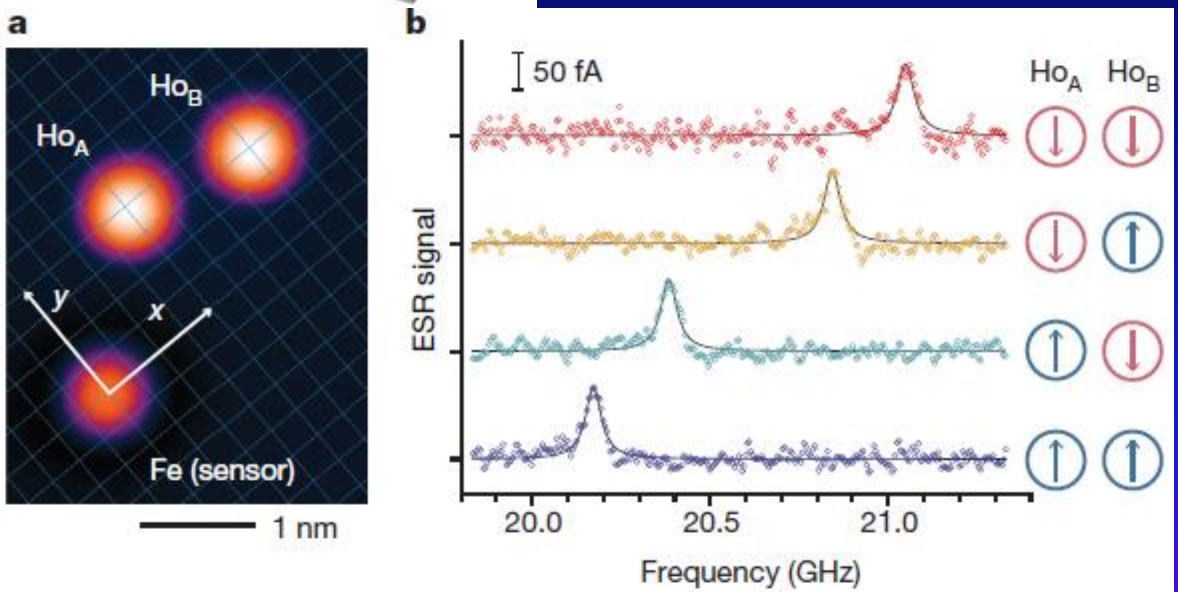

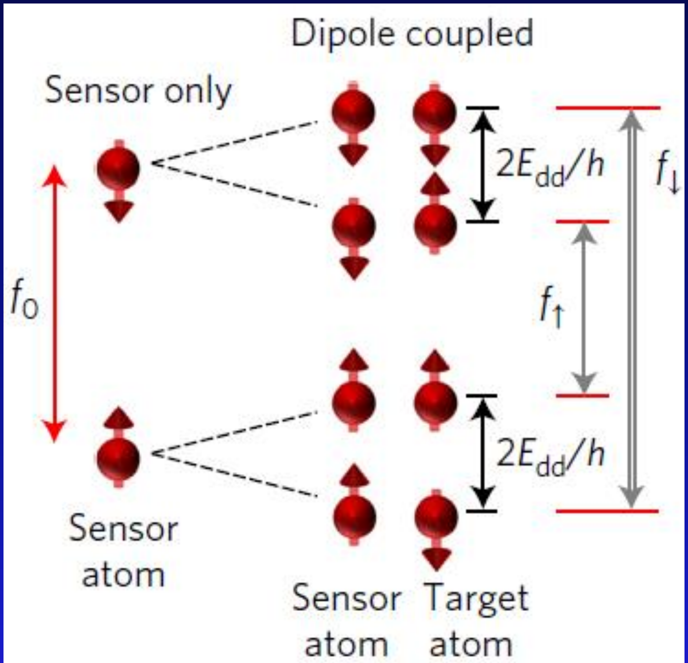

T. Choi *et al*., Nat. Nanotech., 12, 420 (2017)

Summary & Future Highlights

There are more to explore !!

Correlation between

- atomic structure
- electronic structure
- spin structure

at ultimate spatial, time

and energy resolution !

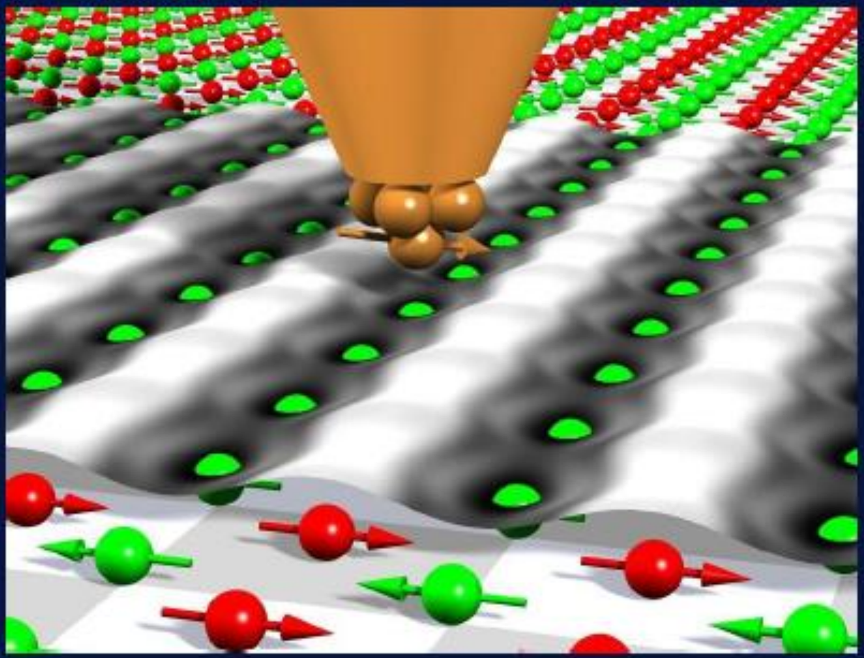

Thanks for your attention !

Imaging and Manipulating Individual Magnetic Skyrmions by Spin-Polarized Scanning Tunneling Microscopy

Pin-Jui Hsu[1,2] (徐斌睿)

1. Institute of Applied Physics, University of Hamburg, Jungiusstrasse 11, D-20355 Hamburg, Germany
2. Department of Physics, National Tsing Hua University, No. 101, Section 2, Kuang-Fu Road, Hsinchu 30013, Taiwan

Fe-DL/ Rh(001)

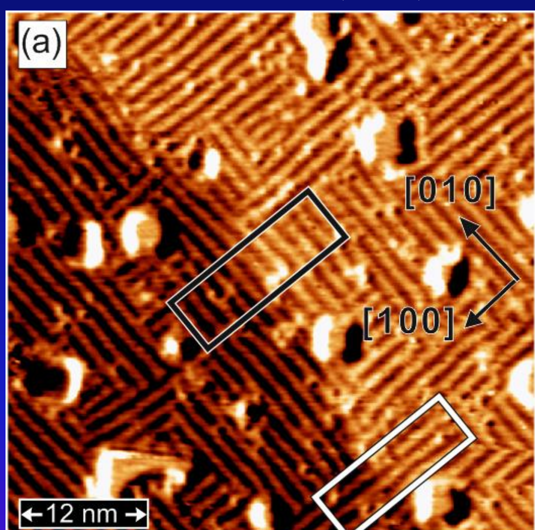

Fe-TL/ Ir(111)

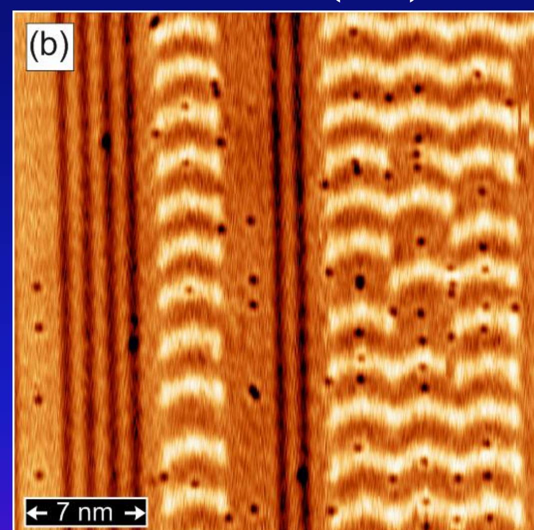

H/ Fe-DL/ Ir(111)

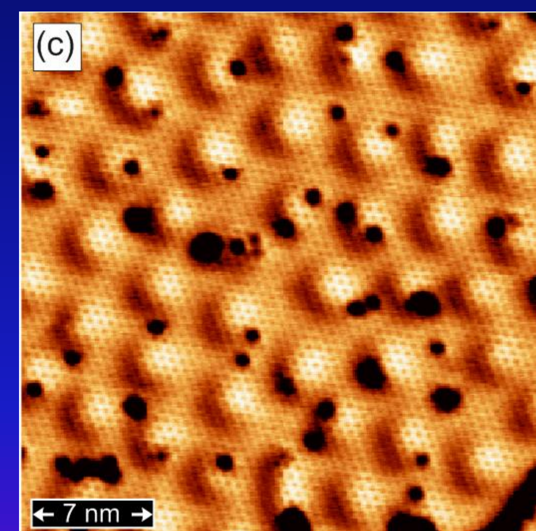

Outline

- ***Research Motivation***
- *Noncollinear magnetic spin structures: chiral domain wall, spin spiral, magnetic skyrmions...*
- ***Introductions & Experimental Results***
- *Spin-Polarized STM & STS (SP-STM/ STS):*
  - *Ferromagnetic Atomic Monolayers : Fe/ Rh(001), Nat. Commun., **7**, 10949, (2016)*
    - *Phase competition between CDW and FM ordering*
  - *Non-collinear Magnetism : Fe-DL/ Ir(111), Phys. Rev. Lett., **116**, 017201 (2016)*
    - *Zigzag spin spiral sate with cycloidal rotation sense at reconstructed surface*
  - *Non-collinear Magnetism : Fe-TL/ Ir(111), Nat. Nanotech., **12**, 123 (2017), Phys. Rev. Lett., **116**, 037202 (2017)*
    - *Electric-field-driven switching of skyrmions; Room temperature spin spiral state*
  - *Non-collinear Magnetism : H/Fe-DL/ Ir(111), Nat. Commun., **9**, 1571 (2018)*
    - *Emergence of isotropic magnetic skyrmions and intrinsic FM state*
- ***Summary & Future Highlights***

Magnetic Skyrmion

Dzyaloshinsky-Moriya Interaction

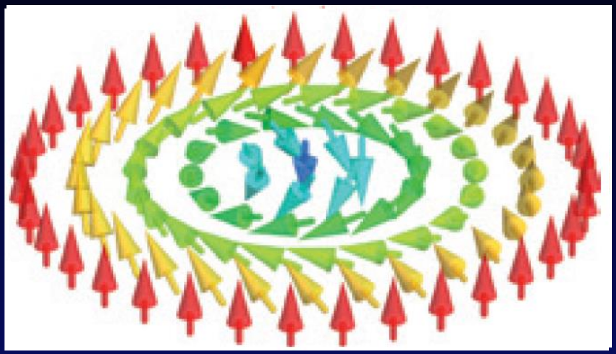

$$E_{\mathrm{DM}} = -\sum_{ij} \mathbf{D}_{ij}\left(\mathbf{S}_i \times \mathbf{S}_j\right)$$

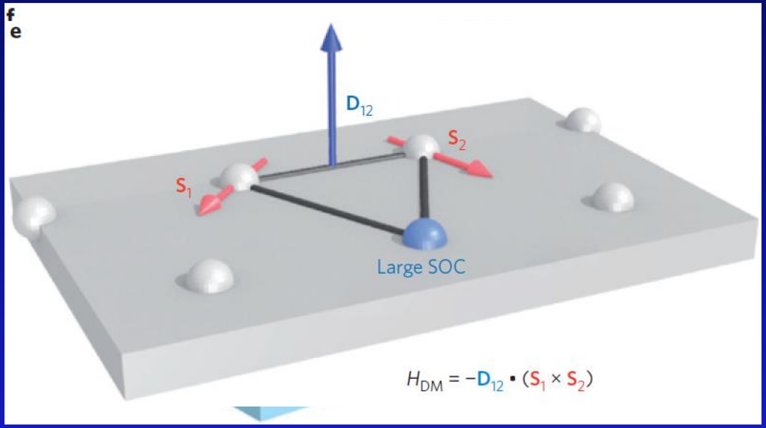

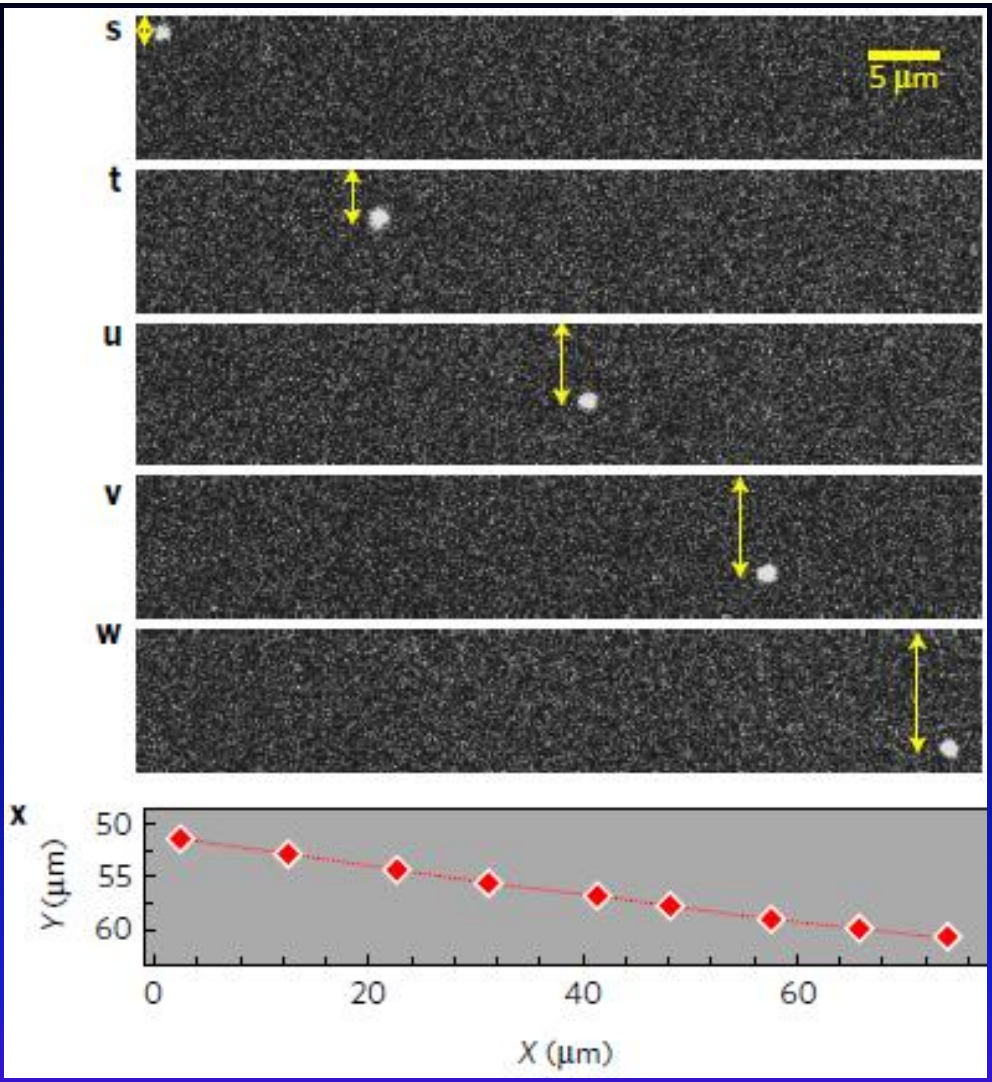

- DMI has the dominant contributions to formation of magnetic skyrmion spin texture.

A, Fert, V. Cros, and J. Sampaio, Nature Nano., 8, 152 (2013)

W. Jiang *et al.*, Nature Phys., 13, 162 (2017)

Magnetic Skyrmion

AFM skyrmion; Antiskyrmion; |Q| > 1

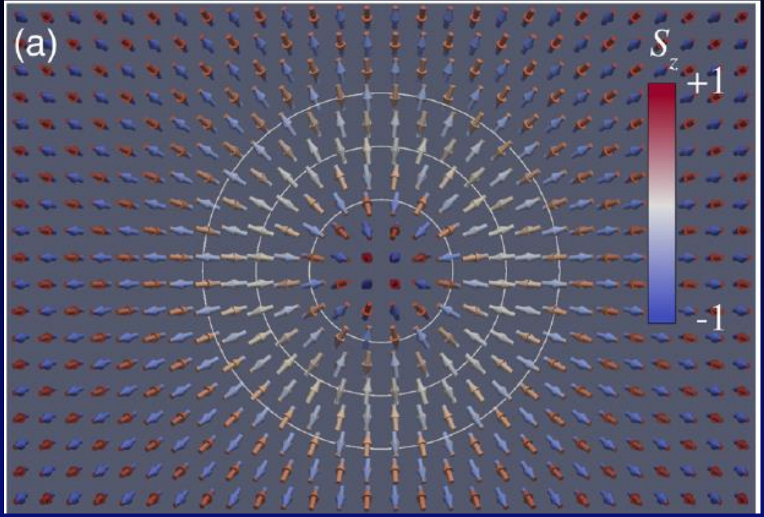

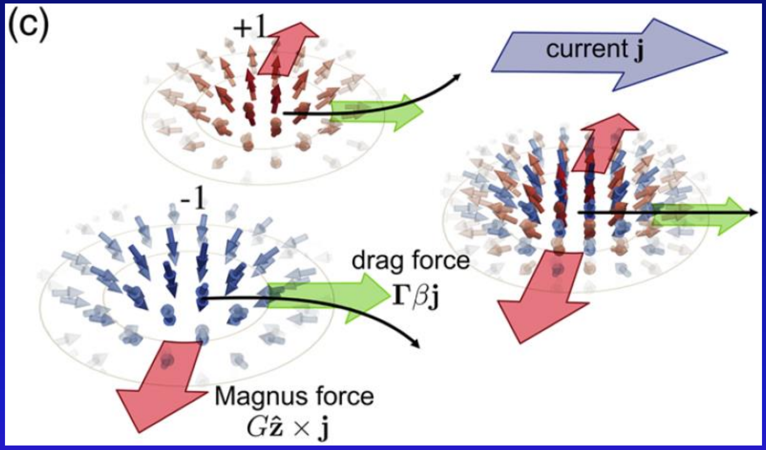

J, Barker, and O. A. Tretiakov, Phys. Rev. Lett., 116, 147203 (2016)

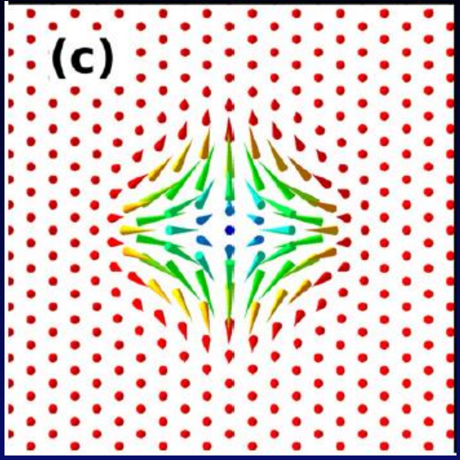

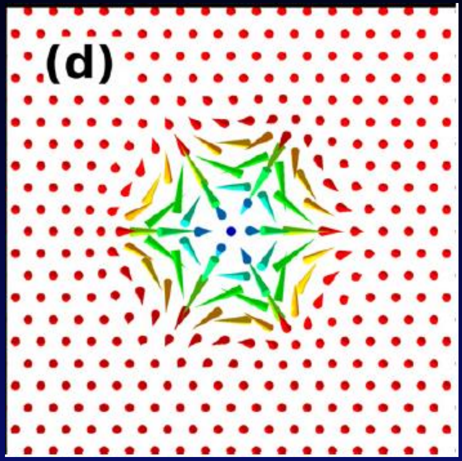

B. Dupé, C. N. Kruse, T. Dornheim, and S. Heinze, New. J. Phys., 18, 055015 (2016)

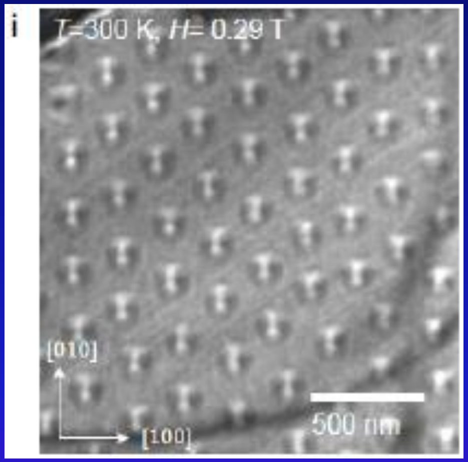

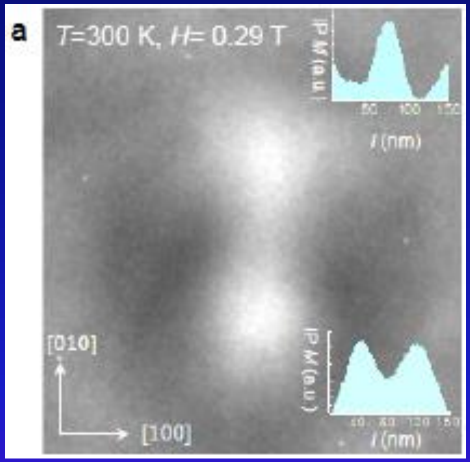

A. K. Nayak, V. Kumar, P. Werner, E. Pippel, R. Sahoo, F. Damay, U. K. Roßler, C. Felser, and S. P. Parkin, Nature, 548, 561 (2017)

Experimental Instruments

Various types of STM in Hamburg

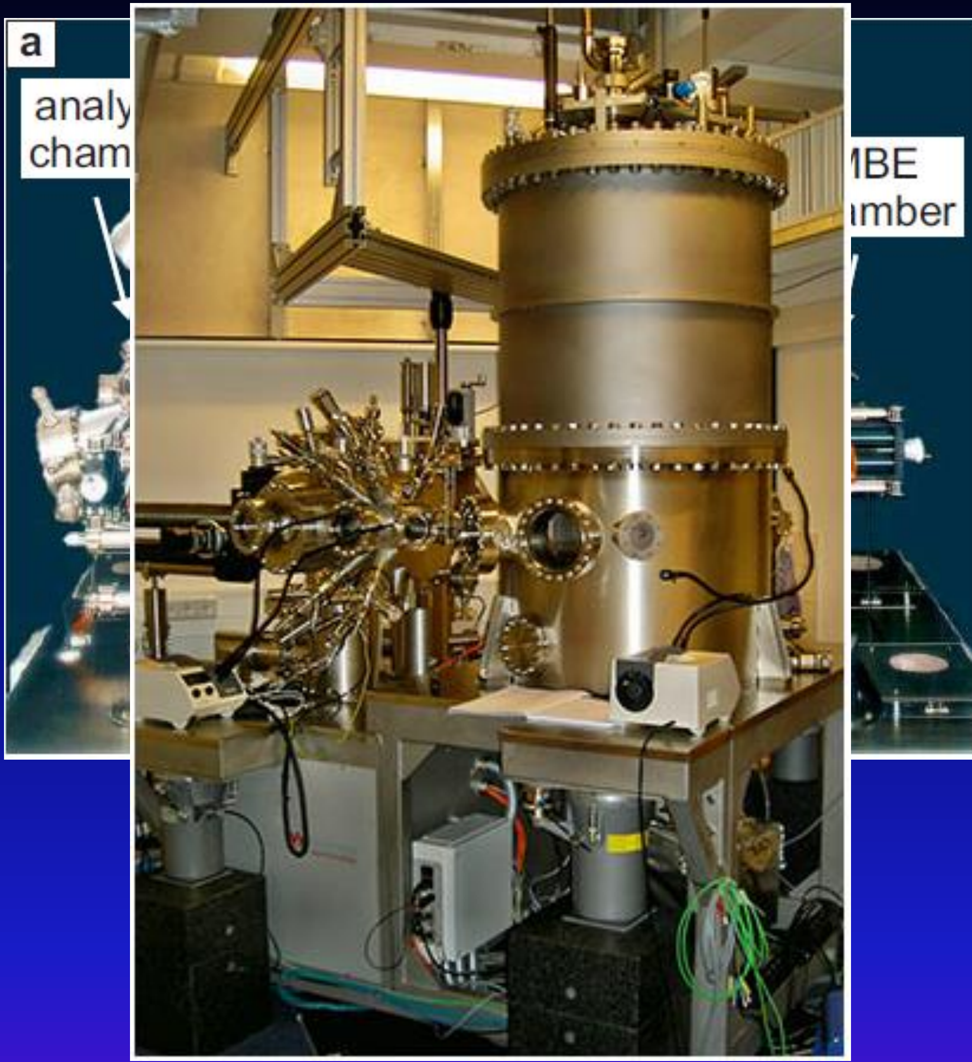

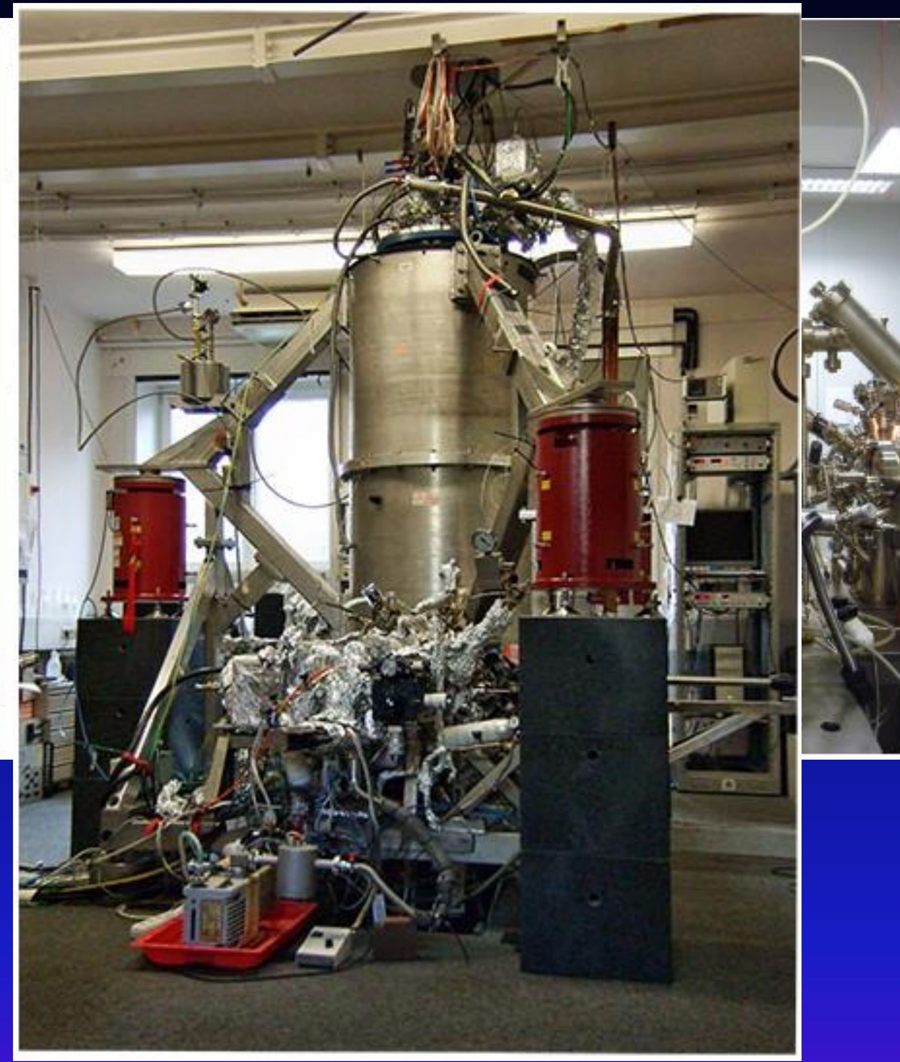

- Home built 4K-STM with 3D Magnets
- Home built 300 mK-STM with 12T Magnet

Spin-Polarized STM
Working Principle

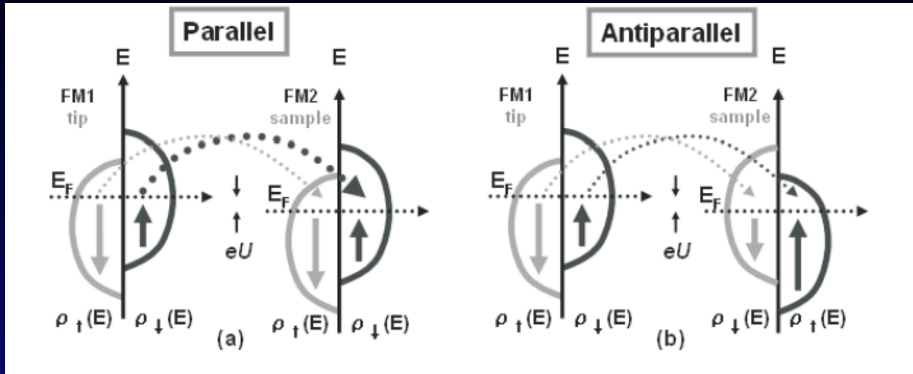

Figure 3.20: Principle of spin-polarized tunneling between two ferromagnetic electrodes with a parallel orientation of the magnetization in (a) and an antiparallel orientation in (b). For elastic tunneling and conservation of the spin, the tunnel current is in case (a) larger than in case (b).

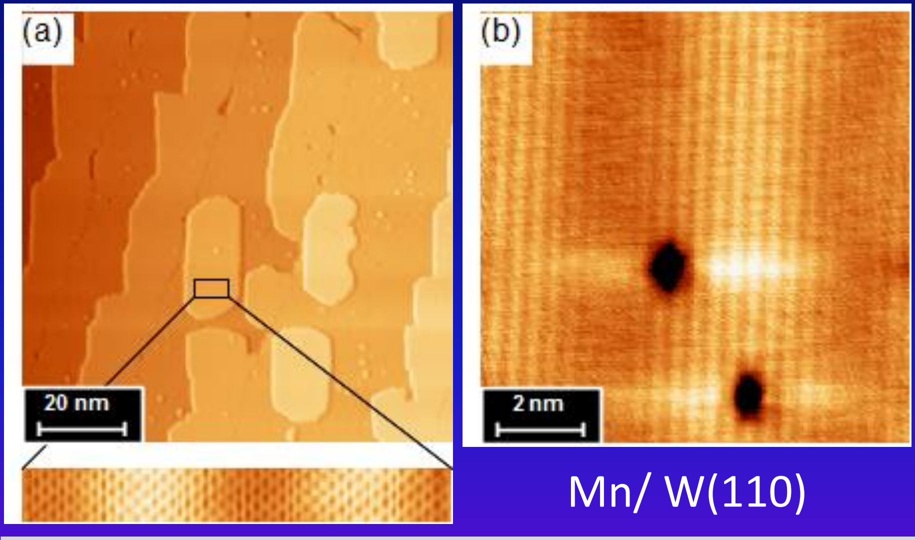

Mn/ W(110)

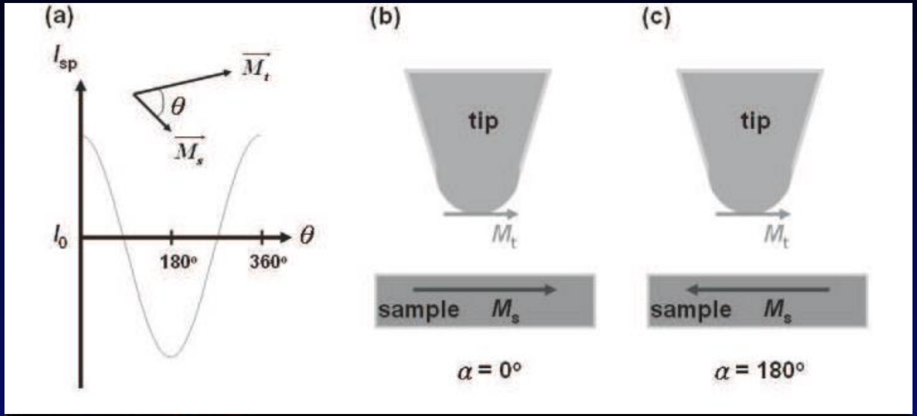

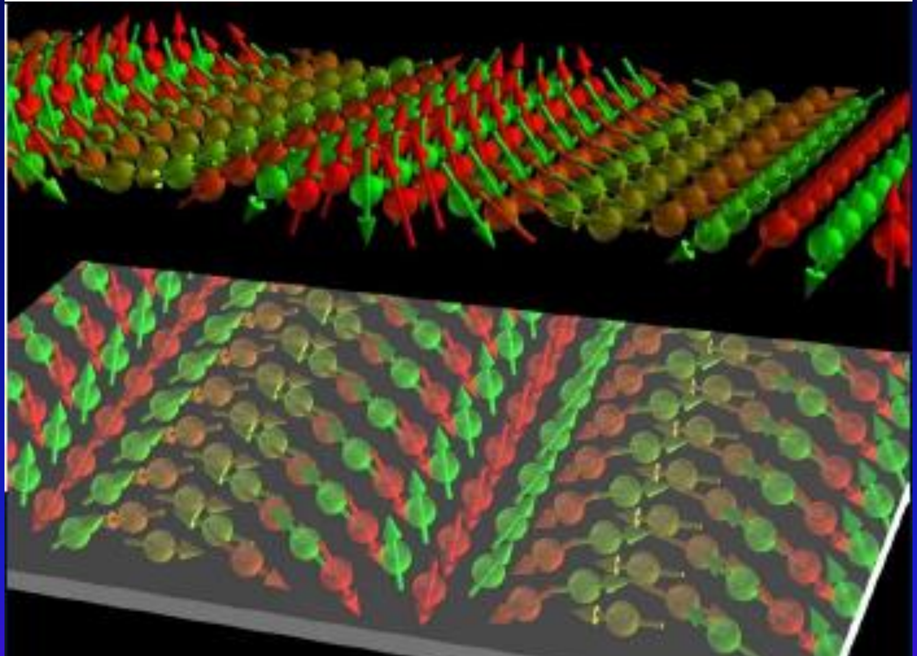

M. Bode *et al*., Nature, 447, 190 (2007)

Outline

- ➢ ***Research Motivation***
- *Noncollinear magnetic spin structures: chiral domain wall, spin spiral, magnetic skyrmions...*
- ➢ ***Introductions & Experimental Results***
- *Spin-Polarized STM & STS (SP-STM/ STS):*
  - *Ferromagnetic Atomic Monolayers : Fe/ Rh(001), Nat. Commun., **7**, 10949, (2016)*
    - *Phase competition between CDW and FM ordering*
  - *Non-collinear Magnetism : Fe-DL/ Ir(111), Phys. Rev. Lett., **116**, 017201, (2016)*
    - *Zigzag spin spiral sate with cycloidal rotation sense at reconstructed surface*
  - *Non-collinear Magnetism : Fe-TL/ Ir(111), Nat. Nanotech., **12**, 123 (2017), Phys. Rev. Lett., **116**, 037202, (2017)*
    - *Electric-field-driven switching of skyrmions; Room temperature spin spiral state*
  - *Non-collinear Magnetism : H/Fe-DL/ Ir(111), Nat. Commun., **9**, 1571 (2018)*
    - *Emergence of isotropic magnetic skyrmions and intrinsic FM state*
- ➢ ***Summary & Future Highlights***

Interfacial Stabilized Dzyaloshinsky-Moria Interaction

Spontaneous Nanoskyrmion lattice of Fe/ Ir(111)

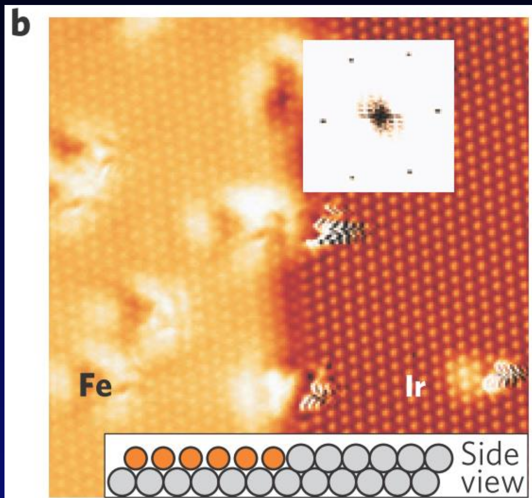

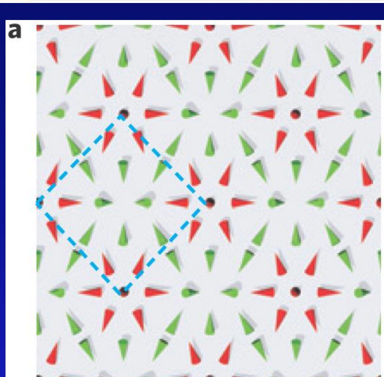

- 1 unit cell contains 15 atoms and period is about 1 nm.

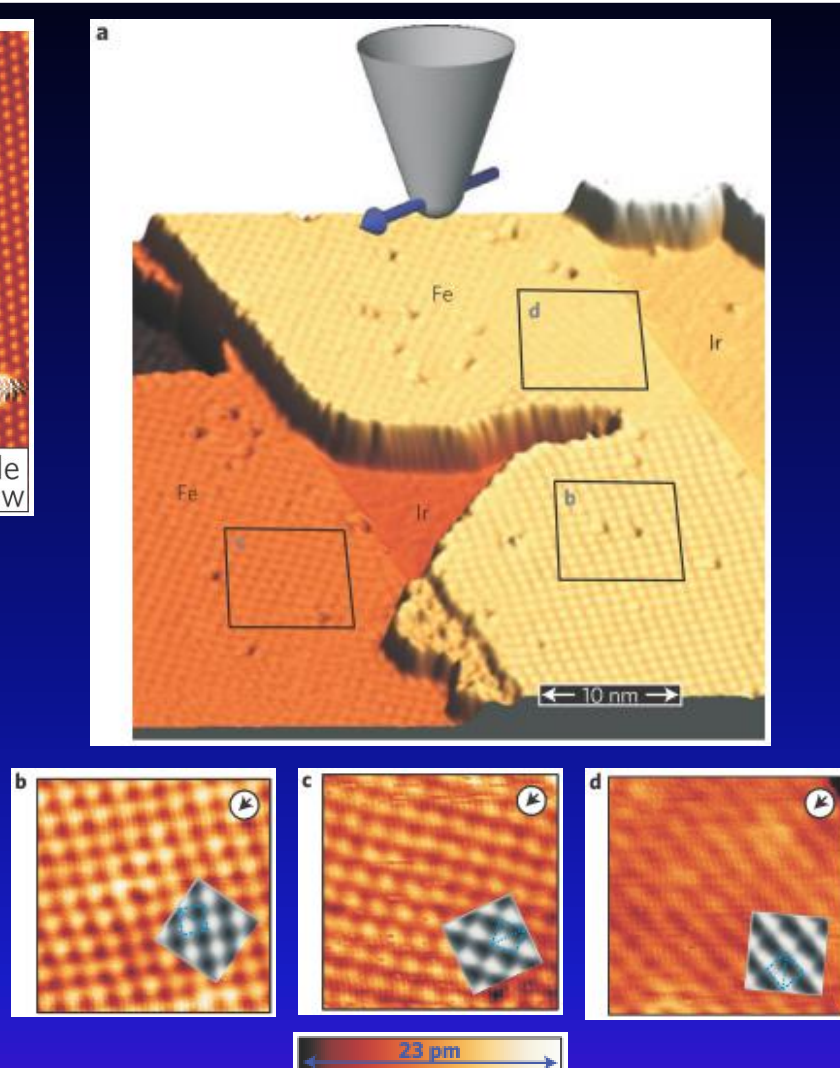

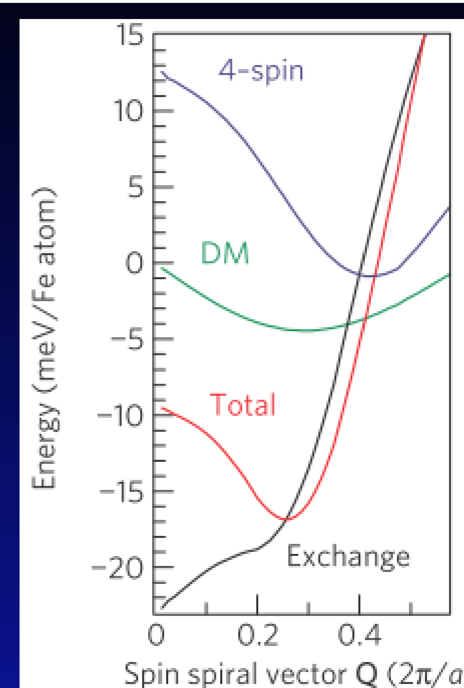

- Four-spin interaction is the driving force for stabilizing skrymion lattice.
- DMI reduces the energy further and it's about 1.8 meV/ atom.

S. Heinze *et al.*, Nature Phys., 7, 713 (2011)

Interfacial Stabilized Dzyaloshinsky-Moria Interaction

Individual Skyrmions in Pd/ Fe/ Ir(111)

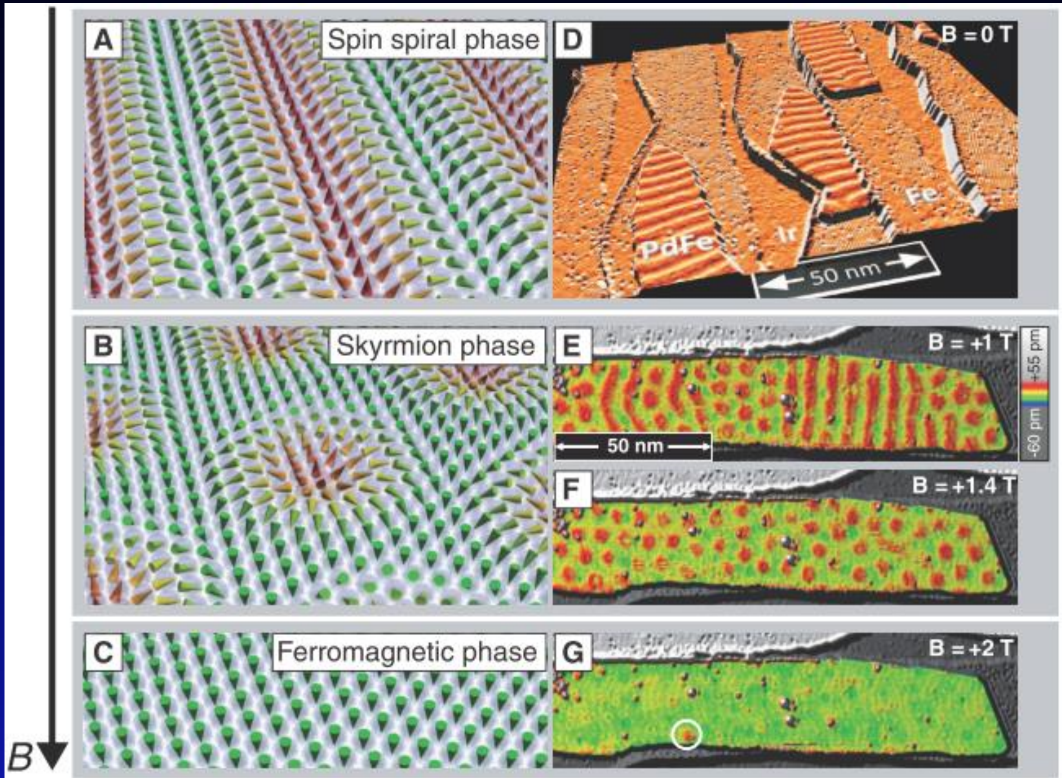

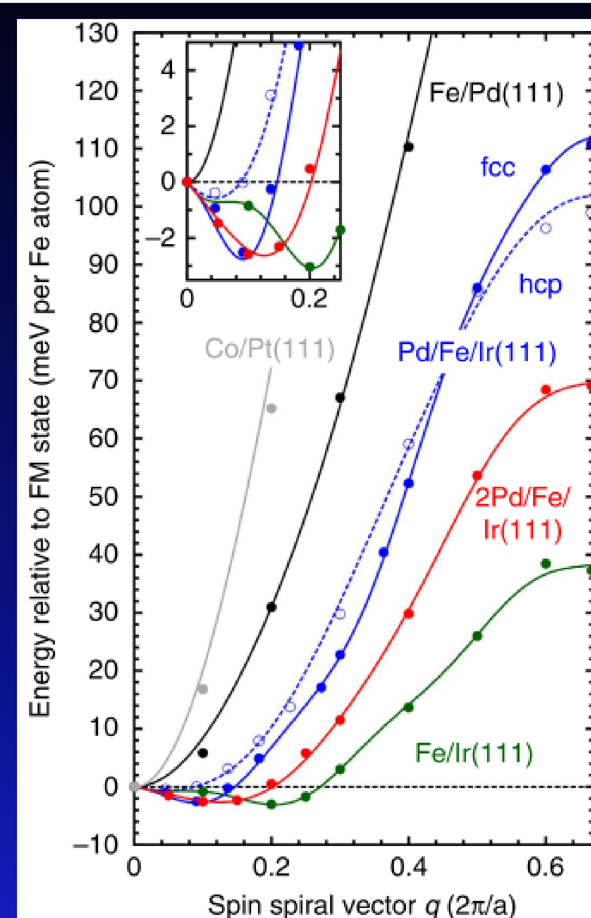

- The spiral period is about 6~7 nm with |D|~1.8 meV/ atom from Fe-Ir interface.
- Pd-Fe interface is crucial for tuning the exchange interaction.
- A phase transition to skyrmion gains the energy with respect to spiral due to Zeeman term.

N. Romming *et al*., Science, 341, 636 (2013)

B. Dupé *et al*., Nature Comm., 5, 4030 (2014)

Double Layer Fe/ Ir(111)
Growth and Electronic Properties

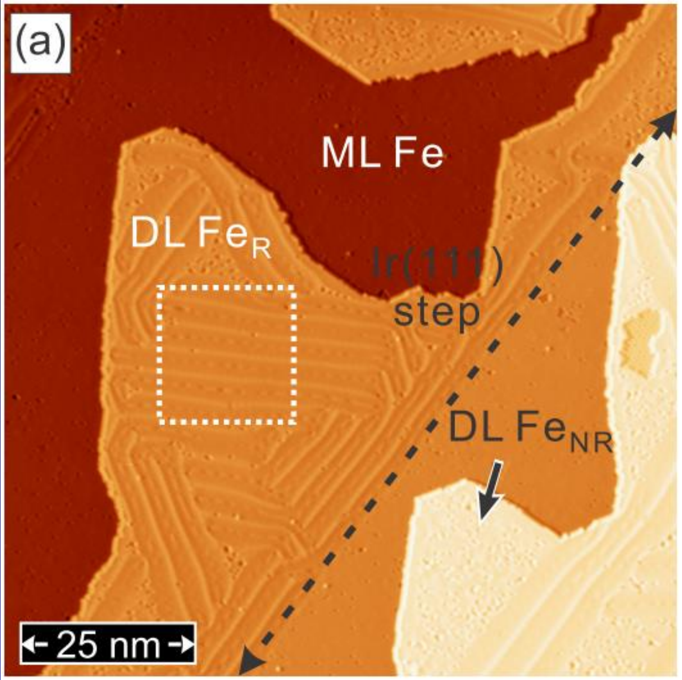

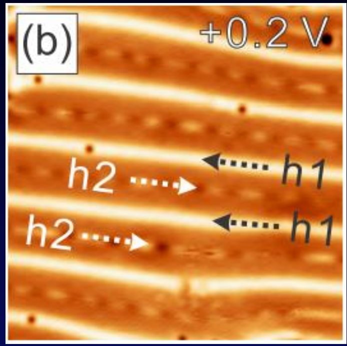

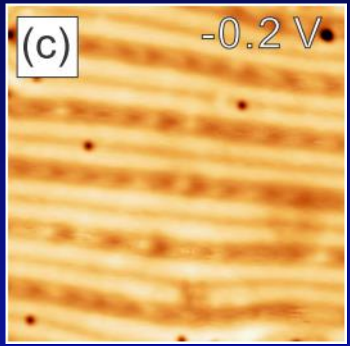

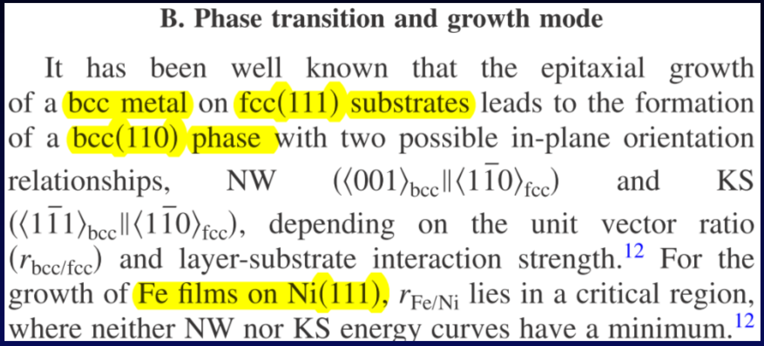
B. Phase transition and growth mode

It has been well known that the epitaxial growth of a bcc metal on fcc(111) substrates leads to the formation of a bcc(110) phase with two possible in-plane orientation relationships, NW $(\langle 001\rangle_{bcc} \| \langle 1\bar{1}0\rangle_{fcc})$ and KS $(\langle 1\bar{1}1\rangle_{bcc} \| \langle 1\bar{1}0\rangle_{fcc})$, depending on the unit vector ratio $(r_{bcc/fcc})$ and layer-substrate interaction strength.[12] For the growth of Fe films on Ni(111), $r_{Fe/Ni}$ lies in a critical region, where neither NW nor KS energy curves have a minimum.[12]

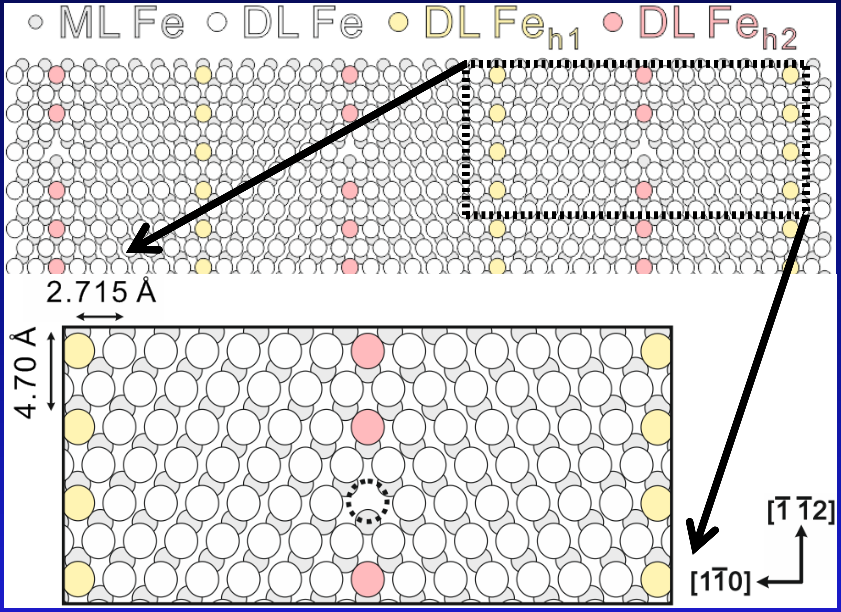

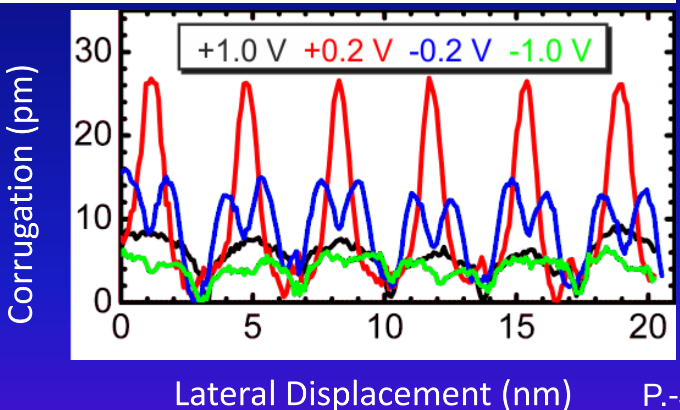

The reconstruction lines run perpendicular to close-packed atomic row and have a typical spacing 3.3 ~ 3.7 nm

B. An *et al*., PRB, 79, 085406 (2009)

P.-J. Hsu, A. Finco, L. Schmidt, A. Kubetzka, K. von Bergmann, and R. Wiesendanger, Phys. Rev. Lett., 116, 017201 (2016)

Double Layer Fe/ Ir(111)

Guiding Spin Spirals by Local Uniaxial Strain Relief

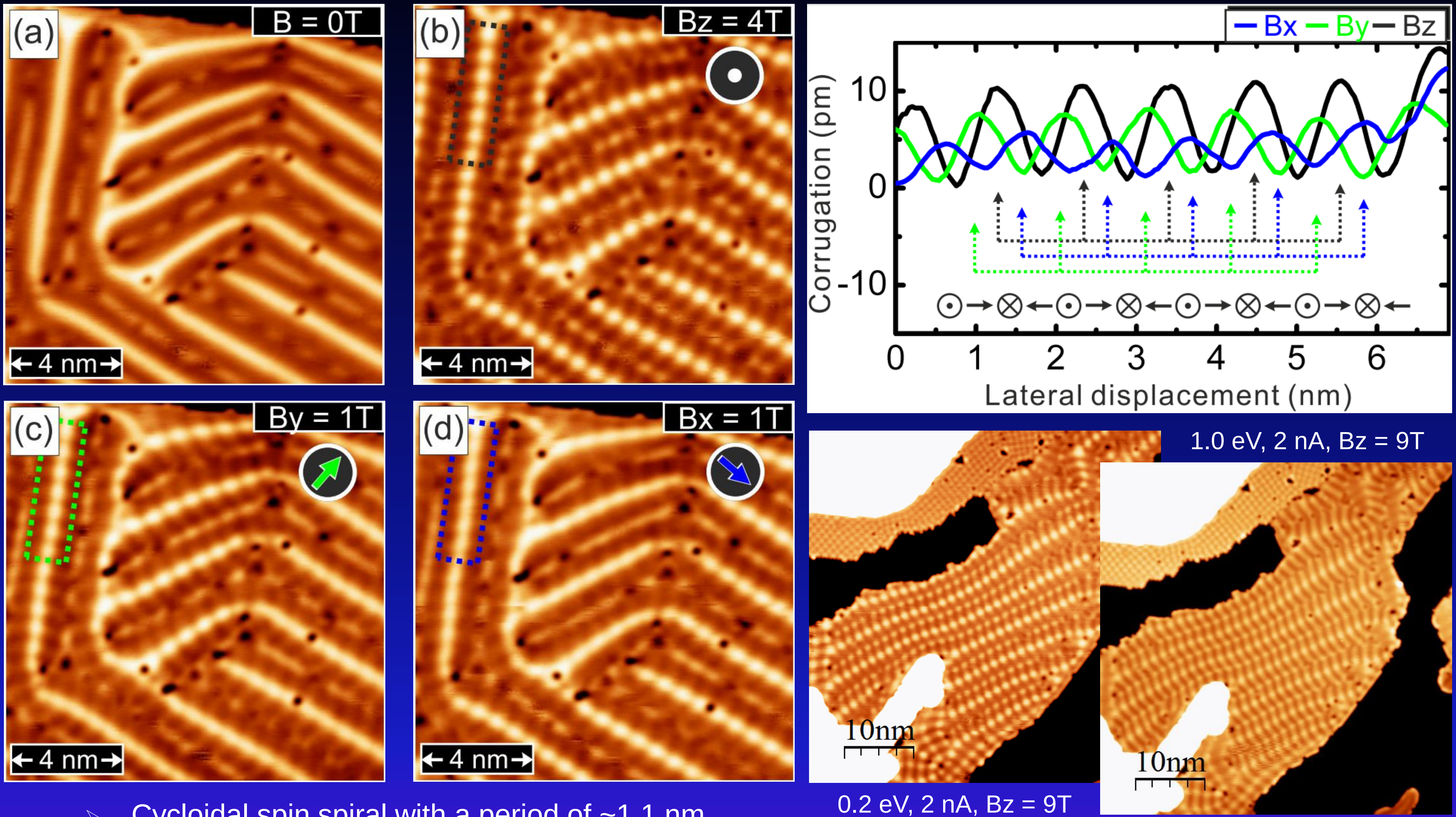

1.0 eV, 2 nA, Bz = 9T

0.2 eV, 2 nA, Bz = 9T

- Cycloidal spin spiral with a period of ~1.1 nm.

P.-J. Hsu, A. Finco, L. Schmidt, A. Kubetzka, K. von Bergmann, and R. Wiesendanger, Phys. Rev. Lett., 116, 017201 (2016)

Outline

- ***Research Motivation***
- *Noncollinear magnetic spin structures: chiral domain wall, spin spiral, magnetic skyrmions...*
- ***Introductions & Experimental Results***
- *Spin-Polarized STM & STS (SP-STM/ STS):*
  - *Ferromagnetic Atomic Monolayers : Fe/ Rh(001), Nat. Commun., **7**, 10949, (2016)*
    - *Phase competition between CDW and FM ordering*
  - *Non-collinear Magnetism : Fe-DL/ Ir(111), Phys. Rev. Lett., **116**, 017201, (2016)*
    - *Zigzag spin spiral sate with cycloidal rotation sense at reconstructed surface*
  - *Non-collinear Magnetism : Fe-TL/ Ir(111), Nat. Nanotech., **12**, 123 (2017), Phys. Rev. Lett., **116**, 037202, (2017)*
    - *Electric-field-driven switching of skyrmions; Room temperature spin spiral state*
  - *Non-collinear Magnetism : H/Fe-DL/ Ir(111), Nat. Commun., **9**, 1571 (2018)*
    - *Emergence of isotropic magnetic skyrmions and intrinsic FM state*
- ***Summary & Future Highlights***

Triple Layer Fe/ Ir(111)

Spin Spirals on Fe-TL/ Ir(111)

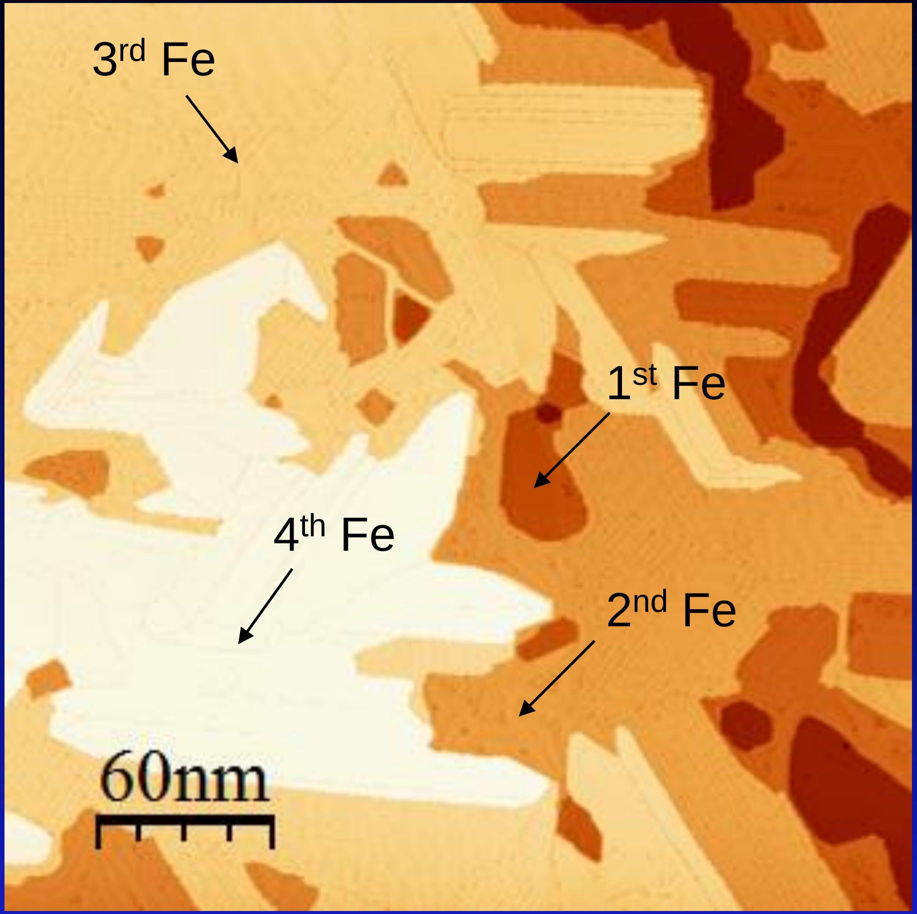

-0.7 V, 1nA, Topo.

- Spin spiral state on the 3rd and FM state on the 4th Fe/ Ir(111).

- Is there a magnetic phase transition on Fe-TL ?

-0.7 V, 1nA, dI/dU mapping

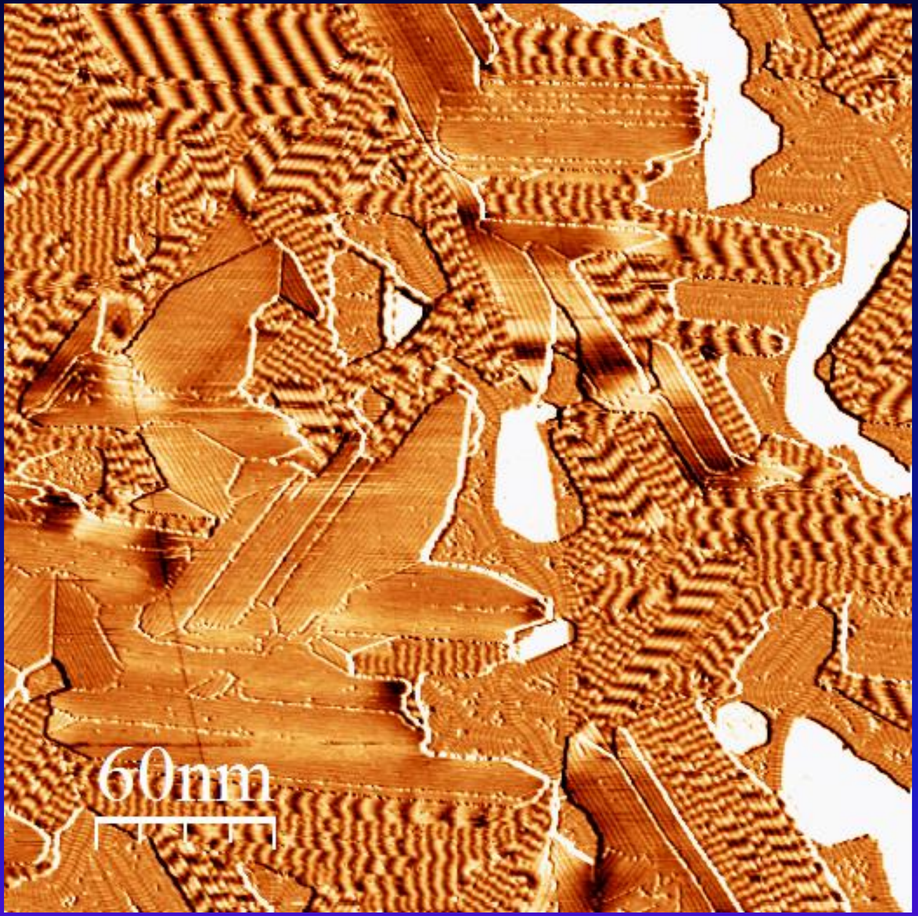

Triple Layer Fe/ Ir(111)

Magnetic Phase Transition

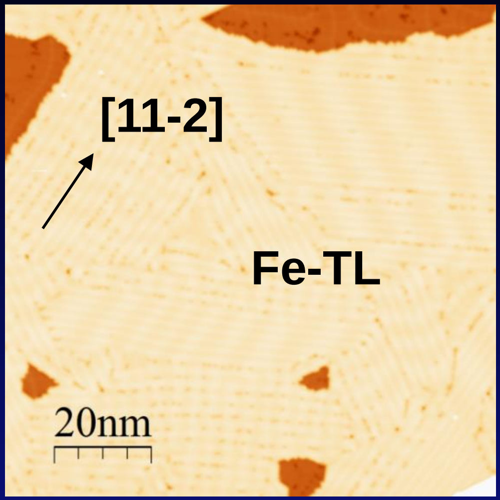

-0.7 V, 1nA, Bz= 0T, Topo.

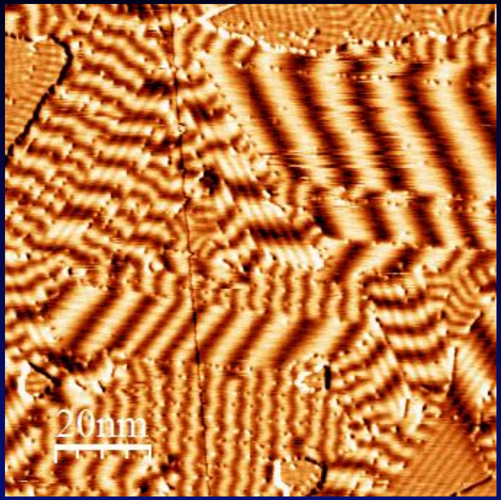

-0.7 V, 1nA, Bz= 0T, dI/dU

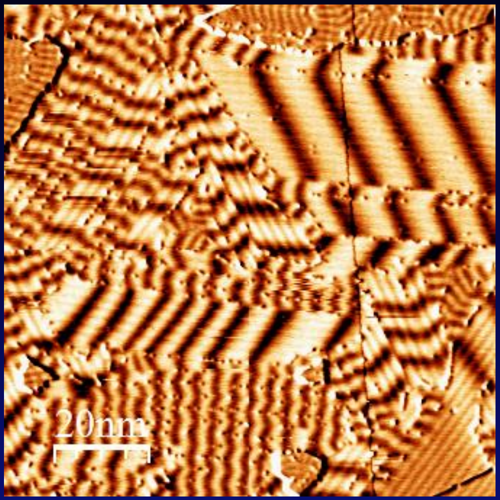

-0.7 V, 1nA, Bz= 0.5T

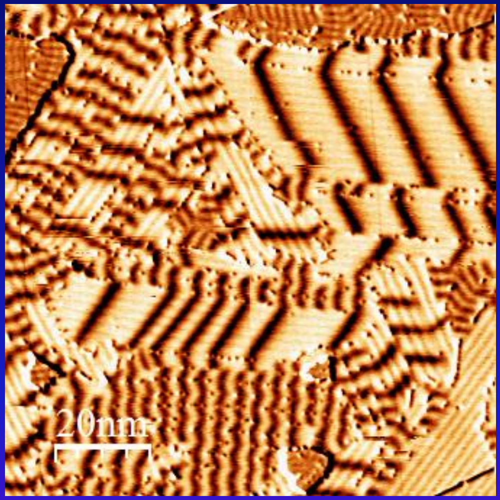

-0.7 V, 1nA, Bz= 1.0T

-0.7 V, 1nA, Bz= 1.5T

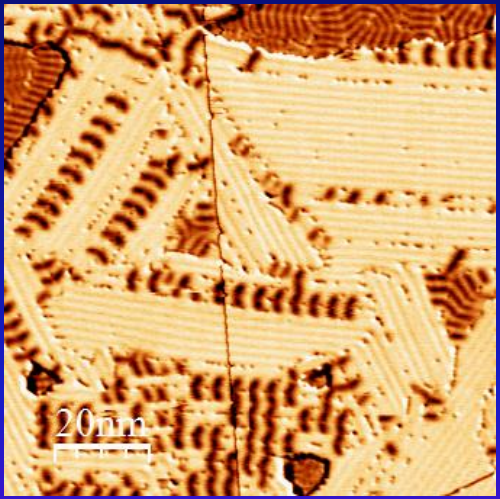

-0.7 V, 1nA, Bz= 2.0T

Triple Layer Fe/ Ir(111)

Unique Rotation Sense of Individual Skyrmions

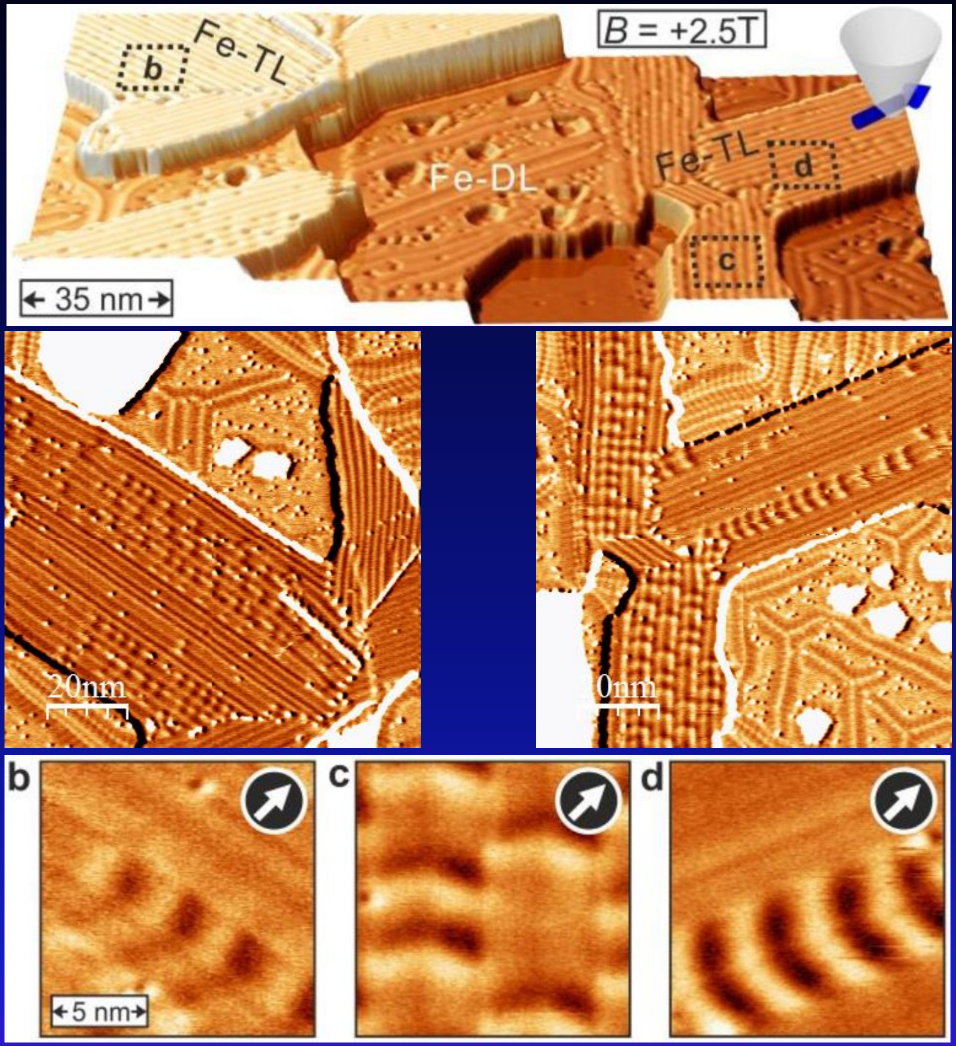

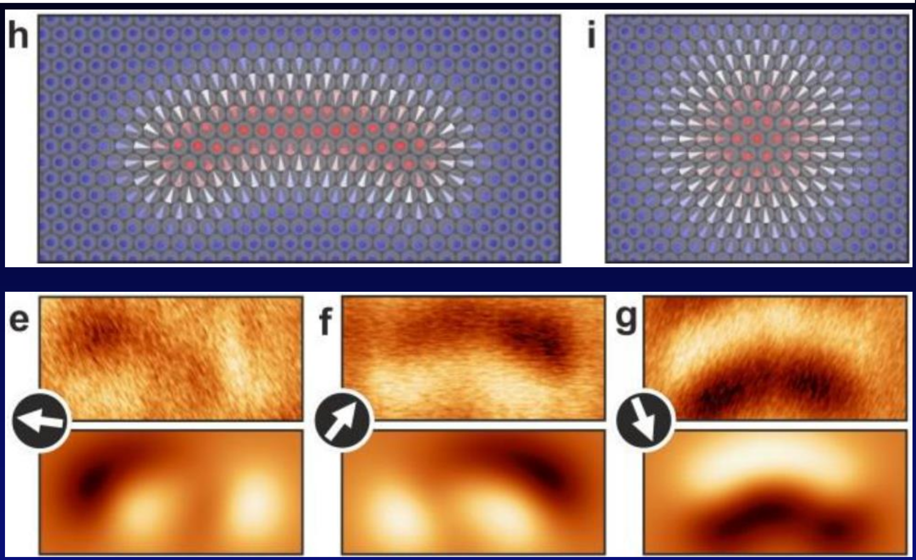

-0.7 V, 1nA, Bz= 2.5T

- Characterizing the spin structures of in-plane spin components on three symmetric rotational domains.
- A deformed skyrmion spin structure has been constructed from experimental results.
- The spin mappings show unique rotational sense indicating the driven force of DM interaction from Fe-Ir interface.

P.-J. Hsu, A. Kubetzka, A. Finco, N. Romming, K. von Bergmann, and R. Wiesendanger, Nat. Nanotech., 12, 123-126 (2017)

Triple Layer Fe/ Ir(111)

Writing and Deleting of Individual Skyrmions, Cr Tip

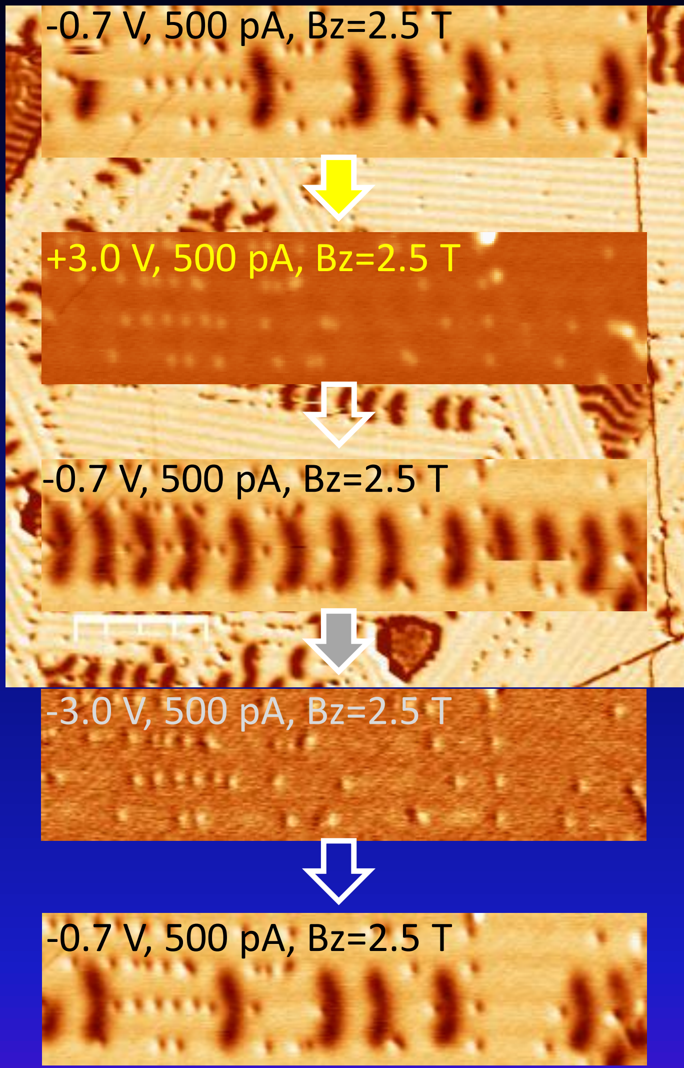

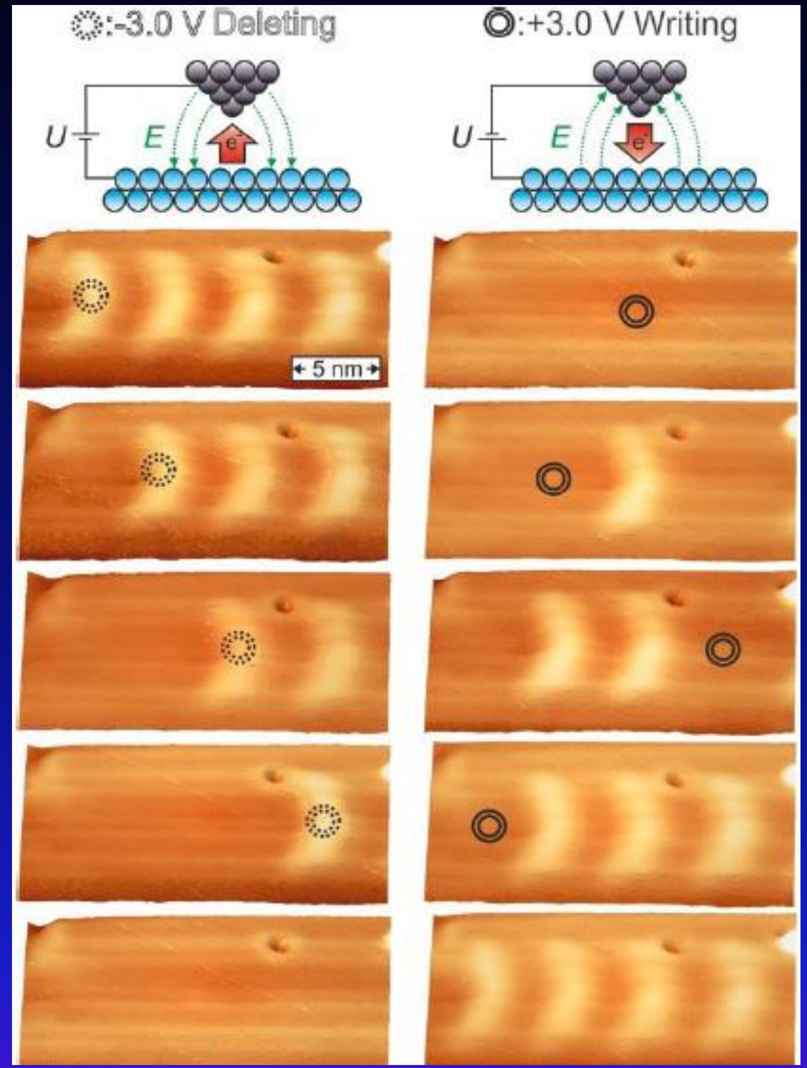

- The writing or deleting events depend on the bias polarity.
- The individual skyrmions can be written and deleted step-by-step.

P.-J. Hsu, A. Kubetzka, A. Finco, N. Romming, K. von Bergmann, and R. Wiesendanger, Nat. Nanotech., 12, 123-126 (2017)

Triple Layer Fe/ Ir(111)

Writing and Deleting of Individual Skyrmions, W Tip

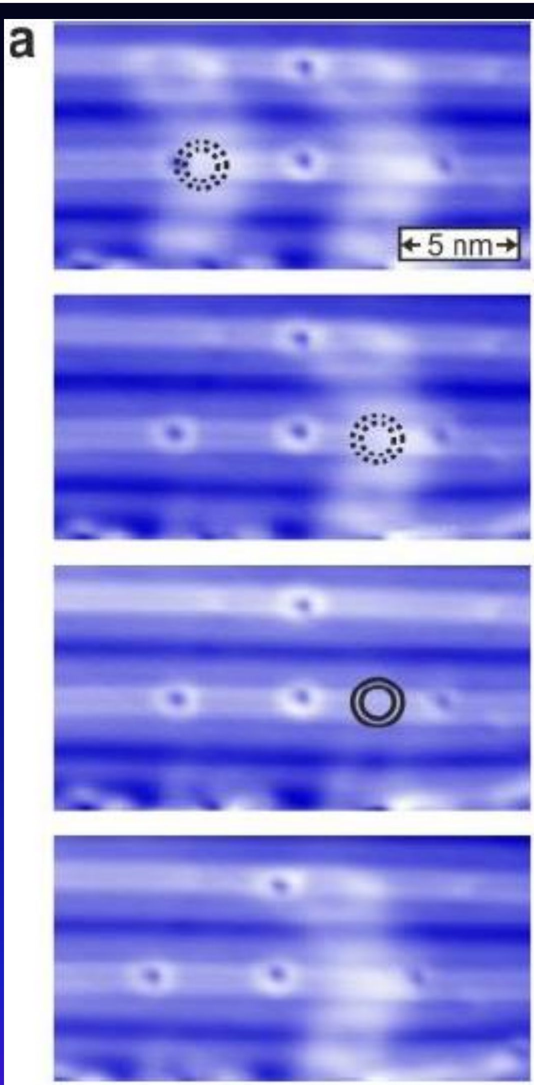

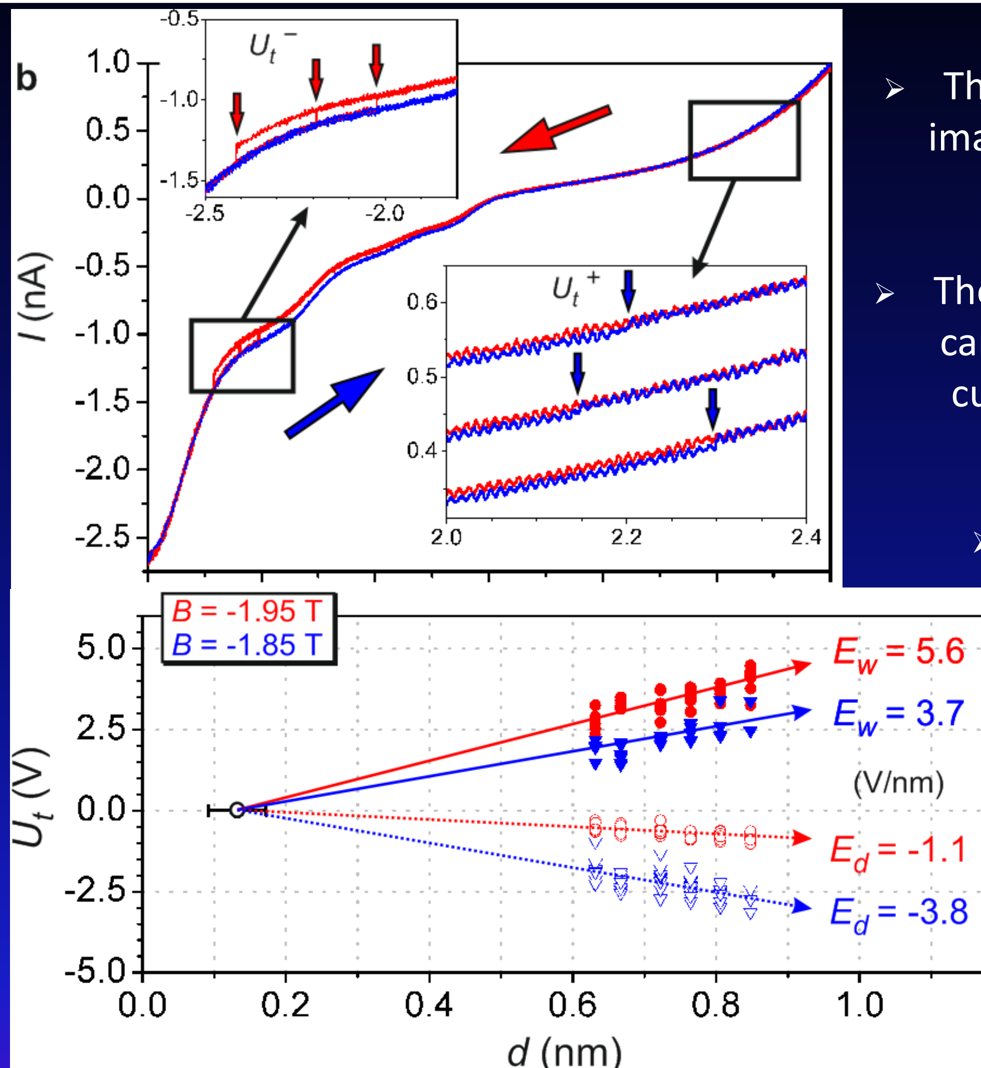

- The skyrmions can be imaged by W tip due to NCMR effect.
- The threshold voltages can be extracted from current jumps in I(U) curves.
- The bias polarity dependence and linear dispersion suggest the decisive role of electric field for the switching behaviour.

P.-J. Hsu, A. Kubetzka, A. Finco, N. Romming, K. von Bergmann, and R. Wiesendanger, Nat. Nanotech., 12, 123-126 (2017)

Triple Layer Fe/ Ir(111)

Temperature-induced increase of spin spiral periods

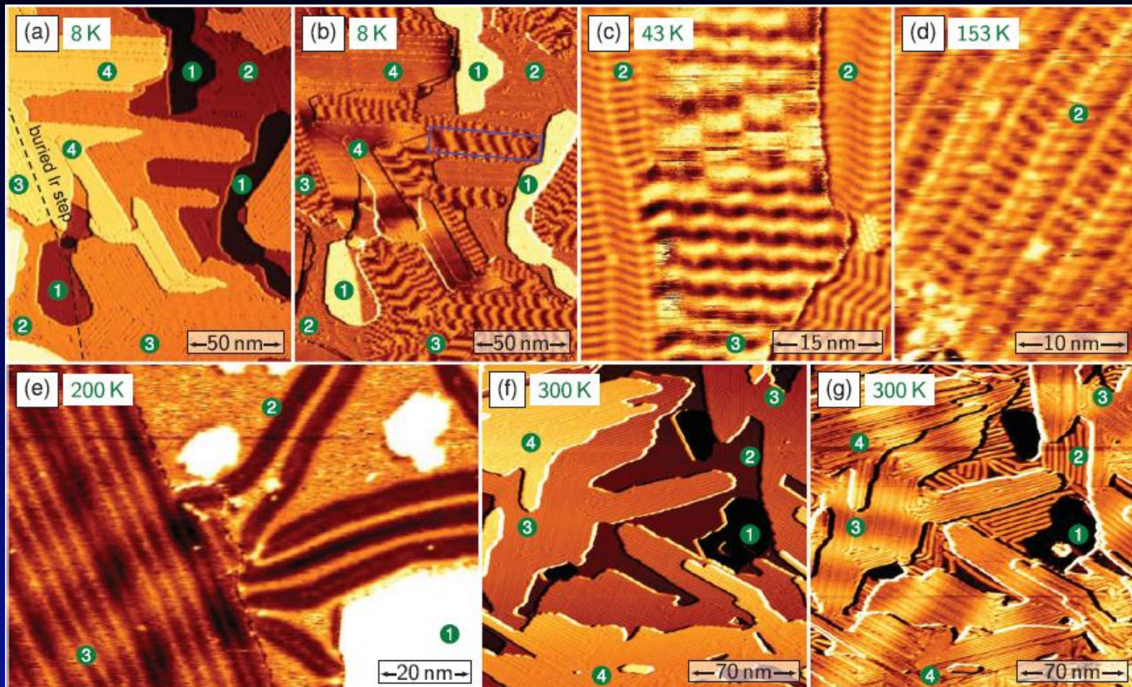

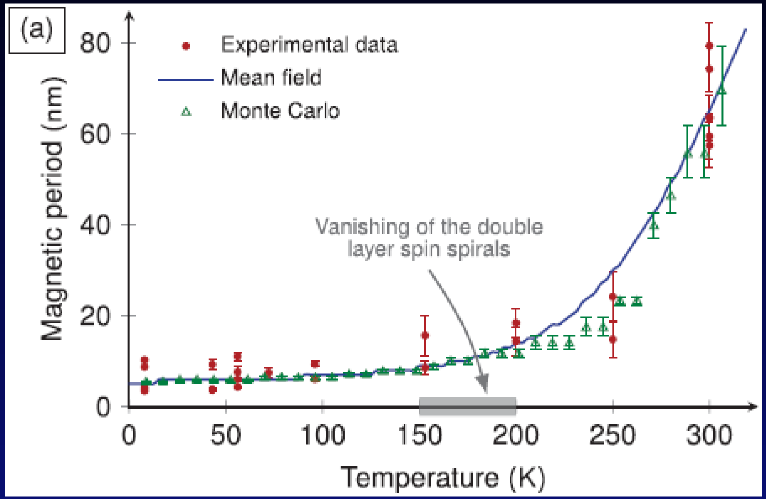

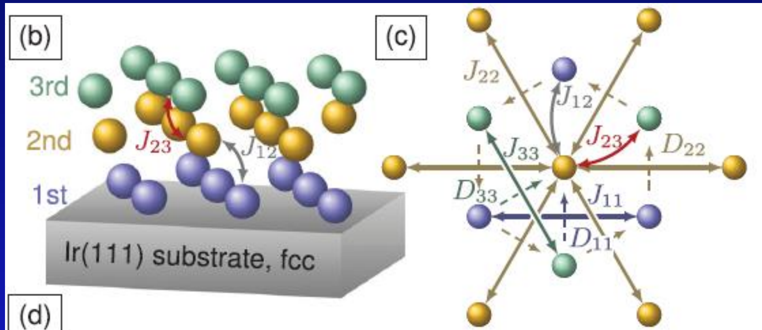

(d)

J_{11}	J_{22}	J_{33}	J_{12}	J_{23}
−8.75 K	−70 K	−245 K	−175 K	−65.63 K

D_{11}	D_{22}	D_{33}
87.5 K	43.75 K	0.88 K

- The period of spin spiral on Fe-TL/Ir(111) increases with temperature, about 16 times larger up to RT.
- With layer-dependent magnetic parameters, the temperature-induced increase of periods can be in agreement with experimental observations.

A. Finco, R. Levente, P. J. Hsu, A. Kubetzka, E. Vedmedenko, K. von Bergmann, and R. Wiesendanger, Phys. Rev. Lett., 119, 037202 (2017)

Outline

- ***Research Motivation***
- *Noncollinear magnetic spin structures: chiral domain wall, spin spiral, magnetic skyrmions...*
- ***Introductions & Experimental Results***
- *Spin-Polarized STM & STS (SP-STM/ STS):*
  - *Ferromagnetic Atomic Monolayers : Fe/ Rh(001), Nat. Commun., **7**, 10949, (2016)*
    - *Phase competition between CDW and FM ordering*
  - *Non-collinear Magnetism : Fe-DL/ Ir(111), Phys. Rev. Lett., **116**, 017201, (2016)*
    - *Zigzag spin spiral sate with cycloidal rotation sense at reconstructed surface*
  - *Non-collinear Magnetism : Fe-TL/ Ir(111), Nat. Nanotech., **12**, 123 (2017), Phys. Rev. Lett., **116**, 037202, (2017)*
    - *Electric-field-driven switching of skyrmions; Room temperature spin spiral state*
  - *Non-collinear Magnetism : H/Fe-DL/ Ir(111), Nat. Commun., **9**, 1571 (2018)*
    - *Emergence of isotropic magnetic skyrmions and intrinsic FM state*
- ***Summary & Future Highlights***

Strained pseudomorphic areas

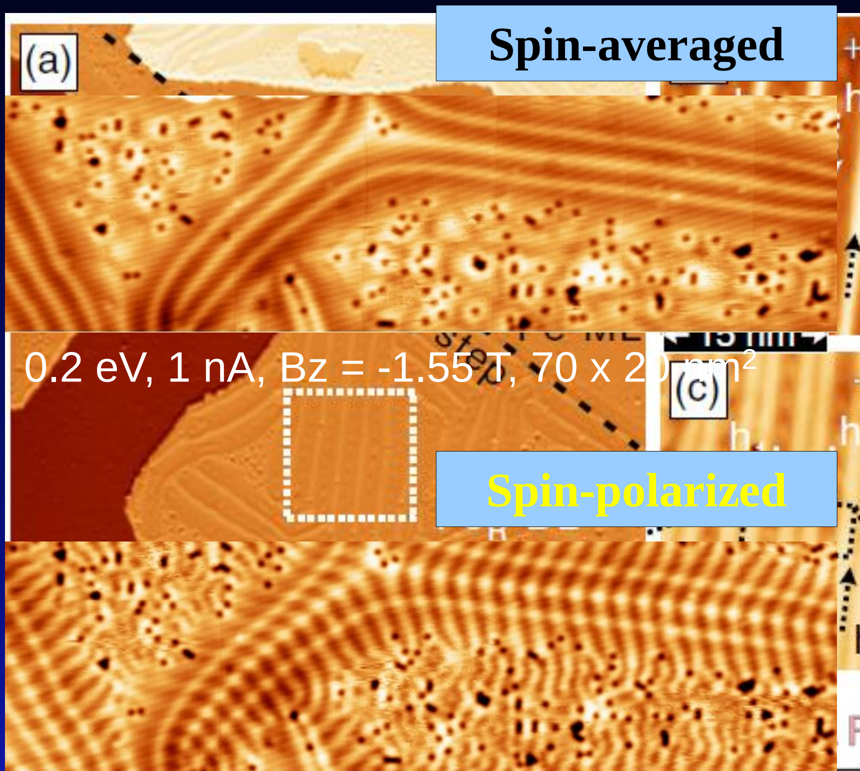

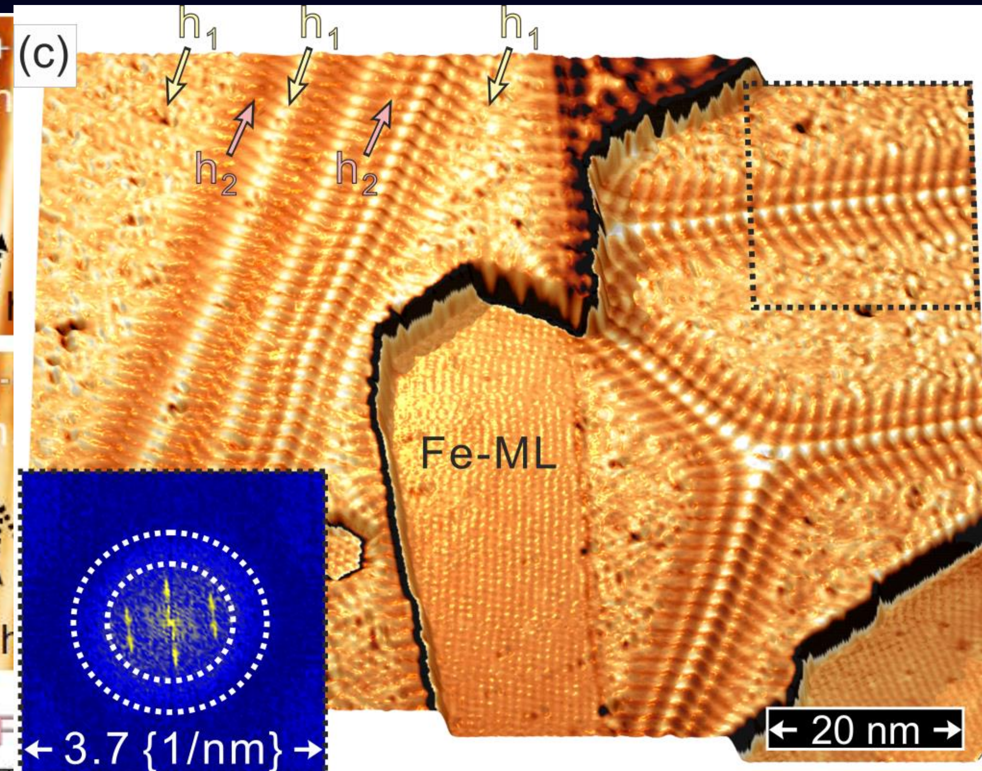

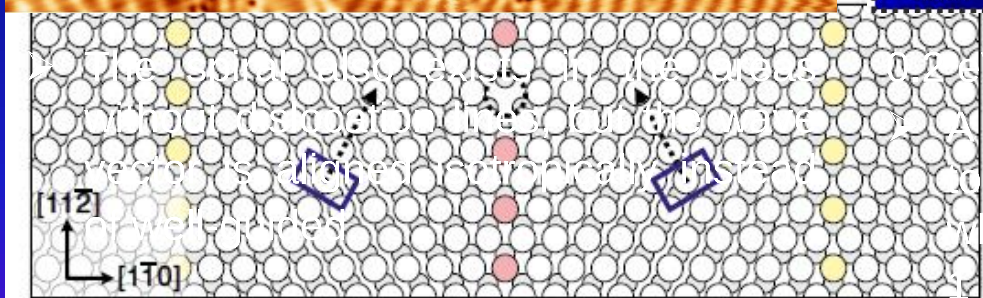

- The spiral also exists in the areas without dislocation lines, but the wave vector is aligned isotropically instead of well-guided.

0.2 eV, 1 nA, Bz = 0T

- A radial average reveals a peak corresponding to a real space periodicity of about 1.2 nm which is close to the nanoskyrmion lattice of ~ 1 nm in Fe-ML.

P.-J. Hsu, A. Finco, L. Schmidt, A. Kubetzka, K. von Bergmann, and R. Wiesendanger, Phys. Rev. Lett., 116, 017201 (2016)

H/ Fe-DL/ Ir(111)

Growth comparison w/ or w/o post annealing

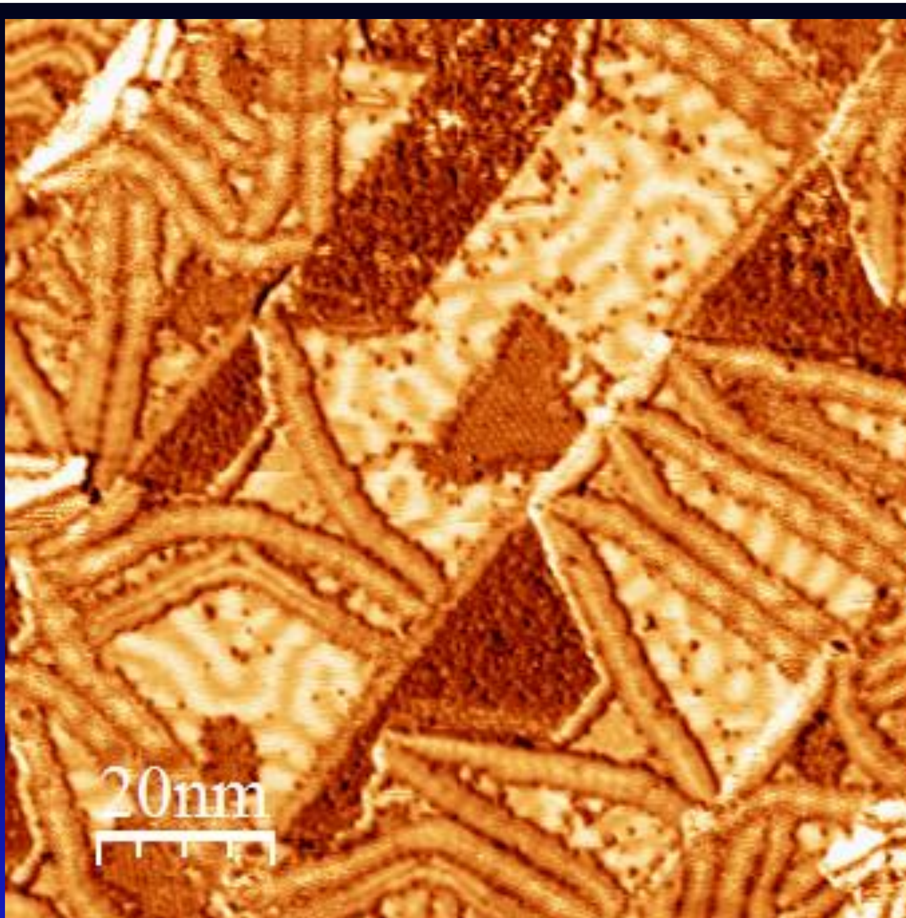

-150mV, 0.5nA, Bz= 0T, dI/dU topo.

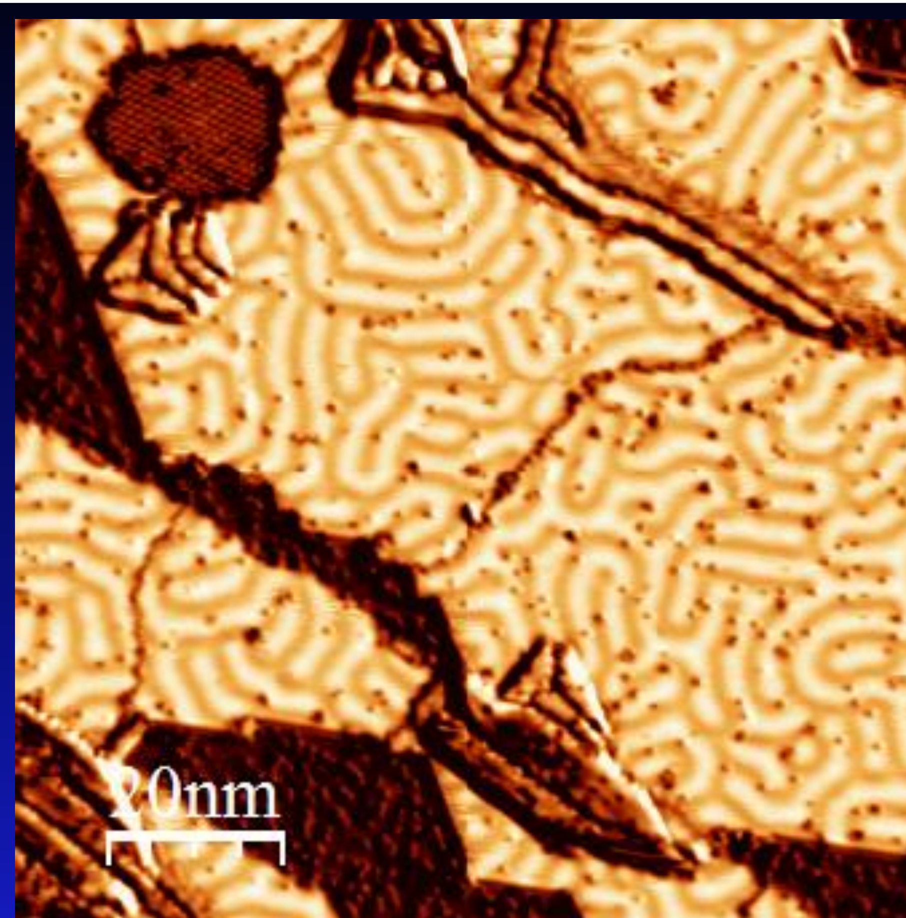

-200mV, 1.0nA, Bz= 0T, dI/dU topo.

- The post annealing assists the growth of hydrogenated Fe-DL to an extended area.
- The period of spiral increases after dosing H atoms onto pseudomorphic Fe-DL.

Field-dependent SP-STM

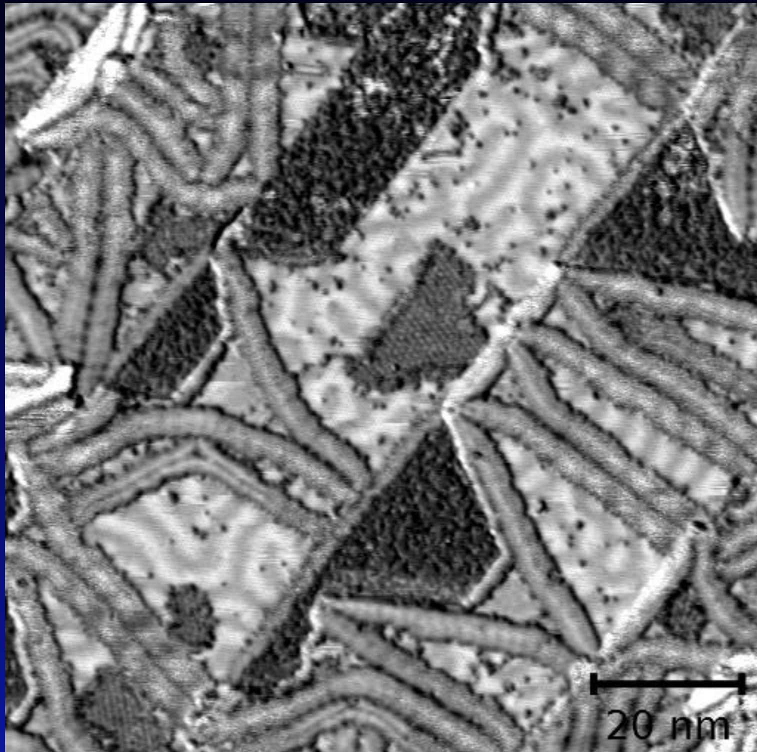

-150mV, 0.5nA, Bz= 0T, dI/dU

- There is magnetic phase transition from spiral to isotropic magnetic object at the strained pseudomorphic areas.

- Also the magnetic phase transition at the reconstruction line areas.

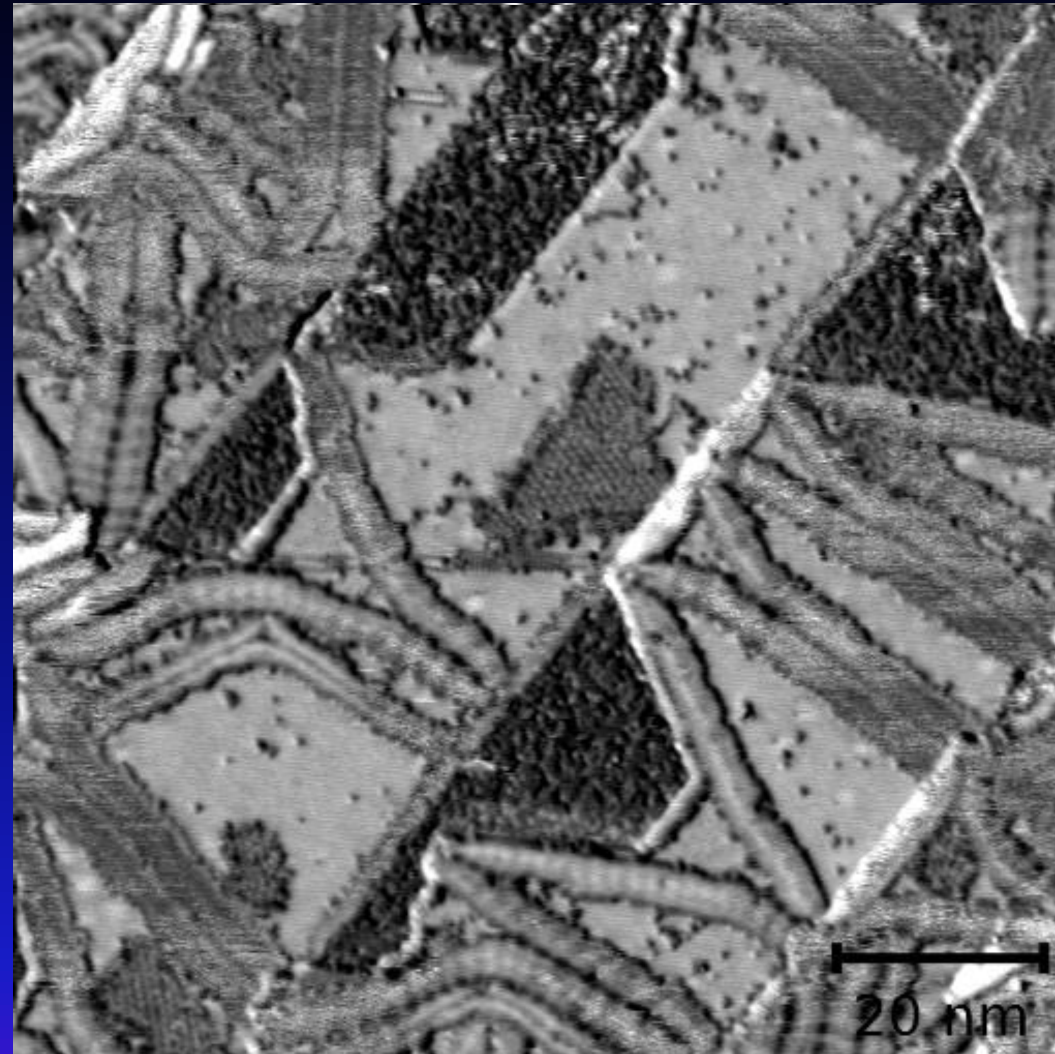

-150mV, 0.5nA, Bz= 4T, dI/dU

Fe-TL; Pd/Fe / Ir(111)
In-plane Spin Contrast

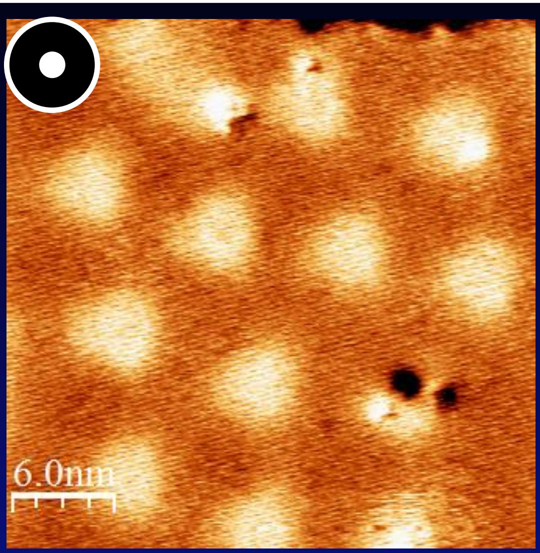

0.2V, 1.0nA, Bz= 1.5T, dI/dU.

- From the out-of-plane spin contrast, they show the same appearance, which is also an indication of unique rotational sense in isotropic skyrmions.

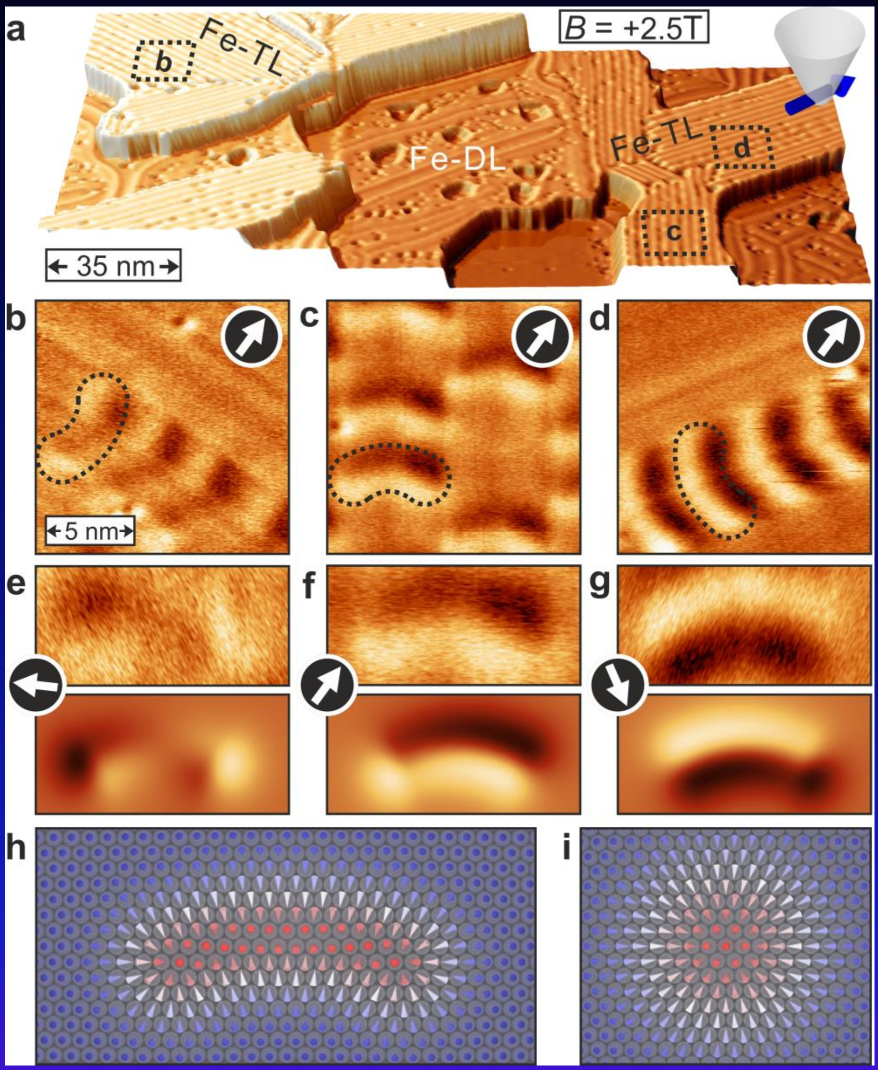

- From the in-plane spin contrasts on 3 rotational domain, the unique rotational sense of anisotropic skyrmion can be determined on Fe-TL/ Ir(111).

  0.2V, 1.0nA, Bz= 1.5T, dI/dU

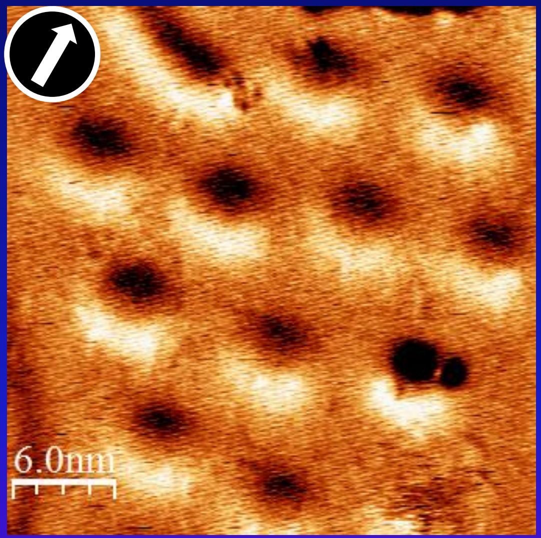

P.-J. Hsu, A. Kubetzka, A. Finco, N. Romming, K. von Bergmann, and R. Wiesendanger, Nat. Nano., 12, 123-126 (2017)

Field-dependent SP-STM with In-plane Spin Contrast

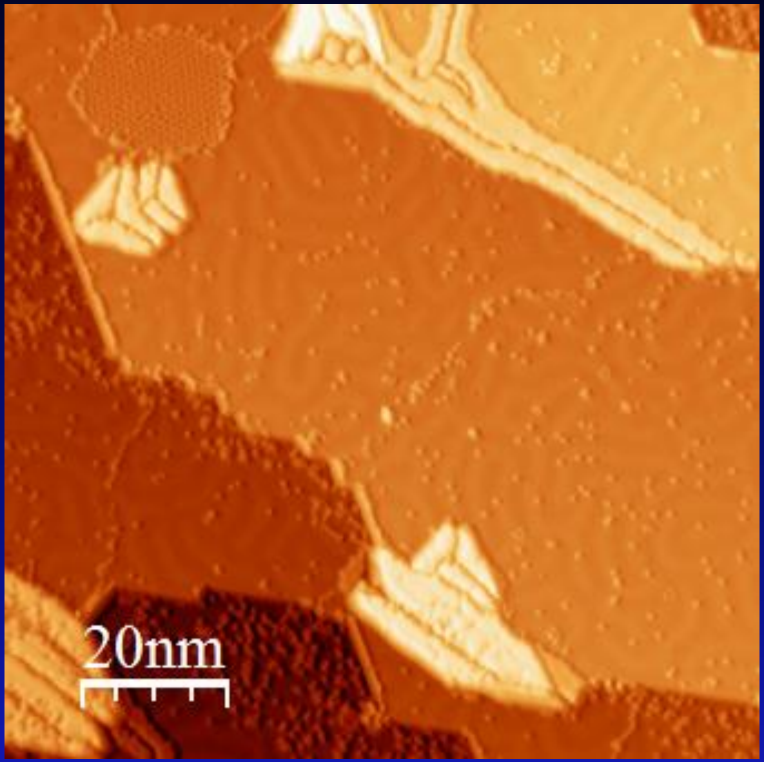

-0.2 V, 1.0 nA, Bz= 0 T, Topo.

- These magnetic object shows unique rotational sense, suggesting they are topologically equivalent to magnetic skyrmions.

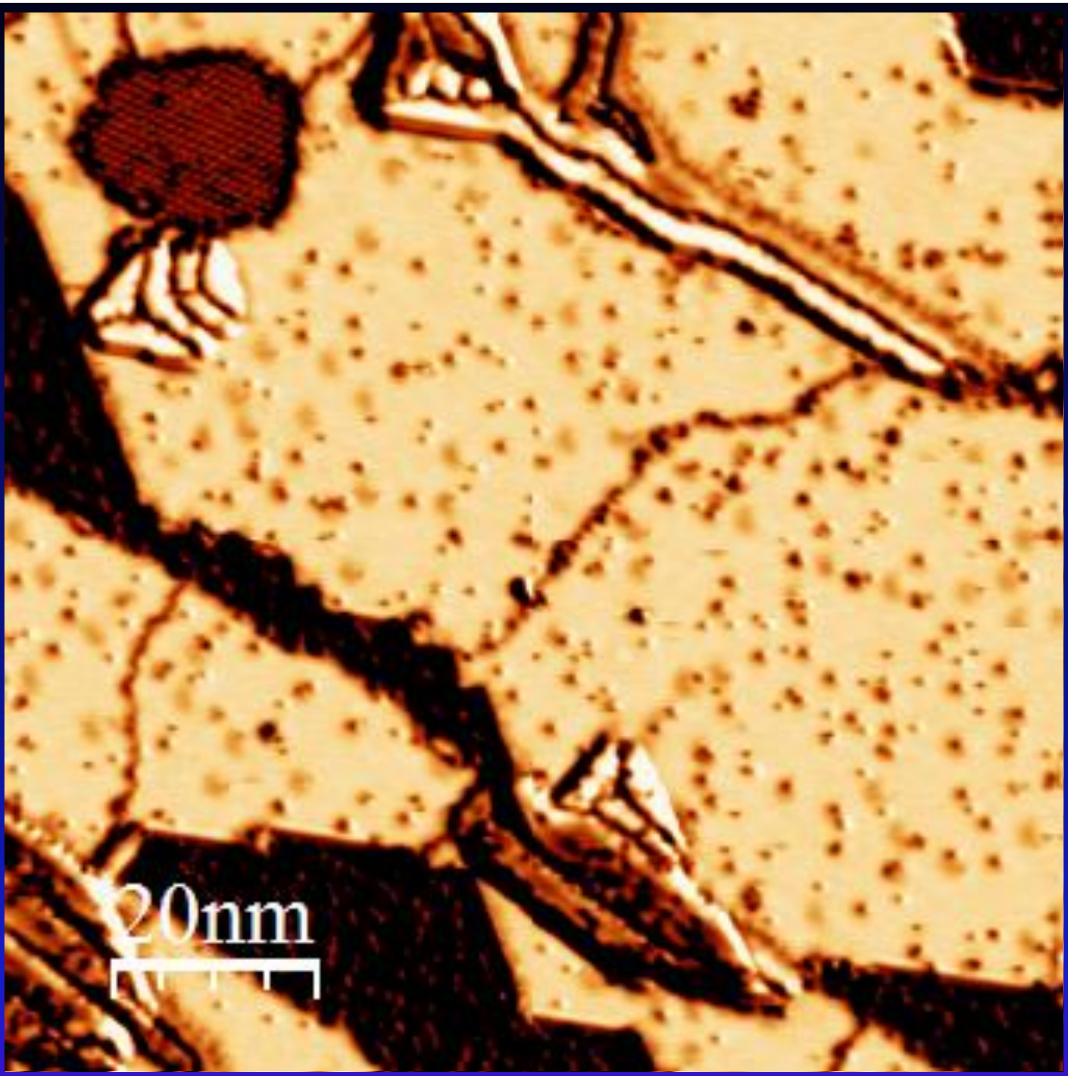

-0.2 V, 1.0 nA, Bz= [illegible] T, dI/dU

Unique Rotational Sense & FM phase, Cr tip, 4 K

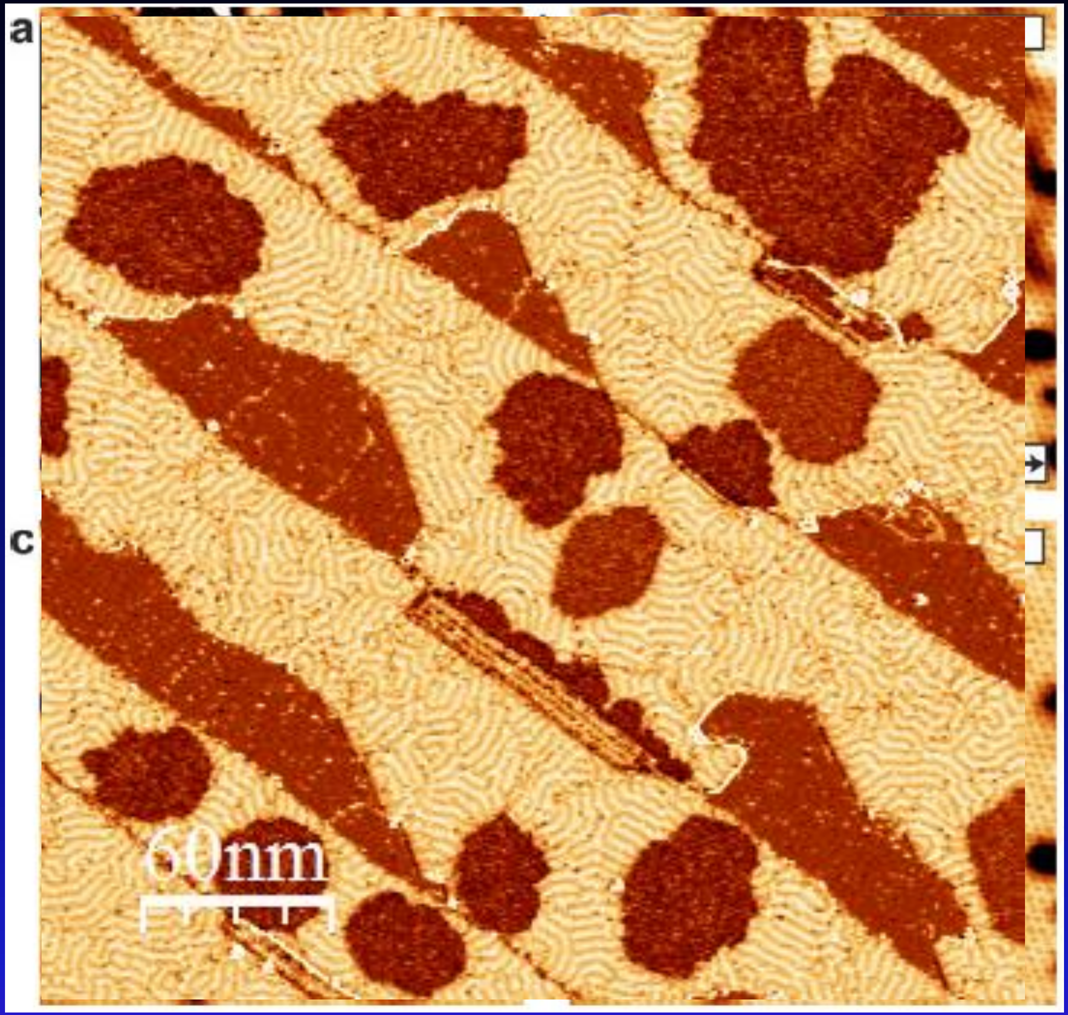

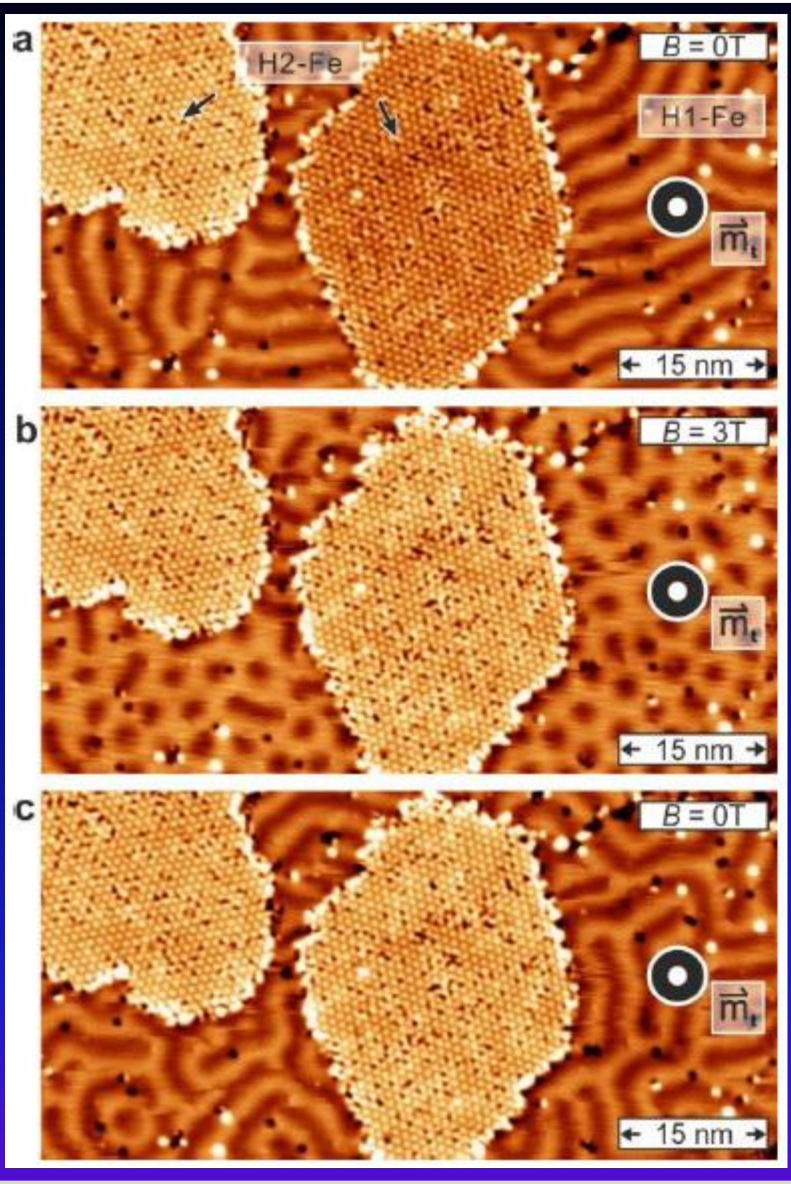

P.-J. Hsu, L. Rózsa, A. Finco, L. Schmidt, K. Palotás, E. Vedmedenko, L Udvardi, L. Szunyogh, A. Kubetzka, K. von Bergmann, and R. Wiesendanger, Nat. Commun., 9, 1571 (2018)

H/ Fe-DL/ Ir(111)

Tailor Heisenberg Exchange & DM Interactions by H

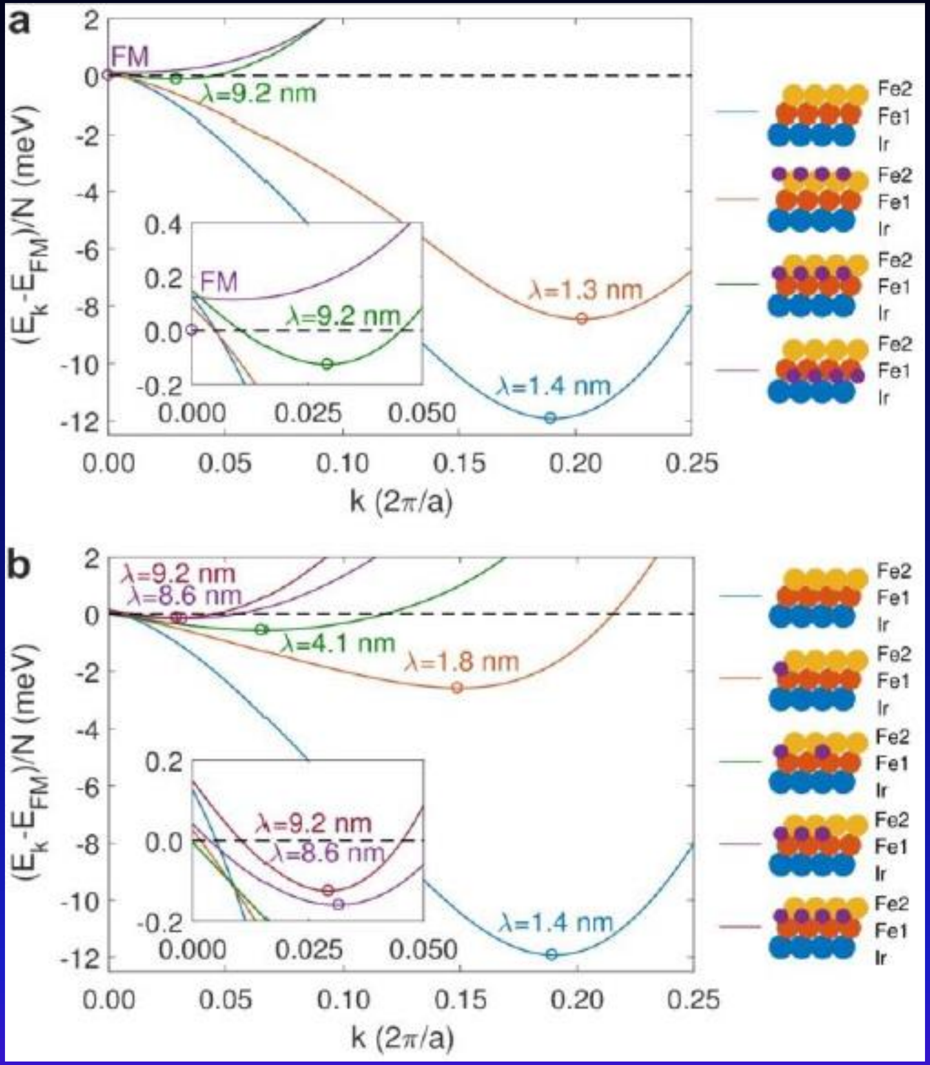

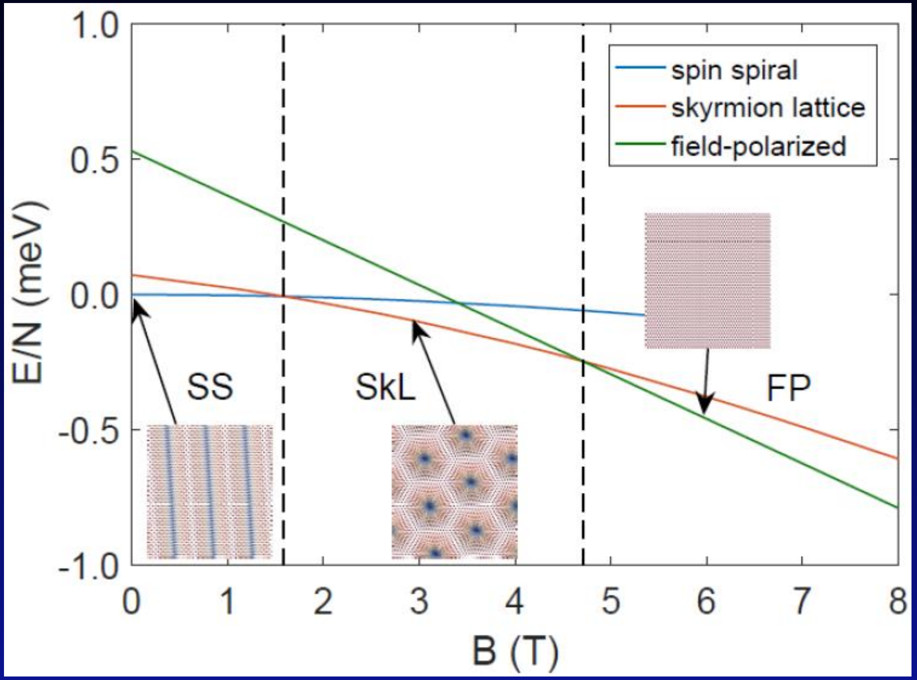

- H enhances the HEI on the H1-Fe phase to increase the spiral's period.
- H reduces the DMI on the H2-Fe phase to develop FM state.

P.-J. Hsu, L. Rózsa, A. Finco, L. Schmidt, K. Palotás, E. Vedmedenko, L Udvardi, L. Szunyogh, A. Kubetzka, K. von Bergmann, and R. Wiesendanger, Nat. Commun., 9, 1571 (2018)

Summary & Future Highlights

➢ **Summary:**

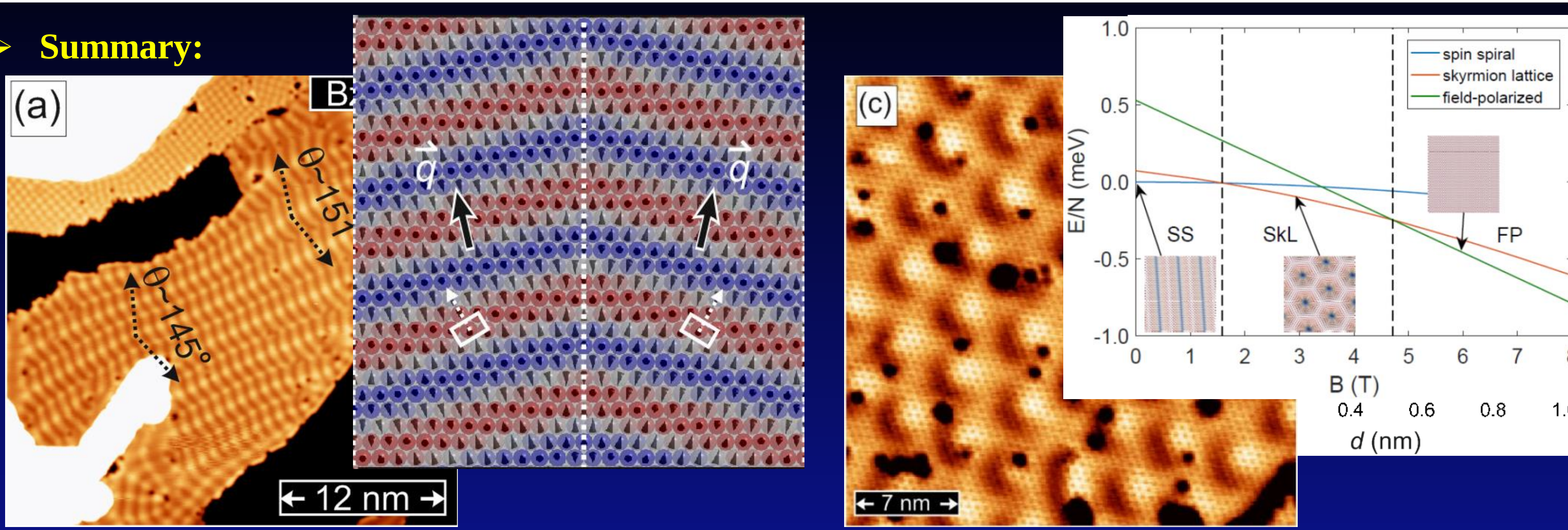

➢ **Future Highlights:**

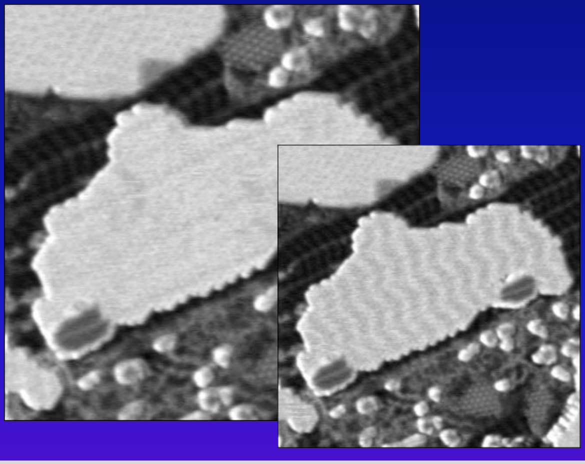

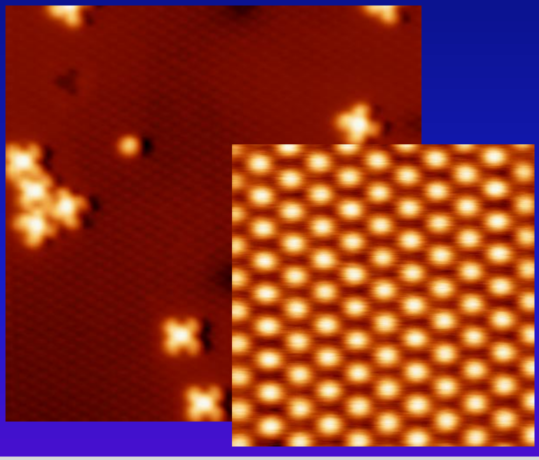

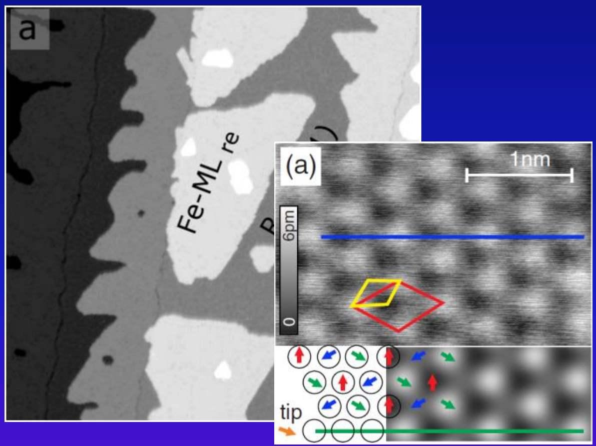

Acknowledgement


L. Schmidt


A. Finco


J. Sassmannshausen


M. Perini


N. Romming


Dr. A. Kubetzka


Dr. K. von Bergmann


Prof. Dr. R. Wiesendanger

H/ Fe-DL/ Ir(111)
Increase of Spiral Period

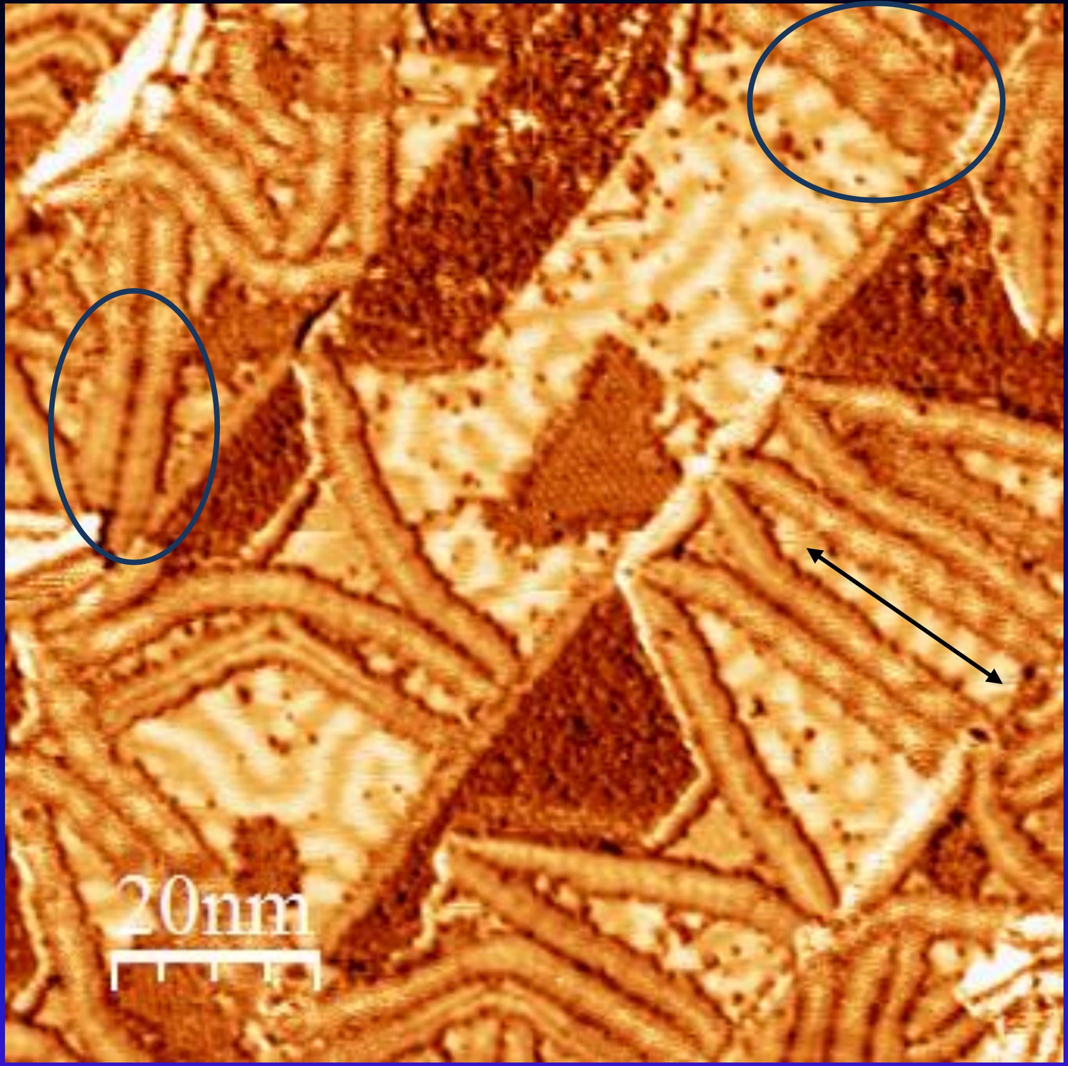

-150mV, 0.5nA, Bz= 0T, dI/dU.

- The spiral period also increases at the dislocation line areas.
- The spiral period increases from 1.2 nm to 3.5 nm at the strained pseudomorphic areas.
- Sine fit of the line profile suggests rather small contribution of magnetic anisotropy.

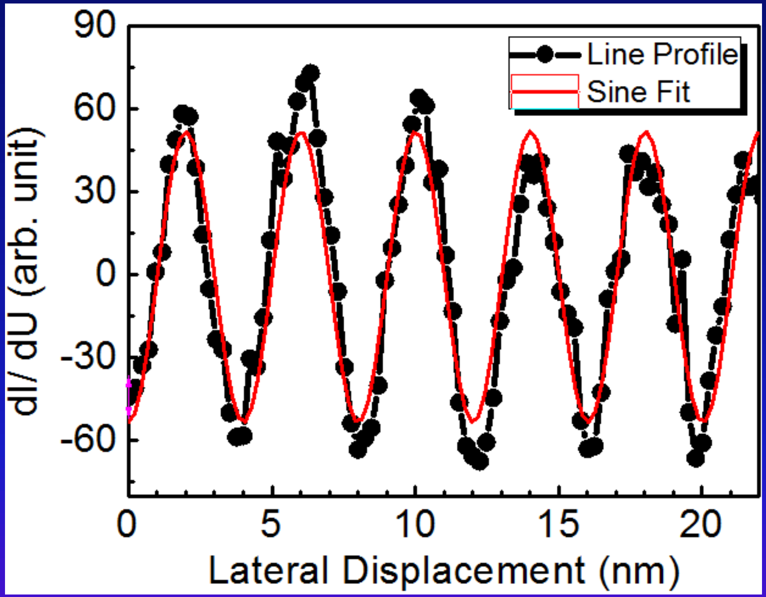

Acknowledgement

(left to right):
Top row: Matthias Bode, Christian Krammel, Jens Krögel, Pin-Jui Hsu, Tobias Mauerer, Paolo Sessi
Front: Jeannette Kemmer, Lydia El-Kareh, Oliver Storz, Annita Gebhardt, Lieselotte Reichert, Weida Wu

Theory : (Kiel Uni.) Markus Hoffmann, Stefan Heinze ;
(Würzburg Uni.) Michael Karolak, Giorgio Sangiovanni; Francesco Toldin, Fakhr Assad;
Experiment : (Würzburg Uni.) Sonja Schatz, Henriette Maaß, Hendrik Bentmann, Friedrich Reinert

Working Principle

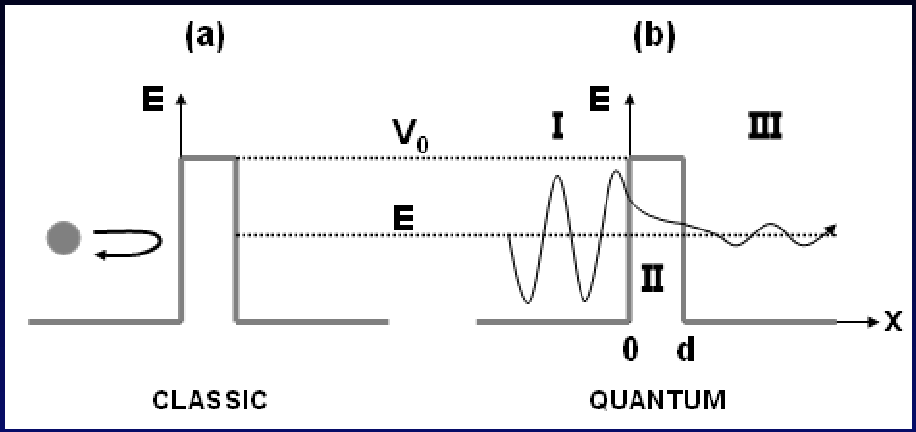

$$T=\frac{j_t}{j_i}=\left|\frac{F}{A}\right|^2=\frac{1}{1+\frac{(k^2+\kappa^2)^2}{(4k^2\kappa^2)}\sinh^2(\kappa d)}$$

$$T\approx\frac{16k^2\kappa^2}{(k^2+\kappa^2)^2}\cdot e^{-2\kappa d},\ \kappa d\gg 1$$

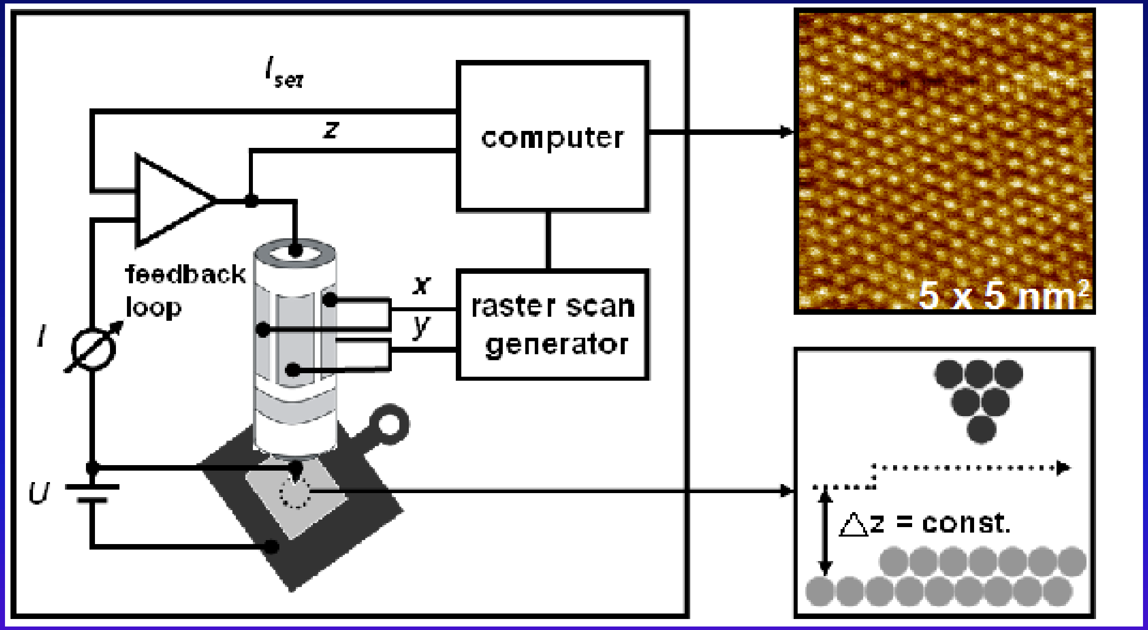

$$I\propto e^{-\lambda z}$$

- **Atomic Resolution**
- **Surface Sensitivity**
- **Local Density of States**

↓

(Tunneling Spectroscopy)

....

Outline

- ***Research Motivation***
- *Noncollinear magnetic spin structures: chiral domain wall, spin spiral, magnetic skyrmions...*
- ***Introductions & Experimental Results***
- *Spin-Polarized STM & STS (SP-STM/ STS):*
  - *Ferromagnetic Atomic Monolayers : Fe/ Rh(001)*
    - *Phase competition between CDW and FM ordering*
  - *Non-collinear Magnetism : Fe-DL/ Ir(111)*
    - *Zigzag spin spiral sate with cycloidal rotation sense at reconstructed surface*
  - *Non-collinear Magnetism : Fe-TL/ Ir(111)*
    - *Electric-field-driven switching of skyrmions; Room temperature spin spiral state*
  - *Non-collinear Magnetism : H/Fe-DL/ Ir(111)*
    - *Emergence of isotropic magnetic skyrmions and intrinsic FM state*
- ***Summary & Future Highlights***

Spin Contrast of 1st & 2nd ML Fe/ Rh(001)

Cr@ W tip; T ~ 4.5 K

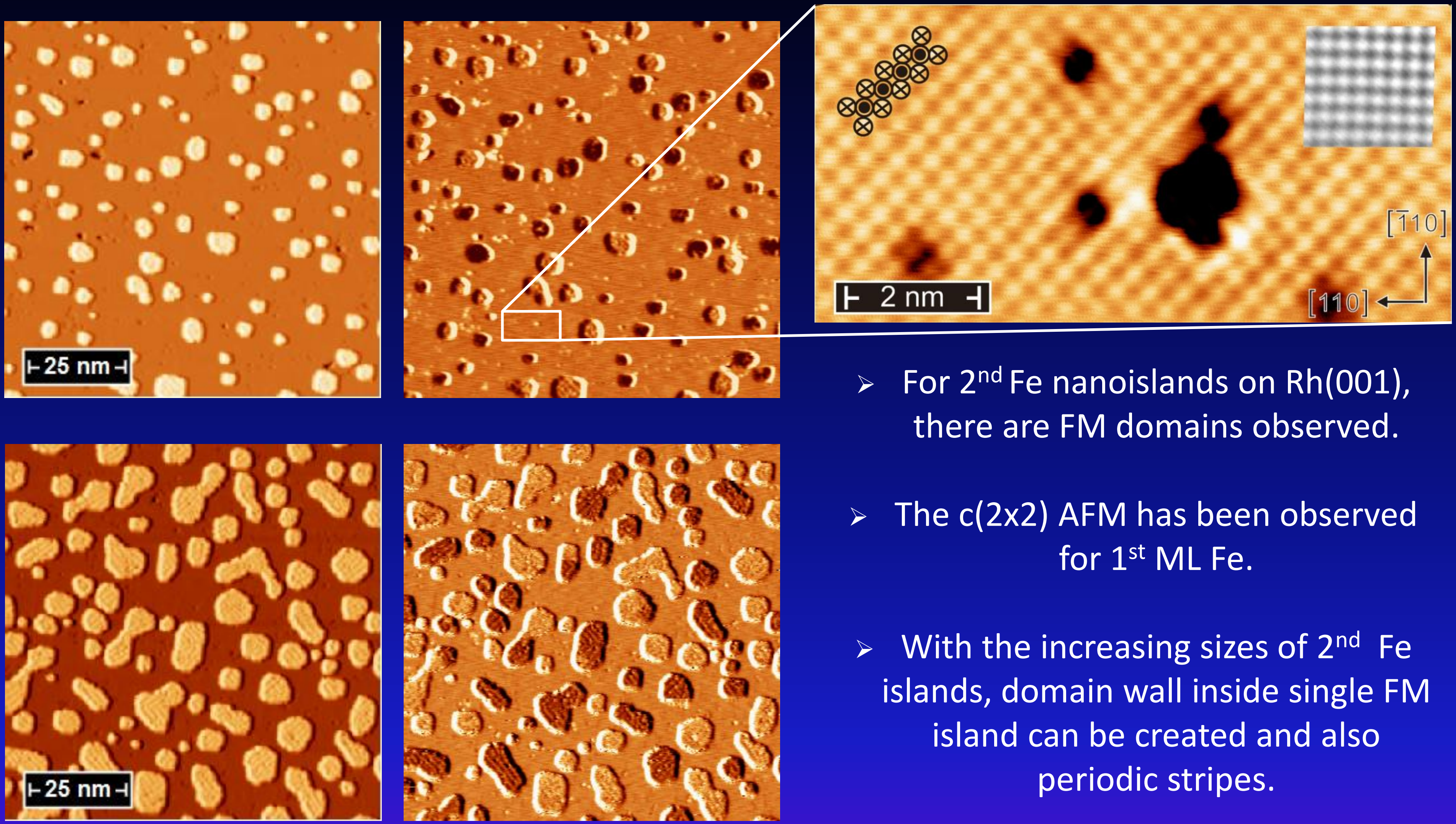

- For 2nd Fe nanoislands on Rh(001), there are FM domains observed.
- The c(2x2) AFM has been observed for 1st ML Fe.
- With the increasing sizes of 2nd Fe islands, domain wall inside single FM island can be created and also periodic stripes.

P. J. Hsu, J. Kröger, J. Kemmer, F. P. Toldin, T. Mauerer, M. Vogt, F. Assaad, and M. Bode, Nat. Comm., 7, 10949 (2016)

Magnetic Domain Walls of 2nd ML Fe/ Rh(001)

Cr@ W tip; T ~ 4.5 K

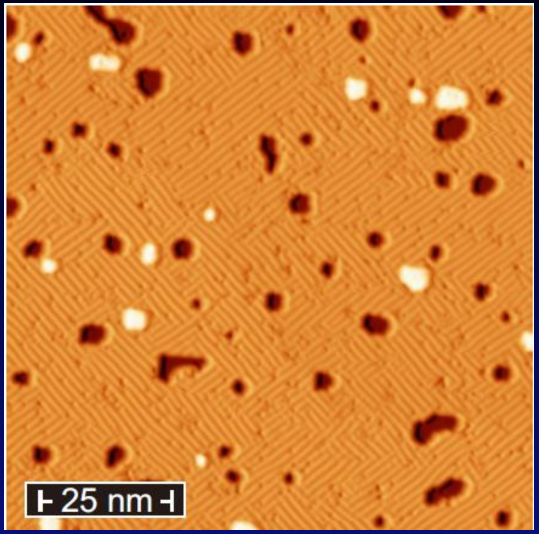

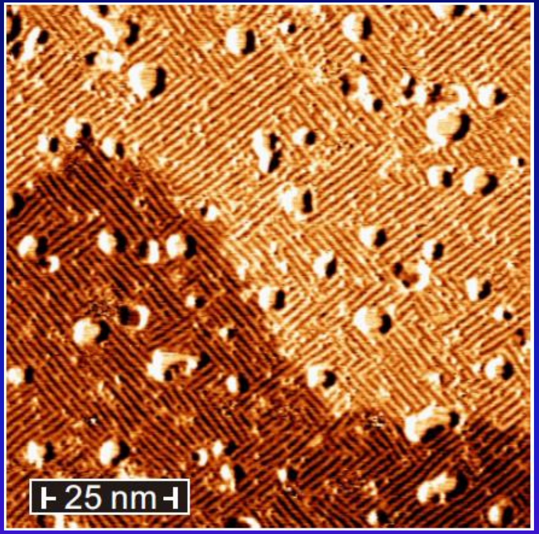

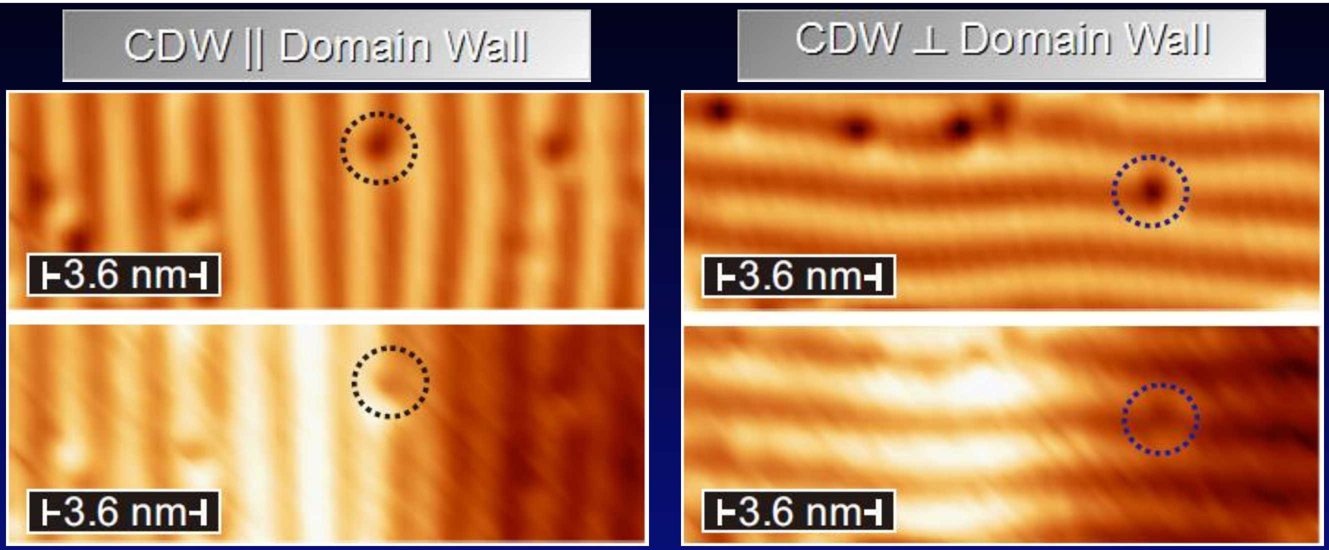

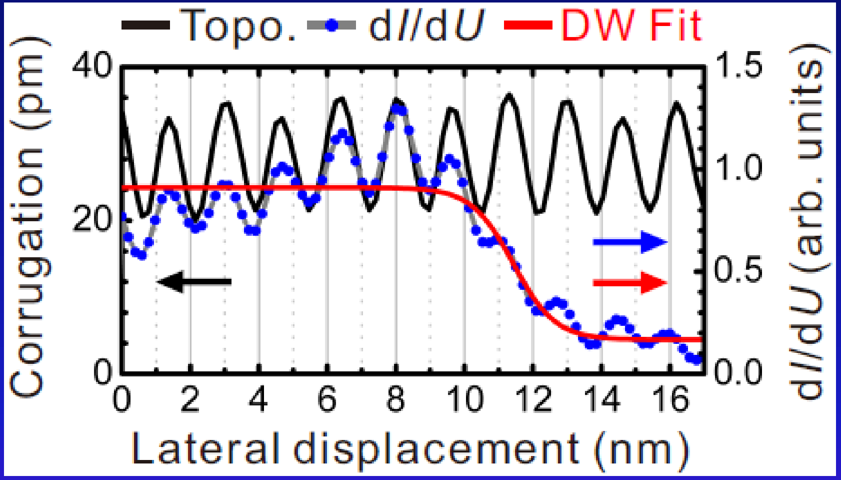

- For the CDW parallel to the domain wall, no detectable correlation with spin structures.
- The same behavior for the CDW perpendicular to the domain wall boundary.

P. J. Hsu, J. Kröger, J. Kemmer, F. P. Toldin, T. Mauerer, M. Vogt, F. Assaad, and M. Bode, Nat. Comm., 7, 10949 (2016)

Competition between Charge and FM Spin Ordering

Temperature Dependence & GL Theory

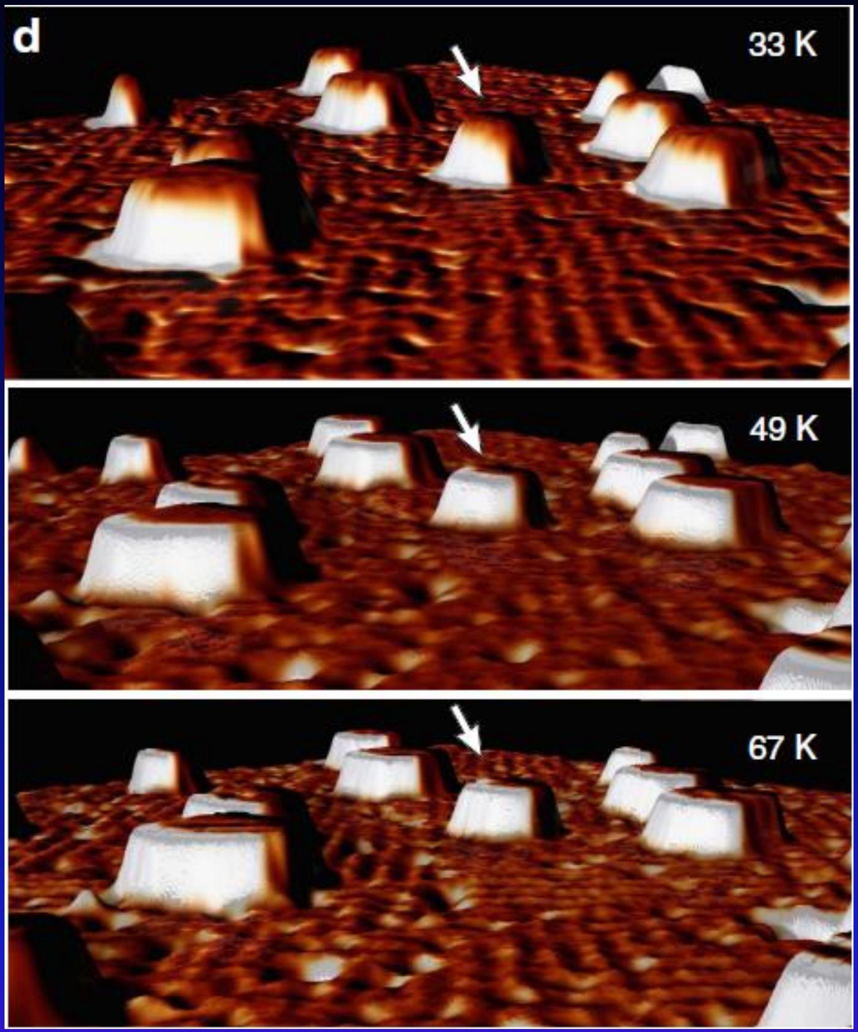

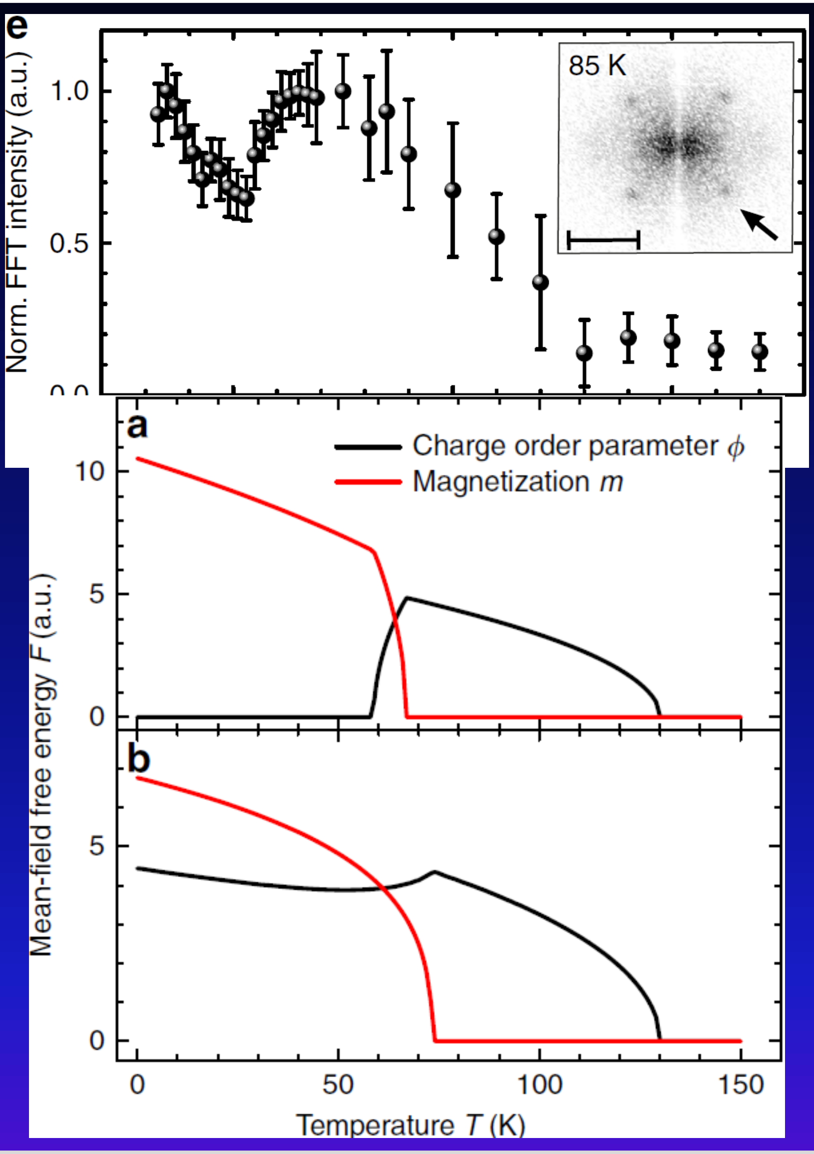

P. J. Hsu, J. Kröger, J. Kemmer, F. P. Toldin, T. Mauerer, M. Vogt, F. Assaad, and M. Bode, Nat. Comm., 7, 10949 (2016)

FeGe(110) on Si holder

Deformation of skyrmion lattice

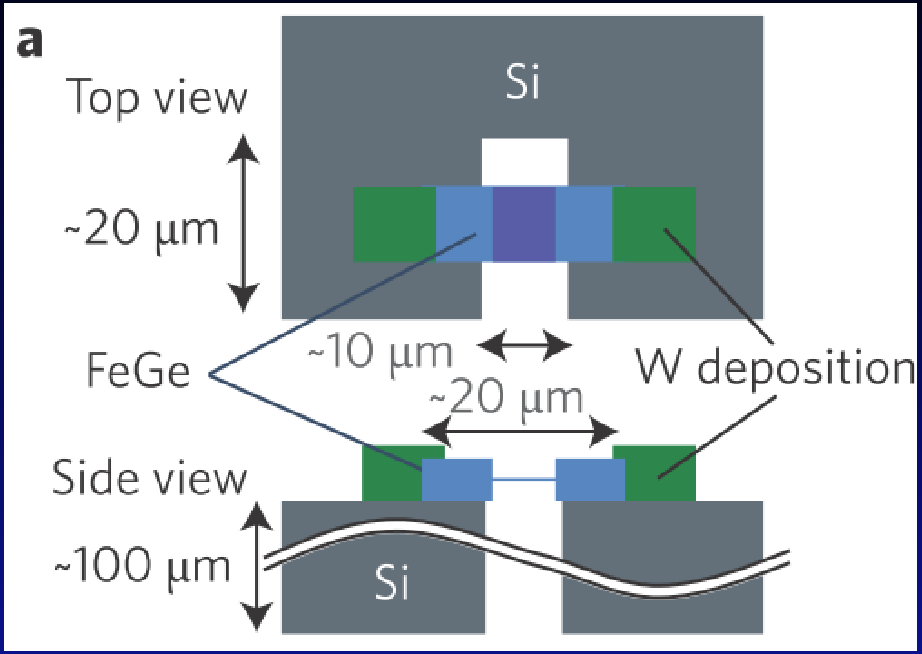

B-20 type FeGe under uniaixal tensile strain

- Thermal strain about 0.3% induces about 20% of deformation of skyrmion lattice.
- Large anisotropic modulation of DMI induced by minute atomic lattice strain.

K. Shibata *et al*., Nature Nano., 10, 589 (2015)

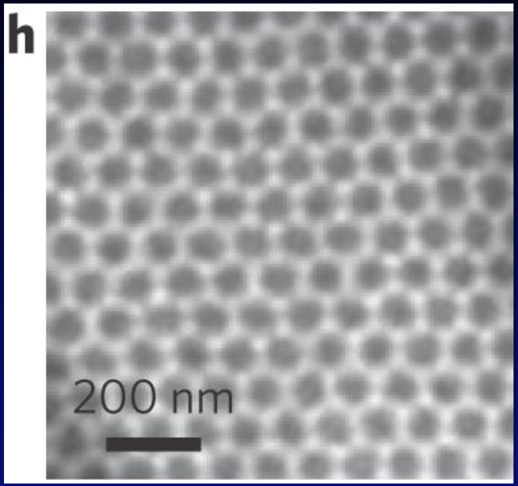

260K

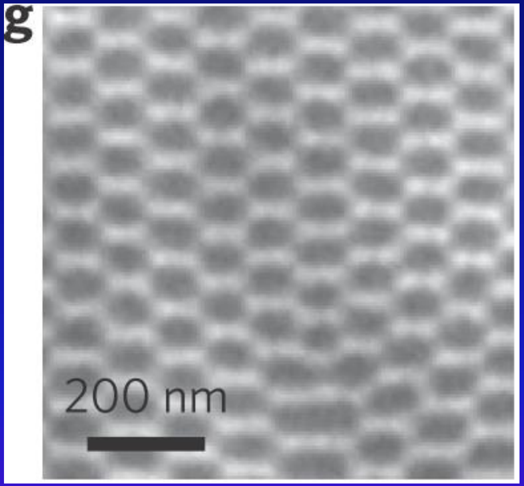

94K

Microscopic Origin of the Skyrmion Lattice

$$H = -\boxed{\sum_{i,j} J_{ij}\,\mathbf{S}_i\cdot\mathbf{S}_j} + \boxed{\sum_{i,j} \mathbf{D}_{ij}\cdot(\mathbf{S}_i\times\mathbf{S}_j)} + \boxed{\sum_i A_i\,(S_i^z)^2}$$

exchange | Dzyaloshinskii-Moriya | anisotropy

$$-\boxed{\sum_{ij} B_{ij}(\mathbf{S}_i\cdot\mathbf{S}_j)^2} - \boxed{\sum_{ijkl} K_{ijkl}\left[(\mathbf{S}_i\mathbf{S}_j)(\mathbf{S}_k\mathbf{S}_l) + (\mathbf{S}_j\mathbf{S}_k)(\mathbf{S}_l\mathbf{S}_i) - (\mathbf{S}_i\mathbf{S}_k)(\mathbf{S}_j\mathbf{S}_l)\right]}$$

biquadratic | 4-spin

- Dzyaloshinskii-Moriya interaction chooses skyrmion lattice out of several possible 2D spin textures for Fe on Ir(111)
- due to 4-spin interaction 2D spin textures are favored over ferromagnetic and 1D spin spiral states

→ Nanoskyrmion lattice is energetically favorable even in zero field !

Various types of STM in Würzburg

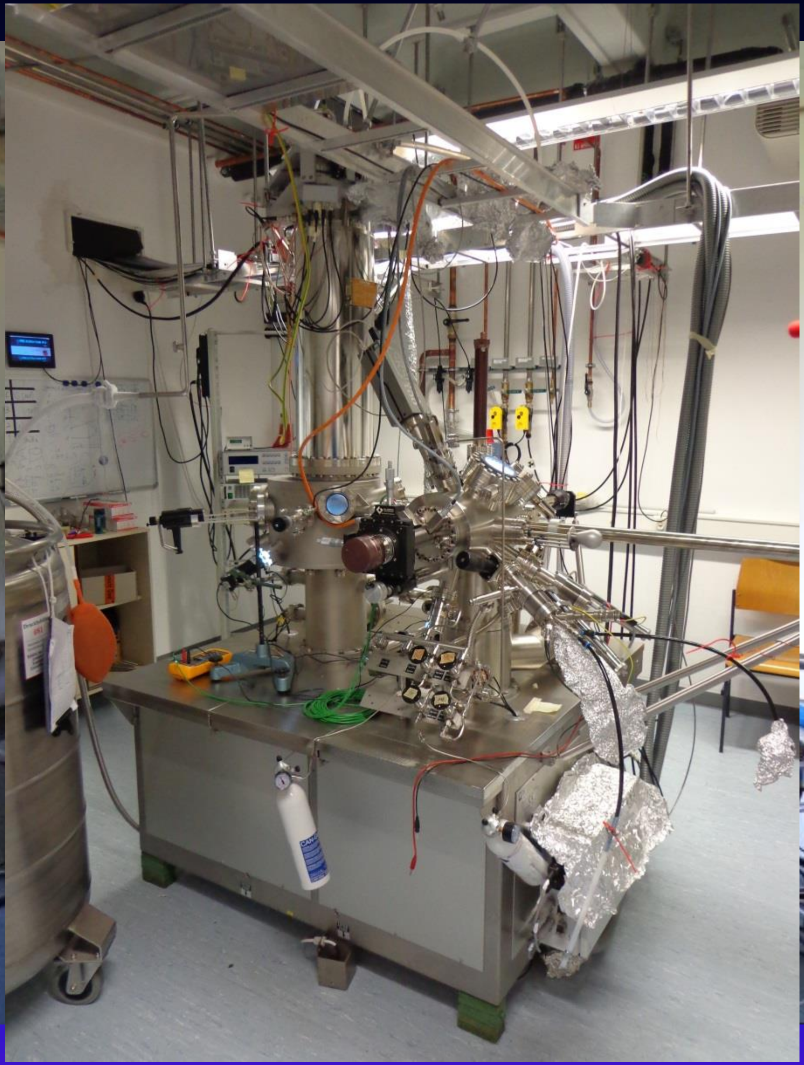

- LT-STM: P< 1E-10 mbar ; T~ 5K ; Ion gun ; E-beam Stage ; RGA ; Evaporators
- VT-STM: P< 1E-11 mbar ; T~ 30 – 400 K ; Ion gun ; E-beam Stage ; RGA ; Evaporators ; LEED/ Auger